ÇUKUROVA UNIVERSITY
INSTITUTE OF NATURAL AND APPLIED SCIENCES

PhD THESIS

Umut ÇELİK

ANALYSIS AND CLASSIFICATION OF VISUALLY EVOKED EEG USING MULTIRESOLUTION APPROXIMATION

DEPARTMENT OF ELECTRICAL AND ELECTRONICS ENGINEERING

ADANA, 2010

ÇUKUROVA UNIVERSITY
INSTITUTE OF NATURAL AND APPLIED SCIENCES

ANALYSIS AND CLASSIFICATION OF VISUALLY EVOKED EEG USING MULTIRESOLUTION APPROXIMATION

Umut ÇELİK

PhD THESIS

DEPARTMENT OF ELECTRICAL AND ELECTRONICS ENGINEERING

We certified that the thesis titled above was reviewed and approved for the award of degree of Doctor of Philosophy by the board of jury on 28 / 10 / 2010.

…….....	……..	…….....
Asst. Prof. Dr. Sami ARICA	Prof. Dr. Hamza EROL	Asst. Prof. Dr. Esen YILDIRIM
SUPERVISOR	MEMBER	MEMBER

…….....	……..
Asst. Prof. Dr. Mustafa ORAL	Asst. Prof. Dr. M. Kerem ÜN
MEMBER	MEMBER

This PhD Thesis is performed in Department of Institute of Basic and Applied Sciences of Çukurova University.
Registration Number:

Prof. Dr. İlhami YEĞİNGİL
Director
Institute of Basic and Applied Sciences

This study was supported by Çukurova University's Scientific Research Fund.
Project Number: MMF2007D14

Not: The usage of the presented specific declarations', tables, figures, and photographs either in this thesis or in any other reference without citation is subject to "The law of Arts and Intellectual Products" number of 5846 of Turkish Republic

ABSTRACT

PhD THESIS

ANALYSIS AND CLASSIFICATION OF VISUALLY EVOKED EEG USING MULTIRESOLUTION APPROXIMATION

Umut ÇELİK

ÇUKUROVA UNIVERSITY
INSTITUTE OF NATURAL AND APPLIED SCIENCES
DEPARTMENT OF ELECTRICAL - ELECTRONICS ENGINEERING

Supervisor: Asst. Prof. Dr. Sami ARICA
Year: 2010, Pages: 131
Jury: Asst. Prof. Dr. Sami ARICA
Prof. Dr. Hamza EROL
Asst. Prof. Dr. Esen YILDIRIM
Asst. Prof. Dr. Mustafa ORAL
Asst. Prof. Dr. M. Kerem ÜN

Electroencephalogram (EEG) is the electrical activity of the brain acquired by recording from electrodes placed on the scalp. The EEG has many usages: It is used to construct a communication channel between human being and his environment; it helps to understand the brain functions; it is used in diagnosis and therapy. Visual Evoked potentials (VEPs) in the EEG that occurs in response to a visual stimulus are a tool to facilitate such advancements.

The objective of this work is to analyze and classify VEPs obtained from familiar and unfamiliar face experiments. EEG signals were recorded from 26 volunteers. Multi-resolution analysis was used as a tool for signal approximation and time-frequency analysis. A custom scaling-wavelet function pair and its bi-orthogonal complements were built by resembling the waveform of the scaling function to excitatory post-synaptic potential (EPSP). The approximation coefficients of the VEPs were obtained from the custom scaling function, and the approximation coefficients of the training set were fed to a Fisher's linear classifier to distinguish the familiar-unfamiliar face specific VEP. The classification performance of the proposed wavelet has been slightly higher than the well-known wavelets with filter lengths which are close to the filter length of the custom scaling function. Furthermore, some EEG data features and common spatial patterns methods were also investigated. The performances of the custom multi-resolution system, ordinary wavelets, the EEG features and, the common spatial patterns methods were examined and compared. The results show that the classification performance of proposed technique has promising success for the EEG signal representation and classification.

Key Words: Electroencephalogram, Visual Evoked Potential, Excitatory Postsynaptic Potential, Multi-resolution Approximation, Linear Discriminant Analysis.

ÖZ

DOKTORA TEZİ

ÇOKLU ÇÖZÜNÜRLÜK YAKLAŞIMI KULLANILARAK GÖRSEL OLARAK UYARILMIŞ EEG'NİN ANALİZİ VE SINIFLANMASI

Umut ÇELİK

ÇUKUROVA ÜNİVERSİTESİ
FEN BİLİMLERİ ENSTİTÜSÜ
ELEKTRİK ELEKTRONİK MÜHENDİSLİĞİ BÖLÜMÜ

Danışman: Yrd. Doç. Dr. Sami ARICA
Yıl: 2010, Sayfa: 131
Jüri: Yrd. Doç. Dr. Sami ARICA
Prof. Dr. Hamza EROL
Yrd. Doç. Dr. Esen YILDIRIM
Yrd. Doç. Dr. Mustafa ORAL
Yrd. Doç. Dr. M. Kerem ÜN

Elektroansefalografi (EEG) kafatası üzerine yerleştirilen elektrotlar vasıtasıyla beynin elektriksel aktivitelerinin ölçülmesidir. EEG'nin bir çok kullanım alanı vardır: Bu sinyaller ile, insanlar ve çevresi arasında bir iletişim kanalı oluşturulmasında veya beynin fonksiyonlarının anlaşılmasında veya birçok tanı ve tedavi sırasında yararlanılabilir. EEG sinyali içerisinde bir görsel uyarana tepki olarak oluşan Görsellikle İlişkili Potansiyeller (GİP) bu tür uygulamaların gelişiminde bir araç olarak kullanılabilir.

Bu çalışmanın temel amacı; tanıdık ve tanımadık insan yüzlerinin fotoğrafları kullanılarak yapılan deneylerden elde edilmiş görsellikle ilişkili EEG sinyallerinin analizi ve sınıflandırılmasıdır. Deneylerde 26 kişiden EEG verisi alınmıştır. Çoklu çözünürlük analizi sinyal yaklaşımı ve zaman frekans analizi için bir araç olarak kullanıldı. Bir ölçekleme ve dalgacık fonksiyon çifti ve onların dikey olmayan tümleyenleri eksitatör post-sinaptik potansiyelin dalga biçimine uygun olarak oluşturulmuştur. GİP'lerin yaklaşım katsayıları bu ölçekleme fonksiyonu sayesinde sağlanmış ve yaklaşım katsayılarından oluşan eğitim setindeki sinyaller tanıdık-tanımadık yüzle ilgili potansiyeli sınıflamak için Fisher lineer sınıflayıcısına giriş olarak uygulanmıştır. Oluşturulan dalgacık ile yapılan sınıflamanın performansı dalgacık filtre uzunlukları bizim oluşturduğumuz ölçekleme fonksiyonunun filtre uzunluğuna yakın olan diğer dalgacıklara göre daha iyi sonuç vermiştir. Bunun yanında, EEG verisinin öznitelikleri ve ortak uzamsal örnekleri yöntemi de sınıflama başarımının karşılaştırılması için kullanılmıştır. Bu sonuçlar bizim yöntemin EEG sinyal işlemede ve sınıflamada başarılı olabileceğini göstermektedir.

Anahtar Kelimeler: Elektroensefalografi, Görsellikle İlgili Potansiyel, Eksitator Postsinaptik Potansiyel, Çoklu Çözünürlüklü Yaklaşım, Lineer Diskriminant Analizi

ACKNOWLEDGEMENTS

I would like to thank my advisor Asst. Prof. Dr. Sami ARICA for his support, suggestions and help. I also thank to Prof. Dr. Yakup SARICA, Cukurova University, Department of Neurology who suggest the main idea of this thesis.

I appreciate Asst. Prof. Dr. Mustafa ORAL and my friends; Mustafa ZATEROĞLU, Durukan ÇOLAK and Zehan KESİLMİŞ for their supports and valuable discussions and also thank staff members of Department of Electrical and Electronics Engineering for their supports.

I also thank my juri members; Prof. Dr. Hamza EROL, Asst. Prof. Dr. Mustafa Kerem ÜN and Asst. Prof. Dr. Esen YILDIRIM for their supports.

I would like to thank students and graduated students participated to the experiments. I also thank Atakan GÜZEL, Deniz İŞLİ and Doç. Dr. Vahide Deniz YERDELEN for their help setting up the experiments. They were too kind and helpful.

I greatly appreciate my dear parents, my sisters, brothers and my friends for their invaluable supports. Especially my mother, she is also my best friend, motivated me and gave the strongest support to me. I would also like to thank for their patience, supports and encouragements. I could not have completed this thesis without their support.

Also, I would like to thank my friends from Adana branch of The Chamber of Electrical Engineer (EMO), especially chairman Mehmet MAK, and Union of Chambers of Turkish Engineers and Architects (TMMOB) Adana provincial coordination committee for their supports, and encouragements.

CONTENTS **PAGE**

ABSTRACT I
ÖZ II
ACKNOWLEDGEMENTS III
CONTENTS IV
LIST OF TABLES VIII
LIST OF FIGURES X
ABREVIATIONS XIV
1. INTRODUCTION 1
1.1. EEG 1
1.2. Visual Evoked Potentials and Familiar - Unfamiliar Face Stimuli 3
1.3. Brain Computer Interface 6
1.4. EEG Preprocessing, Feature Extraction and Classification 7
2. PREVIOUS STUDIES 9
2.1. Face Perception and Processing 9
2.2. Feature Extraction Methods 16
2.3. P300 Speller 17
3. DATA AND METHODS 19
3.1. Face Recognition Experiment 19
3.1.1. Participants 19
3.1.2. Stimuli 19
3.1.3. Procedure and EEG recording 21
3.2. Wadsworth BCI Dataset (P300 Evoked Potentials) 22
3.3. Common Spatial Pattern (CSP) 23
3.4. Wavelet Analysis 25
3.5. Multiresolution Analysis 27
3.6. Multiresolution Analysis based on Excitatory PostSynaptic Potential Approximation Model 34
3.6.1. Neural Activities 34
3.6.2. Multiresolution System Based on EPSP 36

3.7. EEG Signal Features 45
3.7.1. Curve Length 45
3.7.2. Signal Energy 45
3.7.3. Nonlinear Energy 46
3.7.4. Sixth Power Energy 46
3.7.5. Mean Frequency 46
3.7.6. Reyni Entropy 47
3.7.7. Shannon Entropy 47
3.7.8. Average Method 48
3.7.9. Differential Method 48
3.7.10. Barlow Parameters 48
3.7.11. Hjorth Parameters 49
3.7.12. Petrosian Fractal Dimension 49
3.7.13. Max Frequency Match Filter 49
3.7.14. Median Method 50
3.8. Classification Methods 50
3.8.1. Linear Discriminant Analysis (LDA) 50
3.8.2. Neural Networks 53
3.9. Feature Selection Methods 55
3.10. Validation Procedures 57
3.10.1. Bootstrapping 57
3.10.2. N-fold Cross-Validation 58
4. FINDINGS AND DISCUSSIONS 59
4.1. Model Evaluation of the System 68
4.2. Pre-processing of the Visual Evoked EEG Data 69
4.3. Results with Familiar - Unfamiliar Visual Evoked Data 69
4.2.1. Classification with Wavelet Decomposition 70
4.2.2. Classification with features of Section 3.7. 87
4.4. Results of BCI Competition III P300 Speller Data 92
5. RESULTS AND SUGGESTIONS 101
REFERENCES 105

CIRRICULUM VITAE 121
APPENDIXES 122
APPENDIX I.Familiar (Famous) Stimulus Photos and Names 122
APPENDIX II.Unfamiliar Stimulus Photos 126
APPENDIX III.Participant Information 129
APPENDIX IV.Informed Consent Form 130
APPENDIX V.Approved Form by Neurology Department Committee and Management of Başkent University, Adana Application and Research Center. 131

LIST OF TABLES **PAGE**

Table 2.1. Brief Literature Review of the familiar - unfamiliar face.....14
Table 4.1. Familiar and unfamiliar EEG data set size according to volunteers. 59
Table 4.2. Wavelet families, short names and filter length of the wavelet using our work. 71
Table 4.3. Classification accuracies in percent for subject number from 1 to 26 with 5-fold validation using LDA classification. The custom wavelet (epsp) is compared with some well known wavelets. The decomposition filter length of the epsp is 18 and the filter length of the other wavelets is close to or equal to 18. 78
Table 4.4. Specificity (Qn) and Sensitivity (Qd) of classification results of the wavelet decomposition method according to different wavelets. All values are given in % and rounded. 79
Table 4.5. Selected channels by the channel selection steps of the wavelet decomposition method using custom wavelet 'epsp' 80
Table 4.6. Wavelet names and corresponding most selected five channels by channel selection steps of the wavelet decomposition method from all volunteers 80
Table 4.7. Classification accuracies in percent for subject number from 1 to 26 by using excitatory postsynaptic potential approximation method with level 2^J. 82
Table 4.8. Classification accuracies in percent for subject # from 1 to 26 using CSP as the channel selection approach of the wavelet decomposition method. The custom wavelet (epsp) is compared with some well known wavelets. Most discriminative ten channels were selected according to CSP transform. ..83
Table 4.9. Classification accuracies in percent for subject number from 1 to 26. The custom wavelet (epsp) is compared with some well known wavelets. Bootstrapping cross validation was used instead of 5-fold validation 84
Table 4.10. Classification accuracies in percent for subject number from 1 to 26 with 5-fold validation using Backpropagation Neural Network classification. The custom wavelet (epsp) is compared with some well known wavelets.

The decomposition filter length of the epsp is 18 and the filter length of the other wavelets is close to or equal to 18. 85
Table 4.11. Classification accuracies in percent for subject number from 1 to 26. The custom wavelet (epsp) is compared with some well known wavelets. Approximation statistics was used instead of approximation coefficient and 5-fold validation is used. 86
Table 4.12. Feature types for classification algorithm and number of features of each feature type. 87
Table 4.13. Classification accuracy in percent for subject No from 1 to 26 by using feature types with consensus method with sensitivity, specificity and overall accuracy measures. Also, selected feature types by the algorithm are given in right. 90
Table 4.14. Classification accuracy in percent for subject number from 1 to 26 by using feature types with concatenate method with sensitivity, specificity and overall accuracy measures. Also selected channels by the channel selection steps is in right side and most selected channels is in right bottom side 91
Table 4.15. Highest five performance measures of BCI Competition III . The first column of results shows the results of all 15 repetitions and second column only five repetitions (Original Tables in http://www.bbci.de/competition/iii/results/index.html) 97
Table 4.16. Classification accuracy in percent for subject A and subject B for spelling the symbols. The custom wavelet (epsp) is compared with some well known wavelets. The decomposition filter length of the epsp is 18 and the filter length of the other wavelets is close to or equal to 18. 98
Table 4.17. Mean classification accuracy in percent for spelling the symbols. The custom wavelet (epsp) is compared with some well known wavelets. The decomposition filter length of the epsp is 18 and the filter length of the other wavelets is close to or equal to 18. 99

LIST OF FIGURES **PAGE**

Figure 1.1. The different brain rhythms as measured by EEG (pictures from www.wikipedia.org). 2
Figure 1.2. The international 10-20 EEG electrode placement system. A = Ear lobe, C = central, Pg = nasopharyngeal, P = parietal, F = frontal, Fp = frontal polar, O= occipital. 3
Figure 1.3. Three face-selective regions: the FFA in the fusiform gyrus along the ventral part of the brain, the OFA in the lateral occipital area and the fSTS in the posterior region of the superior temporal sulcus (Picture from Kanwisher et al., 1997). 4
Figure 1.4. The model of the distributed human neural system for face perception (Picture taken from Gobbini & Haxby, 2007). 6
Figure 1.5. Architecture of a brain-computer interface 7
Figure 2.1. Functional architecture of face processing described by Bruce and Young (original picture at Bruce & Young, 1986) 10
Figure 3.1. Two examples of face stimuli. a) Familiar (TV actor) b) Unfamiliar 20
Figure 3.2. Experimental setup 20
Figure 3.3. Time course of the experiment 21
Figure 3.4. The user display of P300 Speller paradigm. (Image is from Krusienski & Schalk, 2004) 22
Figure 3.5. Decomposition of discrete wavelet transform 32
Figure 3.6. Symbolic division of time-frequency space for multiresolution wavelet decomposition 33
Figure 3.7. Wavelet packet tree 33
Figure 3.8. A biological neuron 34
Figure 3.9. An action potential 35
Figure 3.10. The neuron membrane potential changes and current flow during synaptic activation (Picture from Sanei & Chambers, 2007) 36
Figure 3.11. EPSP function 37
Figure 3.12. The four filters of custom multi-resolution system 41

Figure 3.13. Bi-orthogonal scaling and wavelet functions and their bi-orthogonal complements for custom wavelet. 41
Figure 3.14. Two dimensional, two class data projected on w. (modified from Alpaydın, 2004). 52
Figure 4.1. Grand average ERPs of all volunteer familiar and unfamiliar data from the each of the channels occipital, temporal, parietal and central regions and corresponding α-value of the t-test under the ERP plots. Red line on the t-test plots are the significant level at α-value=0.05. 60
Figure 4.2. Average ERPs of the volunteers 4, 26, 3 and 22 familiar and unfamiliar data from the central regions and corresponding α-value of the t-test under the ERP plots. Red line on the t-test plots are the significant level at α-value=0.05. Selected subjects have the highest two and lowest two accuracy performance in the 'epsp' wavelet decomposition algorithm in Table 4.3 respectively. 62
Figure 4.3. Signal processing scheme of classification of familiar - unfamiliar evoked EEG using wavelet decomposition. 65
Figure 4.4. Signal processing scheme of classification of familiar - unfamiliar evoked EEG using feature types with consensus methods 66
Figure 4.5. Signal processing scheme of classification of familiar - unfamiliar evoked EEG using feature types with concatenate methods 67
Figure 4.6. Filter coefficients of the wavelet using wavelet decomposition methods. 72
Figure 4.7. Scaling (left) and Wavelet (right) functions of the wavelet using wavelet decomposition methods. 73
Figure 4.8. Histogram of the selected channel by wrapper method. Y axis indicate number of selection for the 26 volunteers 81
Figure 4.9. Selected features by Fishers Criteria in the feature selection unit. X-axis indicates the features, y-axis indicates the number of volunteer, green points indicate selected features and line indicates sum of the selected features over 26 volunteers. 81
Figure 4.10. General signal processing flow chart for the P300 Speller Paradigm. .. 92

Figure 4.11. The 64-channel electrode montage and the predefined channel set. 93
Figure 4.12. Detailed signal processing scheme of the work.....94
Figure 4.13. A P300 Potential averaged responses over Cz electrode. 95
Figure 4.14. A couple of one second speller signals. 96

ABREVIATIONS

ALS	:	Amyotrophic Lateral Sclerosis
AP	:	Action Potentials
BCI	:	Brain Computer Interface
CSP	:	Common Spatial Patterns
DFT	:	Discrete Fourier Transform
DWT	:	Discrete Wavelet Transform
EEG	:	Electroencephalogram
EP	:	Evoked Potential
ERP	:	Event Related Potentials
FFA	:	Fusiform Face Area
FRU	:	Face Recognition Units
GA	:	Genetic Algorithms
LDA	:	Linear Discriminant Analysis
LVQ	:	Learning Vector Quantization
NN:	:	Neural Network
EPSP	:	Excitatory Postsynaptic Potential
IPSP	:	Inhibitory Postsynaptic Potential
ICA	:	Independent Component Analysis
OFA	:	Occipital Face Area
PCA	:	Principal Component Analysis
SVM	:	Support Vector Machines
SL	:	Surface Laplacian
T-F	:	Time - Frequency
VEP	:	Visual Evoked Potentials
WP	:	Wavelet Packet
WT	:	Wavelet Transform
Z	:	Complex Numbers

1. INTRODUCTION

1.1. EEG

Electroencephalography (EEG) is a neurophysiologic measurement of the brain electrical activity recorded from electrodes placed on the scalp, or in the special cases, on the cortex.

The first recording of the electric field of the human brain was made by the German psychiatrist Hans Berger in 1924 in Jena (Teplan, 2002). EEG, also called spontaneous activity, have about 100 μV amplitude when measured on the scalp, and about 1-2 mV when measured on the surface of the brain. The frequency range of this signal is from under 1 Hz to about 85 Hz, as demonstrated in Figure 1.1.

Evoked potentials are components of the EEG. They occur in response to a stimulus such as auditory, visual, etc. Such signals are usually below the noise level and these potential could be distinguished by signal averaging.

Historically four major types of continuous rhythmic sinusoidal EEG waves are recognized that they are alpha, beta, delta and theta. There is no precise agreement on the frequency ranges for each type.

Delta is the frequency range up to 4 Hz and is often associated with the very young and some types of encephalopathy and underlying lesions. It is seen in deep sleep.

Theta is the frequency range from 4 Hz to 8 Hz and is associated with drowsiness, childhood, adolescence and young adulthood.

Alpha (Berger's wave) is the frequency range from 8 Hz to 12 Hz. It is characteristic of a relaxed, alert state of consciousness and is present by the age of two years. Alpha rhythms are best detected with the eyes closed.

Sensorimotor rhythm (SMR) is a middle frequency (about 12–16 Hz) associated with physical stillness and body presence.

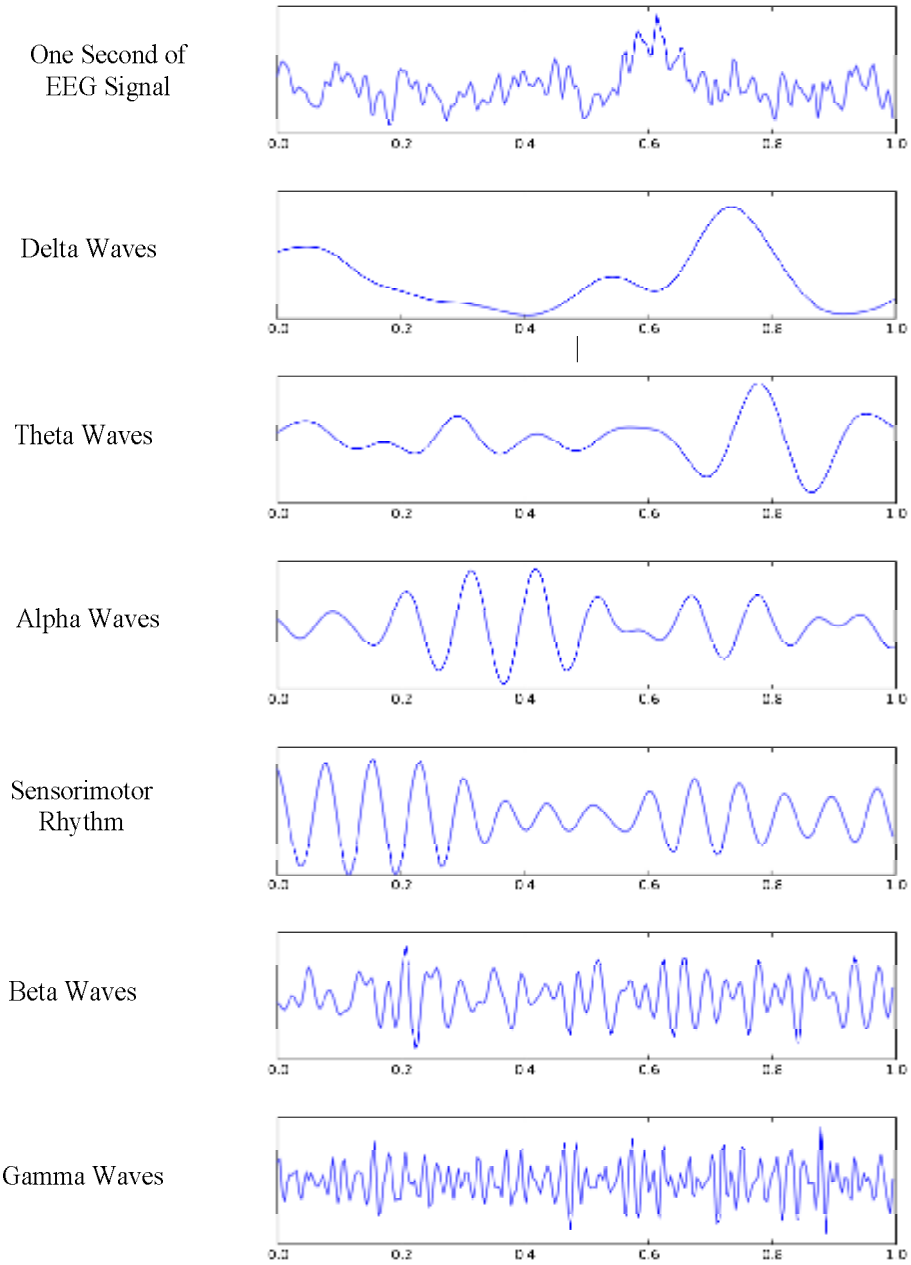


Figure 1.1. The different brain rhythms as measured by EEG (pictures from www.wikipedia.org).

Beta is the frequency range above 12 Hz. Beta rhythms is often associated with active, busy or anxious thinking and active concentration.

Gamma is the frequency range approximately 26–80 Hz. Gamma rhythms appear to be involved in higher mental activity, including perception, problem solving, fear and consciousness.

The samples of one second EEG signal corresponding to the rhythms are shown in Figure 1.1.

EEG is recorded from electrodes placed according to a standard 10-20 international system as indicated in Figure 1.2. This system composed of 19 electrodes. Extended versions have also been proposed for higher spatial resolution.

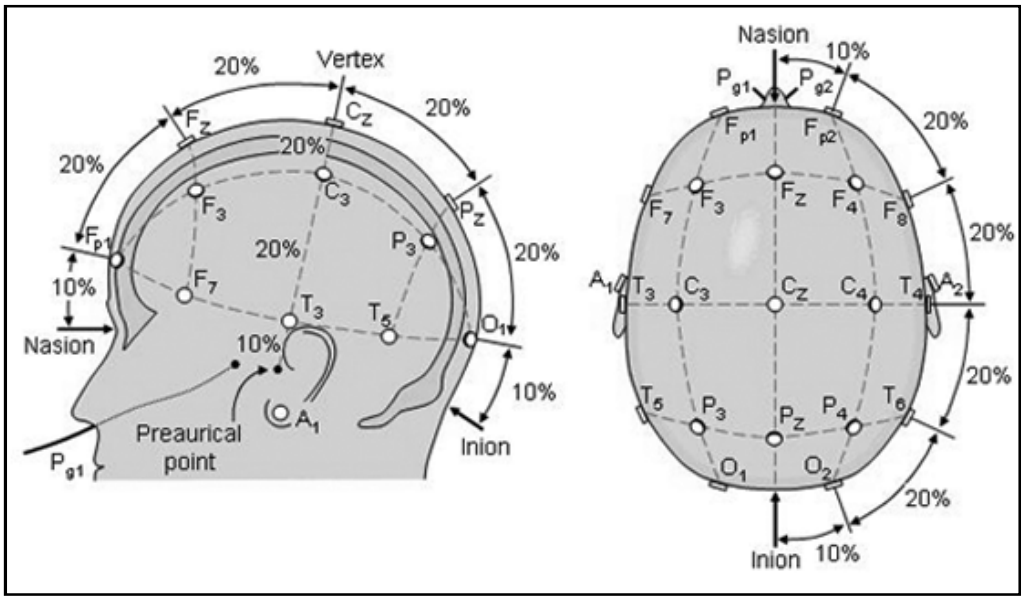


Figure 1.2. The international 10-20 EEG electrode placement system. A = Ear lobe, C = central, Pg = nasopharyngeal, P = parietal, F = frontal, Fp = frontal polar, O= occipital.

1.2. Visual Evoked Potentials and Familiar - Unfamiliar Face Stimuli

Visual evoked potentials (VEPs) are waves in the electroencephalogram which are generated by neural activity in the brain as response to visual stimuli. The VEP can provide important diagnostic information regarding to the functional integrity of the visual system.

Faces are extraordinarily rich sources of information. we determine the person’s age, sex and identify the face in view. Faces include semantic information and we identify person's intentions and emotional state. In addition, we can discover that a person is a relative or not, danger or a threat, etc. These components of face

processing suggest that face processing relies on a distributed neural system (Gazzaniga & Bizzi, 2000).

Functional brain imaging, electroencephalography or magneto encephalography studies indicates that face perception is mediated by a specialized system in the human brain. In fMRI works, processing of faces activates in the region of the superior temporal sulcus (fSTS) and in the occipital lobe in a region named the "occipital face area" (OFA) and bilateral region in the lateral fusiform gyrus, more consistently on the right for many subjects as shown in Figure 1.3 (Kanwisher & Moscovitch, 2000; Haxby et al., 2002; Watanabe et al., 2005). In this region activity by the perception of face is greater than the activity evoked by the perception of non-face objects. These results show that the presence of a neural module in fusiform gyrus. Kanwisher et al. (1997) named this region the "fusiform face area" or FFA.

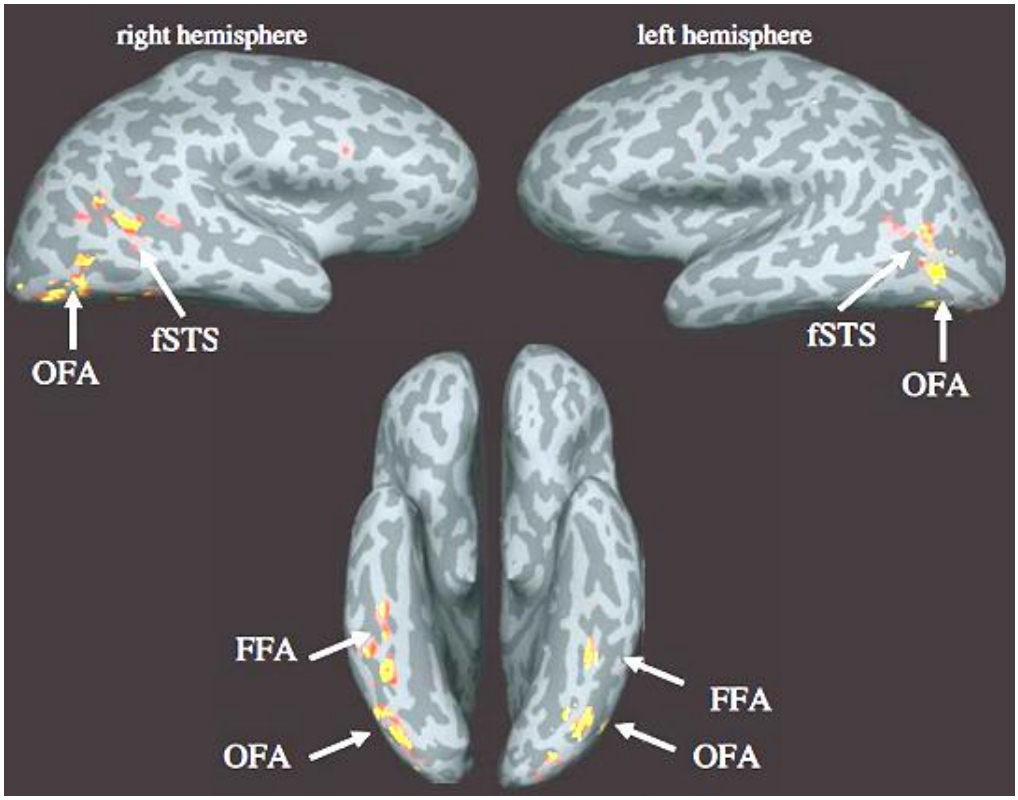


Figure 1.3. Three face-selective regions: the FFA in the fusiform gyrus along the ventral part of the brain, the OFA in the lateral occipital area and the fSTS in the posterior region of the superior temporal sulcus (Picture from Kanwisher et al., 1997).

Familiar and unfamiliar faces are discriminated by the human brain efficiently. But, the neural mechanisms of discrimination of familiar and unfamiliar faces are not fully understood in the brain. There are several difficulties in familiar and unfamiliar faces studies. Task, stimuli factors and volunteers are not standard for such studies. The other problem is that using famous faces for familiar faces in their studies. Famous face stimuli may trigger much semantic and affective information about the persons and difference between familiar and unfamiliar faces may be prevented by activations related to each of these processes (Rossion et al., 2001).

However, it is known that recognizing the identity of a familiar face involves a sequence of events. It begins with processing of the appearance of a familiar individual, followed by processing of semantic information about that person and retrieval of that person's name (Ellis & Rolls, 1992). Haxby et al. (2000) have proposed a neural system model that mediates face perception. The model emphasizes both recognition of unique identity and perception of information that facilitates social communication. The model has a hierarchical structure that distinguishes a core system for the visual analysis of faces and an extended system that processes the meaning of information obtained from faces (Haxby et al., 2002). The model of the distributed human neural system for face perception is shown in Figure 1.4

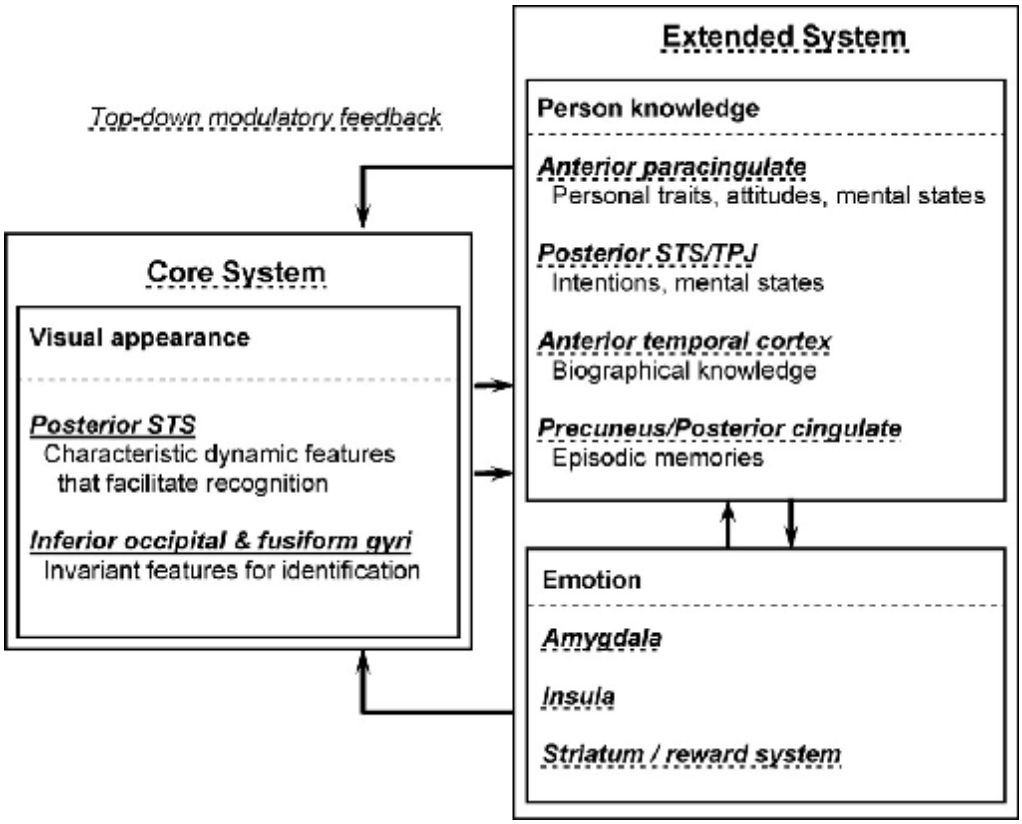


Figure 1.4. The model of the distributed human neural system for face perception (Picture taken from Gobbini & Haxby, 2007).

1.3. Brain Computer Interface

An EEG based brain computer interface (BCI) system extracts specific features online and automatically from EEG signals and uses these to operate computer controlled devices (Pfurtscheller et al., 2006). BCI systems provide communication between disables with severe neuromuscular handicaps and the environment. This communication is accomplished without the need of any muscular act.

A BCI system, as shown in Figure 1.5, is composed of these units: brain activity measurement (data acquisition), signal preprocessing, feature extraction, classification. Signal acquisition module digitizes and stores brain signals and passes them on without any further preprocessing to signal processing part. The signal processing module extracts features from the EEG pass these features to the

classification unit. The classification unit classifies these features and generates control signals that control an output device. The output device can be a robotic arm, a neuroprosthesis or a monitor. The subject learns from his/her experiences in using the device and enhances the features in EEG. This is a feedback which closes the loop of the BCI system.

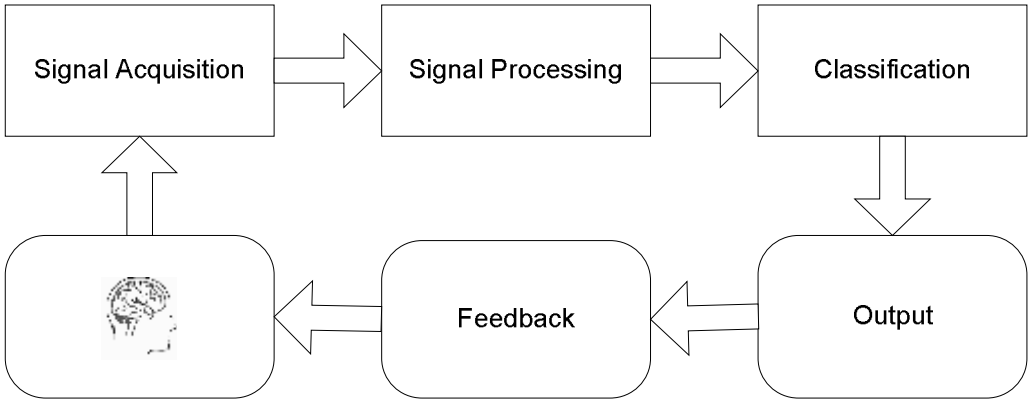


Figure 1.5. Architecture of a brain-computer interface

BCI systems differ from each other with type of electrophysiological signals they employ; VEPs, P300 evoked potentials, mu and beta rhythms, slow cortical potentials, and cortical neuronal action potentials (Wolpaw et al., 2002). The slow cortical potentials and cortical neuronal action potentials are measured invasively while the others are components of the EEG.

1.4. EEG Preprocessing, Feature Extraction and Classification

EEG signals have high dimensionality and contain temporal information. Most of EEG processing systems detect the presence of specific patterns in an ongoing brain activity. The signal processing of EEG is made up of signal enhancement, feature extraction, feature dimensionality reduction, feature classification. Here we have included classification in the signal processing. Various signal processing algorithms are used to detect these patterns and extract the useful information from the brain signal and several methods have been proposed in the literature for the each signal processing steps.

Indeed, EEG signals are known to be very noisy. These signals can be easily influenced by the electrical activity of the eyes or the muscles. The relevant information embedded in the EEG is enhanced by Surface Laplacian (SL) (McFarland et al., 1998; Babiloni et al., 2001) and Common Average Referencing (CAR) techniques (McFarland etal., 1998).

Features are some relevant properties of the signals. Feature extraction process extract features from signals. The performance of the classifier depends on how good a feature represents a class. Spatial filtering, voltage amplitude measurements, spectral analyses, time-frequency analysis and wavelet transform etc., are some techniques of numerous feature extraction methods which have been studied in the past.

In the classification step a class index is assigned to each feature. The classification is categorized into linear and nonlinear methods. Linear Discriminant Analysis (LDA) (Duda et al., 2001; Alpaydın, 2004) and Linear Support Vector Machines (SVM) (Burges, 1998; Gunn, 1998) are most common linear methods. Neural Networks (NN) (Bishop, 1996; Robert et al., 2002) and Bayesian classifiers (Tavakolian & Rezaei, 2004 are widly used nonlinear methods.

BCI features often have very high dimensionality. This necessitates to employ dimensionality reduction methods such as Principal Component Analysis (PCA) (Bashashati et al., 2005) or Independent Component Analysis (ICA) (Serby et al., 2005), () or Genetic Algorithms (GA) which is the most popularly employed (Garrett et al., 2003) and, Common Spatial Patterns (CSP) (Ramoser etal., 2000; Pfurtscheller & Neuper, 2001) These techniques reduce features size and generally lead to better performances.

2. PREVIOUS STUDIES

2.1. Face Perception and Processing

The facial processing has been studied since 70's and a well-known cognitive model of face recognition is proposed by Bruce and Young (1986). According to their model shown in Figure 2.1, pictorial information that provides about lighting, grain and possible imperfections in a photograph are derived and structural information that captures the aspects of the configuration of a face that distinguishes it from other faces respect to age and sex, identity-specific semantics, name, expression of face are obtained. Bruce and Young's model also include the face recognition units (FRU's) which select the pre-stored face model that best fits the currently perceptual representation.

Bruce and Young's model is often accepted as a first contemporary theoretical model. An additional model is proposed by Haxby et al. (2000), they argue in their paper about neural systems for face perception and recognition. In another paper Haxby et al. (2007) suggest that the analysis of a face requires strict cooperation between the core system and the extended system. Core system is responsible for other cognitive functions such as spatial attention, emotional processes, and auditory verbal comprehension. Extended system is responsible for holding biographical information about the face owner.

Numerous neuroimaging and event related potential experiments on face perception and familiar face recognition exist in the literature. Generally studies explore the face responsive region or face processing latency. One of the early studies about object recognition and the distinction between faces and non-face objects is held in Haxby, et al. (1991). The regional cerebral blood flow of the subjects was measured by $H_2{}^{15}O$ positron emission tomography while subjects performed face matching, dot-location matching, or sensorimotor control tasks. They investigated that the face-matching task activated the ventral occipitotemporal cortex while the dot-location task activated the superior parietal lobe. Haxby et al., report that the face-matching task activated the ventral occipitotemporal region bilaterally.

This activation magnitude was greater in the right hemisphere, particularly in the fusiform gyrus (Haxby et al., 1994).

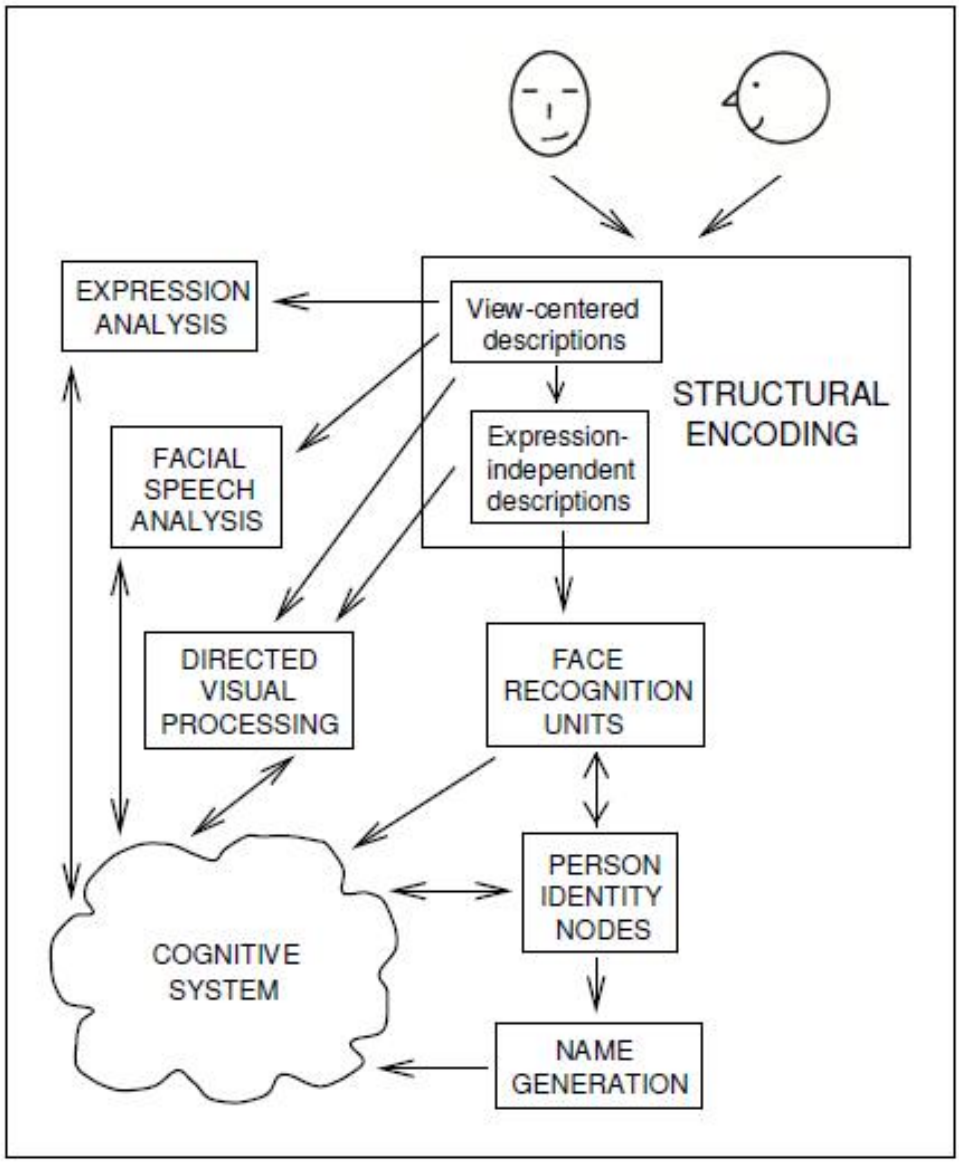


Figure 2.1. Functional architecture of face processing described by Bruce and Young (original picture at Bruce & Young, 1986)

Kanwisher et al (1997) compared faces to common objects and examine that any brain areas was significantly more active during face viewing than object viewing. They discovered an active area in the right fusiform and called this area as fusiform face area (Kanwisher et al., 1996; Kanwisher et al., 1997).

There are several electrophysiological studies in the literature (Jeffreys, 1996; Allison et al., 1999; Bentin & Deouell, 2000; James et al, 2001; Heisz et al., 2006; Tanskanen et al., 2007). Allison et al. (1999) established the existence of ERPs generated by faces; sinusoidal gratings; objects; and letter strings. The face stimuli produced N200, P290, P350, and N700 evoked potentials in the ventral occipitotemporal region. The responses to faces exist bilaterally in left and right hemisphere, especially higher in the right hemisphere.

A number of studies have also examined a negative evoked potential around 170 ms in response to faces. The N170 is thought to related to facial image processing and face detection and it is absent for non-face stimuli and scrambled faces (Bentin et al., 1996; Eimer, 2000a; Eimer, 2000b; Rossion, et al., 2000; Sagiv & Bentin, 2001). Similar responses were occurred for inverted faces but the latency was delayed (Rossion, et al., 1999; Itier & Taylor, 2004; Itier et al., 2006). N170 potential is assumed that it reflects early stages of information processing about the face (Rossion, et al., 1999; Bentin et al., 1999; Itier et al., 2006; Vuilleumier & Pourtois, 2007). However, N170 are independent of whether a face is familiar to the subject or not. It suggests that the N170 is not related to determination of face identity (Bentin & Deouell, 2000; Heisz et al., 2006).

In recent years, some researchers have argued about N170. A recent event-related potential (ERP) study by Thierry et al. (2007), claims that the larger occipitotemporal N170 response to pictures of faces than other categories occurs due to a methodological artifact in stimulus selection. They pointed out that the greater N170 potential occurs according to physical variance between pictures of objects rather than faces. Bruno Rossion and Corentin Jacques (2008) replied to this claim rapidly with their N170 review paper. They claimed that physical variance factor was ill-defined by Thierry et al. and could not account for previous observations;N170 amplitude as response to non-face image is smaller than N170 amplitude as response to face image without latency increase and component “smearing”. Also they provided experiment on a number of methodological and theoretical issues and they found that the largest amplitude of N170 is related to faces.

Face processing and perception have been well documented in the neurophysiological literature as mentioned above in area of fMRI, PET and ERPs. However, familiar and unfamiliar face processing studies are relatively few.

Studies on face recognition can be classified into several specific manners. Especially researchers explore to find cortical sources or temporal components to investigate the factors affecting face recognition. A brief review of literature about familiar face recognition is depicted in Table 2.1.

Numerous experiments on familiar face recognition exist on the findings in the face-responsive regions of cortex. However, the results are inconsistent. The disagreement of these studies could be due to the different types of familiar faces that were used in the experiments. In the experiments, newly learned faces, famous people through the media and faces associated with personal acquaintances have been used. In contrast to the inconsistency, in the extrastriate cortex, anterior temporal regions and medial temporal regions show stronger responses to a variety of familiar stimuli (Haxby et al., 2002; Gobbini & Haxby, 2007; Johnston & Edmonds, 2009).

In the brain studies, temporal latency of familiar and unfamiliar face processing is investigated in the 300–600 ms interval for brain electrical responses According to the Bruce and Young (1986) model for face processing, first face structure is encoded, then the face is further analyzed for the expression and recognition . The N170 component corresponds to the structural encoding stage and later component may be related to familiarity.

Generally some factors in experiments affect the recognition of familiar and unfamiliar faces. Face viewpoint is a well researched affecting factor (Troje & Kersten, 1999; Eger et al., 2005). Miyakoshi et al. (2008) suggests that familiar faces are recognized in a relatively viewpoint-independent manner. They conclude that familiar faces are first recognized viewpoint-dependently and then represented viewpoint-independently. An another factor may be face internal and external feature. The internal features are eyes, nose, and mouth area and external features are shape of the face, hair and etc. It is suggested that internal features are more important for the recognition of familiar faces than the external features (Ellis et al.,

1979; Young et al., 1985). Inversion is another affecting factor for face recognition (Eimer, 2000a; Anaki et al., 2007). Anaki et al (2007) suggest that N170 amplitude to inverted faces was higher than to upright faces and was not influenced by face familiarity. In contrast, induced gamma activity was higher for upright than for inverted faces and for familiar than unfamiliar faces.

Table 2.1. Brief Literature Review of the familiar - unfamiliar face

Aim	Subjects	Images	Department	References
Memorize	8 women, 4 men	40 Familiar, 80 new faces	Psychology	(Paller et al., 2000)
Memory and cognition	17 females, 9 males	An unknown face, own grandmother, light stimulation	Biophysics,Psychology	(Özgören et al, 2005)
Explorations the nature of neural mechanisms	11 females, 13 male	360 faces, half of them famous	Psychology,Center for Neural Computation	(Anaki et al., 2007)
Examine the effects of repetition priming, event-related potential (ERP) correlate of a visual memory	22 males	120 famous faces, 120 non-famous faces	Psychiatry,	(Begleiter et al., 1995)
Memories related to social–emotional significance	4 females, 6 males	15 different familiar faces and 75 different unfamiliar faces,and every face was presented twice	Cognitive Neuroscience	(Bobes et al., 2007)
Face-identification processes on the formation of structural representation of faces	60 undergrad. students	30 butterflies of different kinds, 60 unfamiliar people, 60 famous, 30 famous politicians	Psychology	(Bentin & Deouell, 2000)
Examine N170 ERP	5 women, 6 men	An unknown face, a famous face (the French president), and the own subject's own face	Faculté des Sciences	(Caharel et al., 2002)
Face perception	11 male	40 printed photographs, 20 videotape for train,	Laboratory of Neurophysiology	(Dubois, et al., 1999)
Cortical sources responsible for face recognition and comparison	13 females, 6 males	11 persons familiar	Brain Research and Rehabilitation Center Neuron	(Mnatsakanian & Tarkka, 2005)
Repetition priming in the recognition	10 women, 8 men	90 famous people, 90 unfamiliar people	Psychology,	(Schweinberger et al., 2002)
ERP study investigated how different processing stages	13 female, 11 males	50 images of familiar faces, 50 images of unfamiliar faces and 32 images of houses	Psychology,	(Eimer, 2000b)
Repetition effects in the recognition of famous faces	8 women, 4 men	90 famous people,90 unfamiliar faces	Psychology,	(Schweinberger et al., 2002)
Analyzing the modulation of two types of event-related potentials	6 females, 5 males	80 pictures of famous and 80 pictures of non-famous persons were presented on a black background	Epileptology,Psychology,	(Dietl, et al., 2005)

Table 2.1. Continued

Aim	Subjects	Images	Depart.	Paper Title
Patients with schizophrenia are deficient relative to controls in the processing of faces	Schizophrenia patients (8men and 10women)	The subject's own face, a face personally known and two totally unknown faces	Faculté des Sciences	(Caharel, et al., 2007)
Recognized in a relatively viewpoint independent	10 women, 6 male	One's own face, SELF; famous person's face, FAMOUS; and unfamiliar other's face, UNFAMILIAR	Psychology,	(Miyakoshi et al., 2008)
Interhemispheric cooperation	19 females, 11 males	60 men and 30 women Faces of well-known politicians, actors, singers and sport stars 90 faces unfamiliar	Psychology, Cognition and Brain Sciences	(Mohr et al., 2002)
Familiarity and recollection processes	14 female,10 males	360 faces and 240 occupations	Psychology,	(Curran & Hancock, 2007)
Repetition processes which are specific to each material	6 Females, 6 males	100 famous faces ,100 scrambled faces, 100 drawings of everyday objects and 100 scrambled drawings	Neurosciences cognitive	(Guillaume, et al., 2009)
Cortical activity during face recognition	10 male	50 stimuli. Familiar faces were randomly presented at 10% probability	Electronic Engineering	(Xu et al., 2005)
Face specific erp	Some Subjects	53 unfamiliar, one familiar(53 times display),	Biomedical Engineering	(DeMarco & Micheli-Tzanakou, 2009)
Perceptual and structural encoding stages of face processing	6 females, 3 males,	360 black-and-white photographs of familiar and unfamiliar faces that were digitally scanned	Psychology,	(Marzi & Viggiano, 2007)
Face perception, recognition and priming	10 men, 8 women	32 famous men and 32 famous women; theUnfamiliar faces were of 32 men and 32 women previously unseen byParticipants	Neuroscience , Neurology,	(Henson et al., 2003)
Dynamics of the neuronal activity	18 patients who had drug-refractory epilepsy		Recherche Cerveau et Cognition	(Barbeau et al., 2008)
Emotional processing and memory processes	26 female subjects	30 trials of each person shown randomly intermixed	Brain Dynamics, Biophysics,	(Basar et al., 2008)

2.2. Feature Extraction Methods

Numerous feature extraction techniques have been proposed and examined for EEG based studies (Pfurtscheller & Neuper, 2001; McFarland et al., 2006; Bashashati et al., 2007; Lotte et al., 2007). In these studies, features extraction methods are related to the temporal or frequential information or both embedded in the signals. Temporal methods are used as features of the temporal variations of the signals. Temporal feature extraction methods are simplification of the time course of the EEG signals (Kaper et al., 2004), auto-regressive modeling (Pfurtscheller et al., 1998), filtering (Sykacek et al., 2004; Serby et al., 2005). Frequential feature extraction methods are used to find specific oscillations known as rhythms. Well known methods are band power features (Pfurtscheller G. , et al., 1999; Boostani et al., 2007) and power spectral density features (Babiloni, et al., 2001; Blanchard & Blankertz, 2004; McFarland et al., 2006; Bashashati et al., 2007). Hybrid method of feature extraction is known time-frequency representations. They extract both frequential and temporal information from the signals. The time-frequency representations can catch relatively sudden temporal variations of the signals, while still keeping frequential information (Lotte F. , 2008). Short-time Fourier transform and wavelet transform are this kind of feature extraction methods (Unser & Aldroubi, 1996; Bostanov, 2004; Bashashati et al., 2005; Merzagora et al., 2006; Subasi, 2007).

Wavelet and time-frequency analysis have been used successfully in analyzing EEGs and ERPs. However, they have not been applied to human brain face recognition researches(DeMarco & Micheli-Tzanakou, 2009). DeMarco and Micheli-Tzanakou (2009) investigated continuous wavelet transform for familiar versus unfamiliar face distinction. Wavelet and wavelet packet decomposition methods have not been used for classification familiar unknown faces.

2.3. P300 Speller

P300 is an event-related potential (ERP), described as a positive peak in an EEG recording at approximately 300 ms from an event. It follows unexpected, rare, or particularly informative stimuli. The shape of the P300 depends on the characteristics of the stimuli and their presentation. The P300 component of the ERP was discovered by Sutton et al. (1965) and the first P300-based BCI was proposed by Farwell and Donchin (1988). P300 speller is a BCI model aimed to aid user spell a word. In this model 36 characters are displayed in a 6x6 matrix. According to this paradigm, each row and column of the matrix is intensified in a random sequence and the intersection of the row and column of target letter represents the address of the letter (Farwell & Donchin, 1988). A user communicates with the external world by the help of this matrix. The P300 speller is similar to oddball paradigm which is the rare presentation of the target stimuli in the random sequence of stimuli.

The P300 Speller procedure consists of three steps; experimental design, signal processing / feature selection-extraction, and classification and determination of characters. Numerous of studies have been focused on each step.

A variety of studies on experimental design have been proposed to improve the transfer rates and accuracy. Inter-stimulus interval, matrix size, character size, matrix color and matrix content for different applications were explored by researchers (Sellers et al., 2006; Mugler, et al., 2008; Salvaris & Sepulveda, 2009; Takano et al., 2009; Nam, Li, & Johnson, 2010).

Wavelets (Bostanov, 2004; Salvaris & Sepulveda, 2009), spatial filters (Hoffmann et al., 2006; Rivet et al., 2008), common spatio-temporal patterns (Krusienski et al., 2007), perceptual characteristic (Lin & Zhang, 2005), independent component analysis (Serby et al., 2005), principal component analysis (Mirghasemi et al., 2006), amplitude quantization (Krusienski et al., 2009), genetic algorithm (GA) (Dal Seno et al., 2010), have been implemented as feature extraction and signal processing-preprocessing methods Several classifier have been implemented for classifying P300 components: linear discriminant (FLD) (Lenhardt et al., 2008), stepwise linear discriminant analysis (SWLDA) (Krusienski et al., 2008), support

vector machine (SVM) (Kaper et al., 2004; Li et al., 2008), matched filtering (Serby et al., 2005), learning vector quantization (LVQ) (Liang & Bougrain, 2008). Krusienski et al (2006) compared various classification techniques regarding P300. They suggest that SWLDA and FLD provide the best overall performance and implementation characteristics for practical classification of P300 speller data.

P300 speller studies aims to help completely or nearly locked-in individuals to spell a text on a computer. Amyotrophic Lateral Sclerosis (ALS) (Rowland & Shneider, 2001) is one of the most common causes of the locked-in syndrome and they may benefit from such BCI and they could use a P300-based matrix speller to spell spontaneous words (Sellers & Donchin, 2006; Sellers, Kubler, & Donchin, 2006; Nijboer, et al., 2008). Researchers have indicated that P300 speller may benefit better than other systems by allowing the user to answer yes/no questions. It provides to communicate at an acceptable rate of speed with high accuracy (Sellers E. , 2004).

3. DATA and METHODS

3.1. Face Recognition Experiment

3.1.1. Participants

Twenty nine healthy volunteers, 6 females and 23 males, aged from 20 to 33 years, with an average of 24.2 years and standard deviation of 3.52, participated in this study. The EEG of three volunteers was removed because of corrupted records. Therefore, twenty six subjects were used in the analysis. Volunteers' information is given in Appendix III.

All participants had normal or corrected-to-normal vision (3 of them uses glasses), and no history of neurological or psychiatric disorders. Two of them were left-handed and others were right-handed. They were non-medicated, and did not receive any payment for their participation. The experiment was carried in neurology department of Başkent University, Adana Hospital and Research Center. All participants signed a written informed consent form and the experiment was approved by local ethics committee of the hospital (see appendix IV and V).

3.1.2. Stimuli

The stimuli consisted of 172 digitized photographs of faces, half of them famous, which were selected from various public-accessed websites. All photos were software-edited by using Adobe Photoshop®. Editing these pictures includes removing background and homogenizing with respect to luminance, contrast and color range. All faces were consisted of frontal views and almost neutral facial expression. The color depth of the images was 24 bits and rescaled proportionally to a size of 425pixel×600pixel and resolution was 200 pixel/cm (5.4×7.6 cm).

Famous faces (as familiar) were selected from well known personalities in the entertainment, movie and TV world, politics and the sports world. Unfamiliar faces were also obtained from various sources including members of abroad universities

and firm websites, model agencies and magazine websites. The unfamiliar faces were matched the famous faces in terms of general visual appearance and attractiveness during they were selected. Stimuli samples one from familiar and one from unfamiliar image are shown in Figure 3.1. The images used during the experiment are shown in Figure 3.2. All famous stimuli and their names are given in Appendix I. All unfamiliar stimuli are also given in Appendix II.



a b

Figure 3.1. Two examples of face stimuli. a) Familiar (TV actor) b) Unfamiliar



Figure 3.2. Experimental setup

3.1.3. Procedure and EEG recording

Participants sat on a comfortable chair in front of an LCD monitor at a distance of about 1 m in a sound-attenuated, dimly lighted room as shown in Figure 3.2. After electrode placement, they were fully informed about the purpose of the study. The subjects pressed a button which generates a pulse if they are familiar to the images. The pulses were recorded along EEG synchronously to identify the familiar faces for the subjects. The participants were instructed to look at images carefully, minimize blinking and movements at each stimulus and were asked to respond as quickly and accurately as possible.

The experimental procedure is as follows. At first black-white check board was presented for 2 s, a white fixation cross for concentration was followed for 30 s. After that, "experiment start" warning was shown on screen. The image was shown for 800 ms and then a gray screen appeared for 1200 msec. Next, a question mark was followed and was present for 3000 ms for participant to decide that if the shown face image is familiar or unfamiliar. Participant pressed the button during this interval if the stimulus was familiar. Then a black fixation cross presented for 2500 ms for resting and then next trial was followed. One trial lasted 7.5 seconds and the experiment lasted about 22 minutes. The time course for each trial is shown in Figure 3.3.

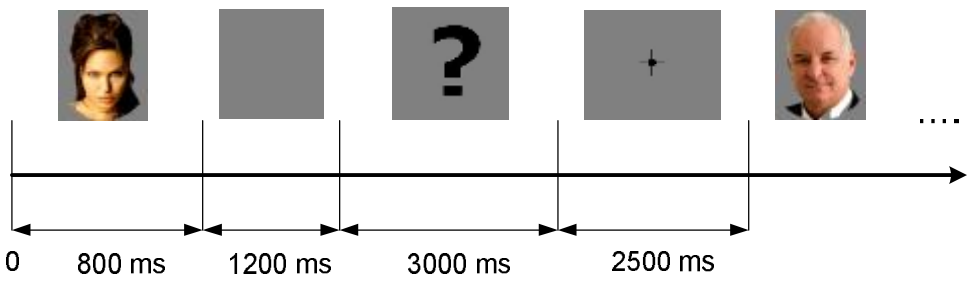


Figure 3.3. Time course of the experiment

The EEG was recorded using 10-20 standard system referenced to mastoids with a forehead ground. The type of the electrodes was Ag/AgCl. EEG recording device was Nihon Kohden EEG1100 NeuroFax®.

The EEG signals were filtered with an analog band pass filter with bandwidth of 0.53-70 Hz. The sampling rate was 200 Hz and, a notch filter was used to remove 50 Hz power line interference while the EEG signals was being recorded. The recorded EEG data was exported to ASCII for further analysis in PC. All analysis and signal processing methods was implemented offline.

3.2. Wadsworth BCI Dataset (P300 Evoked Potentials)

This dataset is one of the dataset of BCI Competition III held in 2004. As it is described by Krusienski and Schalk (2004), the experiment paradigm and data collection are given as follows.



Figure 3.4. The user display of P300 Speller paradigm. (Image is from Krusienski & Schalk, 2004).

A 6 by 6 matrix of characters as shown in Figure 3.4 was displayed to the user. The user's task was to focus on character of a word (one character at a time) that was specified previously. All rows and columns of this matrix were randomly intensified at a rate of 5.7 Hz. One particular row and one particular column of 12 intensifications of rows or columns contained the desired character (2 out of 12 stimuli). The responses evoked by these infrequent stimuli that contain the desired

character are different from those evoked by the stimuli that did not contain the desired character.

P300 speller data was collected from two subjects. Then the data was 0.1-60Hz bandpass filtered and sampled at 240Hz rate. Each session consisted of a number of runs. In every run, the subject focused on a series of characters. For each character epoch in the run, user display was as follows: the matrix was displayed for a 2.5 s period, and during this time each character had the same intensity and the matrix was blank. Subsequently, each row and column in the matrix was randomly intensified for 100ms. 12 different stimuli – 6 rows and 6 columns – were occurred. After intensification of a row/column, the matrix was blank for 75ms. Row/column intensifications were block randomized in blocks of 12. The sets of 12 intensifications were repeated 15 times for each character epoch. Thus, any specific row/column was intensified 15 times and total intensifications for each character epoch became 180. Each character epoch was followed by a 2.5 s period, and during this time the matrix was blank. This period informed the user that this character was completed and he should focus on the next character in the word that was displayed on the top of the screen (Krusienski & Schalk, 2004).

3.3. Common Spatial Pattern (CSP)

The Common Spatial Pattern (CSP) algorithm is a technique to analyze multi-channel data and highly successful in calculating spatial filters for detecting two classes. Aim of the CSP is to construct spatial filters which maximize the variance of the spatially filtered EEG signal from one class while minimizing the variance of EEG signal from the other class. These spatial patterns provide a weighting to the electrodes. The method based on the simultaneous diagonalization of two covariance matrices of the classes (Ramoser et al., 2000; Blankertz et al., 2008).

Consider that E is EEG data matrix with size of NxT, where N stands for number of channels and T denotes the number of samples per channel.

The normalized spatial covariance is

$$C = \frac{EE'}{trace(EE')} \tag{3.1}$$

with E^T is the transpose of E and trace computes the sum of diagonal elements of E. Eigen-value decomposition of the composite spatial covariance;

$$\mathrm{Z} = \overline{C_1} + \overline{C_2} \tag{3.2}$$

is computed:

$$\mathrm{Z} = U_c \, l_c \, U_c' \tag{3.3}$$

Here, U_c is the matrix of eigenvectors and l_c is the diagonal matrix of Eigen-values.

The columns of the matrices of the two classes are pooled to form two origin-centered point clouds. It is always possible to find a linear transformation that renders a point cloud isotropic. This transformation composes a change of coordinate defined by the point cloud's principal axes and called the whitening transformation. It equalizes the variances in the space spanned by U_c (Müller-Gerking et al., 1999).

The whitening transformation is extracted from the Eigen-value decomposition;

$$P = l_c^{-1/2} U_c' \tag{3.4}$$

The transformed covariance matrices S_1 and S_2 are respectively;

$$S_1 = P\overline{C_1}P' \qquad S_2 = P\overline{C_2}P' \tag{3.5}$$

S_1 and S_2 share common eigenvectors B. The sum of the corresponding Eigen-values will always add up to the identity matrix. The eigenvector with largest Eigen-value for S_1 has the smallest eigenvalue for S_2 and vice versa.

The projection matrix is defined as

$$W = (B'P)' \tag{3.6}$$

The original EEG is transformed into uncorrelated components with the projection matrix;

$$\mathrm{D} = WE \tag{3.7}$$

The columns of W^{-1} are the common spatial patterns and can be seen as time-invariant EEG source distribution vectors.

The original data E is simply

$$E = W^{-1}D \tag{3.8}$$

In order to obtain discriminative channels the spatial patterns are arranged in the descending order of the variances from left to right; the Eigen-values of the spatial patterns matrix are arranged from the highest to the lowest. The Eigen-vector associated with the highest Eigen-value explains that the majority of the variance in the combined data and the weight values for each channel can be found out from the spatial patterns matrix.

3.4. Wavelet Analysis

EEG recordings from multiple electrode arrays vary in their frequency content over their time courses and across recording sites on the scalp. Accordingly, EEG and ERP data sets are non-stationary in both time and space (Samar et al., 1999). Wavelets provide us information about how frequency changes over time and particularly it provide us the value of magnitude change and when the this change occur in the frequency (Mallat, 1989; DeMarco & Micheli-Tzanakou, 2009).

Wavelet analysis refers to a class of signal processing techniques and wavelet transform (WT) is designed to address the problem of non-stationary signals. WT uses wavelets which are actually a family of functions derived from a single

generating function called the mother wavelet by translation and dilation operations. Dilation, also known as scaling, compresses or stretches the mother wavelet and translation shifts the mother wavelet along the time axis.

WT provides good frequency resolution in low and good time resolution in high frequencies. Let *x(t)* be a signal continuous wavelet transform is defined as

$$X_{CWT}(a,b) = \int_{-\infty}^{\infty} x(t) y^{*}_{a,b}(t) dt \tag{3.9}$$

Here the, $y^{*}_{a,b}(t)$ term is derived from the mother wavelet $y(t)$ by scaling and shifting

$$y^{*}_{a,b}(t) = \frac{1}{\sqrt{a}} y\left(\frac{t-b}{a}\right) \qquad a \in \Re^{+},\ b \in \Re \tag{3.10}$$

where a is the scale and b is the time shift.

However, calculating wavelet coefficients for every possible scale need a considerable effort and result in a vast amount of data. A more efficient and computationally simpler wavelet analysis, known as the Discrete Wavelet Transform (DWT), was introduced by Mallat (1989).

In DWT, time remains continuous but time-scale parameters are sampled by choosing $a = 2^{i}$ and $b = k2^{i}$, where $i, k \in Z$, so the wavelets then become

$$y_{i,k}(t) = 2^{-i/2} y\left(2^{-i}t - k\right) \tag{3.11}$$

It then follows that the values $c_{i,k}$ are the analysis coefficients for these functions;

$$c_{i,k} = \int_{-\infty}^{\infty} x(t) y^{*}_{i,k}(t) dt \tag{3.12}$$

The recovery of the signal through the synthesis formula is called the Inverse Discrete Wavelet Transform:

$$x(t) = \sum_{i \in Z} \sum_{k \in Z} c_{i,k} y_{i,k}(t) \tag{3.13}$$

The wavelet function $y(t)$ is assembled by a scale function $f(t)$, which is a solution of a two-scale difference equation:

$$y(t) = \sqrt{2} \sum_{k} g_k f(2t - k) \tag{3.14}$$

The sequence $\{g_k\}$ has high-pass characteristics. filter Similarly, the scaling function is generated from itself by dilation equation

$$f(t) = \sqrt{2} \sum_{k} h_k f(2t - k) \tag{3.15}$$

where $\{h_k\}$ has low-pass characteristics.

3.5. Multiresolution Analysis

A signal can be decomposed into its approximation and detail by using scaling and wavelet functions:

$$x(t) = a(t) + d(t) \tag{3.16}$$

where $a(t)$ is approximation signal:

$$a(t) = \sum_{k} a_k 2^{J/2} f\left(2^J t - k\right) \tag{3.17}$$

and $d(t)$ is detail part:

$$d(t) = \sum_{k} d_k 2^{J/2} y\left(2^J t - k\right) \tag{3.18}$$

The coefficients a_k and d_k are approximation and detail coefficients respectively. Here, 2^J represents resolution and J is the resolution index. As the resolution increases; J increases, the signal is better approximated by the approximation signal. The approximation signal can also be decomposed with lower resolution index; $J-1$, which is also called as decomposition level 1. The decomposition is again applied to the approximation signal at resolution index, $J-1$, to obtain approximation signal at resolution index; $J-2$ (level 2). This can be repeated until a certain level. Mathematically (Strang & Nguyen, 1996) :

$$x(t)=\sum_k a_{J-L,k}\,2^{(J-L)/2} f\left(2^{J-L}t-k\right) + \sum_{\mathbf{l}=0}^{L}\sum_k d_{J-\mathbf{l},k}\,2^{(J-L)/2} y\left(2^{J-\mathbf{l}}t-k\right) \tag{3.19}$$

where $a_{J-l,k}$ is approximation coefficients at level L(resolution 2^{J-L}) and translation $2^{L-J}k$ and $d_{J-l,k}$ is detail coefficients at level $\mathbf{l}$ (resolution $2^{J-\mathbf{l}}$) and translation $2^{\mathbf{l}-J}k$. The relation between the coefficients of lower and upper levels can be easily established by using dilation and two-scale equations. This leads to fast wavelet transform; discrete wavelet transform.

A signal at resolution index J can be represented by a sum of approximation and detail components of resolution index $J-1$. Therefore,

$$\sum_k a_{J,k}\,2^{J/2} f\left(2^J t-k\right)=\sum_k a_{J-1,k}\,2^{(J-1)/2} f\left(2^{J-1}t-k\right) + \sum_k d_{J-1,k}\,2^{(J-1)/2} y\left(2^{J-1}t-k\right) \tag{3.20}$$

Using dilation and two-scale equations we can write

$$f\left(2^{J-1}t-k\right)=\sum_m h_m\sqrt{2} f\left(2^J t-2k-m\right) \tag{3.21}$$

$$y\left(2^{J-1}t-k\right)=\sum_m g_m\sqrt{2}f\left(2^J t-2k-m\right) \tag{3.22}$$

And we replace these equations to the above equation

$$\begin{aligned}\sum_k a_{J,k}2^{J/2}f\left(2^J t-k\right)&=\sum_k a_{J-1,k}2^{(J-1)/2}\sum_m h_m\sqrt{2}f\left(2^J t-2k-m\right)\\&\quad+\sum_k d_{J-1,k}2^{(J-1)/2}\sum_m h_m\sqrt{2}f\left(2^J t-2k-m\right)\\&=\sum_m h_m a_{J-1,k}\sum_k 2^{J/2}f\left(2^J t-2k-m\right)\\&\quad+\sum_m g_m d_{J-1,k}\sum_k 2^{J/2}f\left(2^J t-2k-m\right)\end{aligned} \tag{3.23}$$

by change of variable: $2k+m=n$, we obtain

$$\sum_k a_{J,k}2^{J/2}f\left(2^J t-k\right)=\sum_n 2^{J/2}f\left(2^J t-n\right)\left[\begin{matrix}\sum_k a_{J-1,k}h_{n-2k}\\+\sum_k d_{J-1,k}g_{n-2k}\end{matrix}\right] \tag{3.24}$$

It yields

$$\begin{aligned}a_{J,n}&=\sum_k a_{J-1,k}h_{n-2k}+\sum_k d_{J-1,k}g_{n-2k}\\&=\left[a_{J-1,n}\right]_{\uparrow 2}*h_n+\left[d_{J-1,n}\right]_{\uparrow 2}*g_n\end{aligned} \tag{3.25}$$

Where $[\ ]_{\uparrow M}$ stands for up sampling by a factor M and $*$ stands for convolution sum.

This result shows that upper level approximation coefficients are synthesized from lower level approximation and detail coefficients.

In order to extract approximation and detail coefficients bi-orthogonal complement of the scaling and wavelet functions are need which have the following dilation and two-scale identities:

$$\phi(t) = \sqrt{2}\sum_k h_k \phi(2t-k) \tag{3.26}$$

$$\psi(t) = \sqrt{2}\sum_k g_k \phi(2t-k) \tag{3.27}$$

The approximation and scaling coefficients of resolution index J are extracted by the following inner products:

$$a_{J,k} = \int_{-\infty}^{\infty} x(t) 2^{J/2} \phi(2^J t-k) dt \tag{3.28}$$

$$d_{J,k} = \int_{-\infty}^{\infty} x(t) 2^{J/2} \psi(2^J t-k) dt \tag{3.29}$$

At resolution index $J-1$ the coefficients are then computed by the following integrals:

$$a_{J-1,k} = \int_{-\infty}^{\infty} x(t) 2^{(J-1)/2} \phi(2^{J-1} t-k) dt \tag{3.30}$$

$$d_{J-1,k} = \int_{-\infty}^{\infty} x(t) 2^{(J-1)/2} \psi(2^{J-1} t-k) dt \tag{3.31}$$

We replace the dilation and two-scale equations of bi-orthogonal scaling and wavelet functions:

$$a_{J-1,k} = \int_{-\infty}^{\infty} x(t) 2^{(J-1)/2} \sqrt{2}\sum_m h_m \phi(2t-2k-m) dt \tag{3.32}$$

$$d_{J-1,k} = \int_{-\infty}^{\infty} x(t) 2^{(J-1)/2} \sqrt{2}\sum_m g_m \phi(2t-2k-m) dt \tag{3.33}$$

Continuing by change of variable $2k+m=n$,

$$a_{J-1,k} = \sum_n \bar{h}_{n-2k} \int_{-\infty}^{\infty} x(t) 2^{J/2} \bar{f}(2t-n)dt = \sum_n \bar{h}_{n-2k} a_{J,n} \tag{3.34}$$

$$d_{J-1,k} = \sum_n \bar{g}_{n-2k} \int_{-\infty}^{\infty} x(t) 2^{J/2} \bar{f}(2t-n)dt = \sum_n \bar{g}_{n-2k} d_{J,n} \tag{3.35}$$

we obtain

$$a_{J-1,k} = \left[a_{J,k} * \bar{h}_k \right]_{\downarrow 2} \tag{3.36}$$

$$d_{J-1,k} = \left[d_{J,k} * \bar{g}_k \right]_{\downarrow 2} \tag{3.37}$$

where $[\ ]_{\downarrow M}$ stands for down sampling by a factor M.

These outcomes provide us fast wavelet transform or discrete-wavelet transform. At highest resolution the approximation coefficients are nearly equal to the signal samples and the signals samples can be used as approximation coefficients of the highest resolution. Actually, these equations are synthesis and analysis equations of a two-band filter bank system. From the examination of a two band filter bank system, we obtain

$$\begin{aligned} \bar{G}(z) &= -zH(-z) \\ G(z) &= -z^{-1}\bar{H}(-z) \end{aligned} \tag{3.38}$$

$$\bar{H}(z)H(z) + \bar{H}(-z)H(-z) = 2 \tag{3.39}$$

in z-domain. The time domain of equivalent of these equations

$$\begin{aligned} \bar{g}_n &= (-1)^n h_{n+1} \\ g_n &= (-1)^n \bar{h}_{n-1} \end{aligned} \tag{3.40}$$

$$\sum_{\mathbf{l}=-\infty}^{\infty} \bar{h}_{\mathbf{l}} h_{2n-\mathbf{l}} = d_n \tag{3.41}$$

Where in these equations $h_n = h(n)$. The procedure of the decomposition of discrete wavelet transform schematically shown in Figure 3.5.

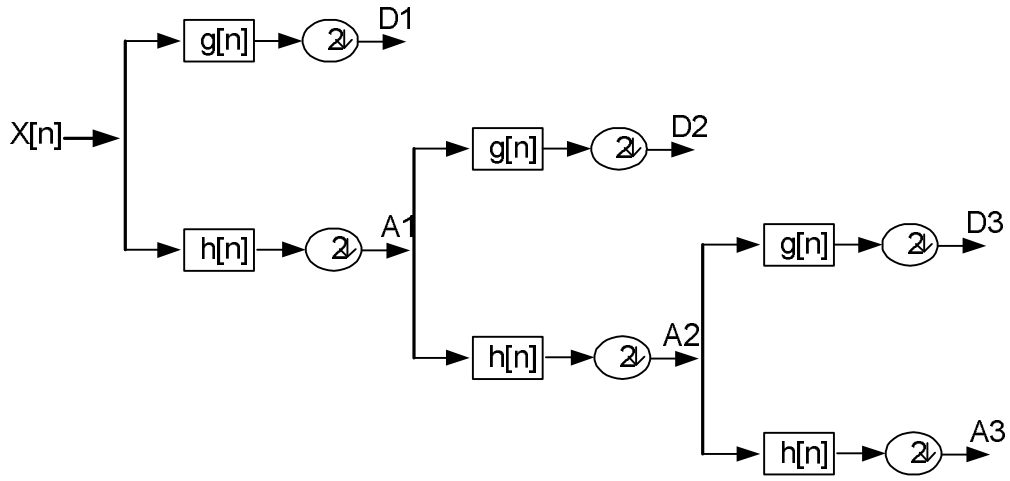


Figure 3.5. Decomposition of discrete wavelet transform

The generalized version of wavelets transform is wavelet packets. A wavelet packet is a family of signals derived from a single mother wavelet. Figure 3.6 represents symbolic division of the time-frequency plane, corresponding to ranges of time and frequency parameters. Wavelet packet decomposition is generated by a filtering scheme similar to DWT. The difference between the two is that wavelet packet decomposition permits the detail functions to be further split into two or more subbands. This procedure is shown in Figure 3.7 (Samar et al., 1999).

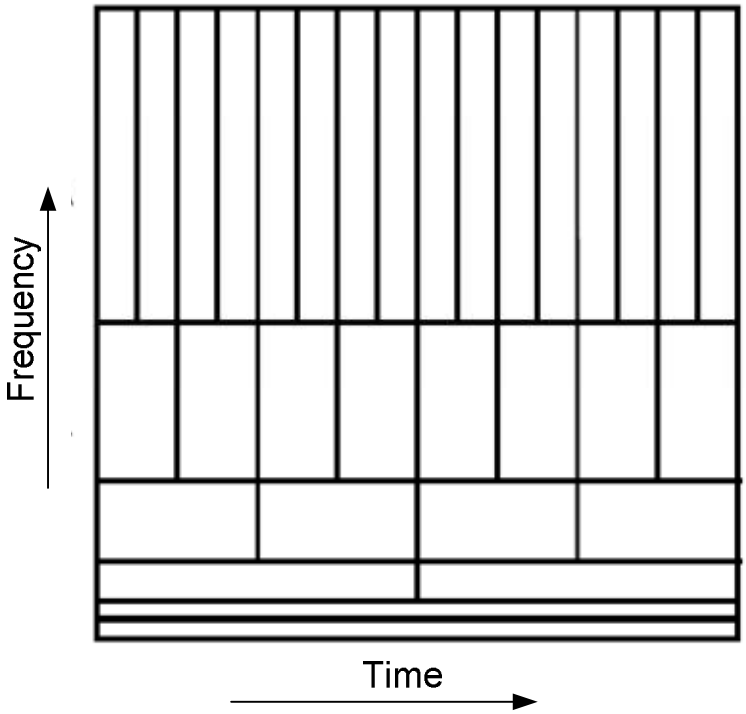


Figure 3.6. Symbolic division of time-frequency space for multiresolution wavelet decomposition

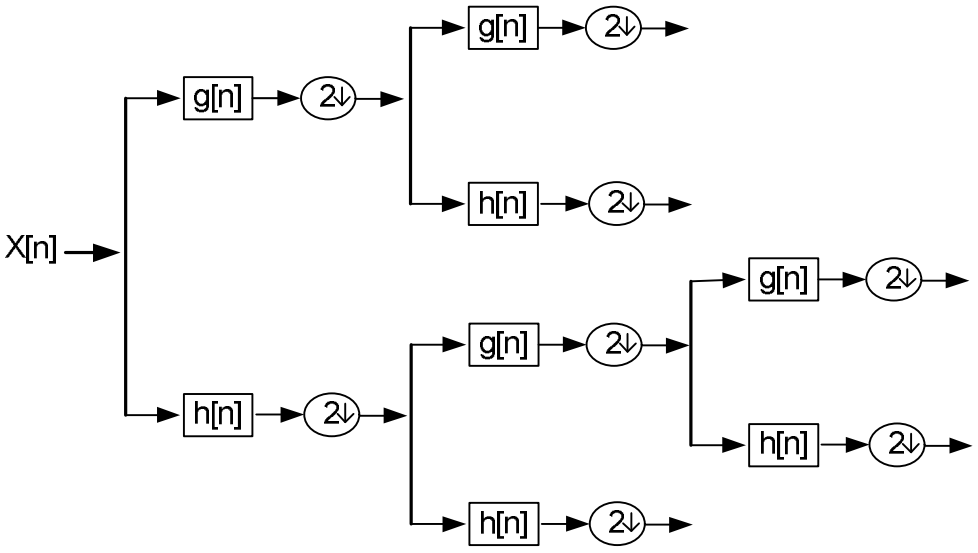


Figure 3.7. Wavelet packet tree

3.6. Multiresolution Analysis Based on Excitatory PostSynaptic Potential Approximation Model

3.6.1. Neural Activities

EEG signals are electrical potential generated by the nerve cell in the cerebral cortex. These signals represents from a large number of neurons. A nerve cell consists of axons, dendrites, and cell bodies shown in Figure 3.8 and nerve cells respond to stimuli and transmit information over long distances.

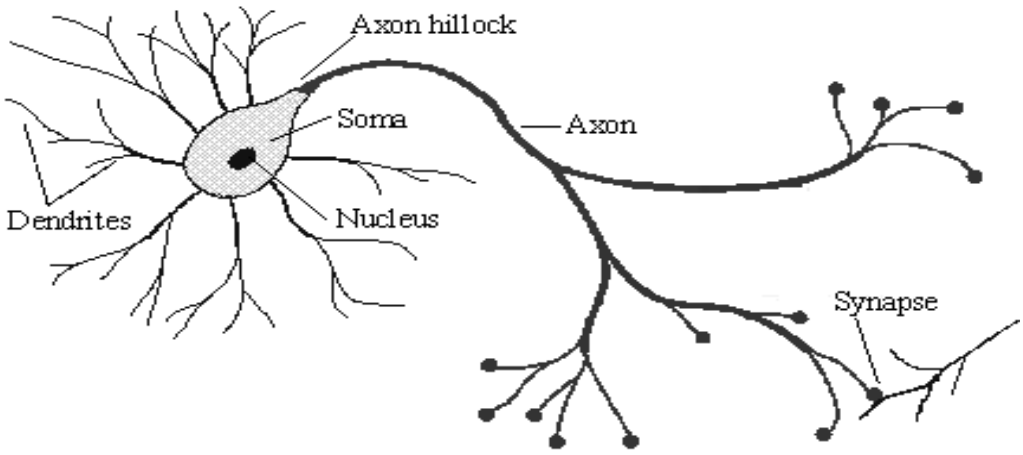


Figure 3.8. A biological neuron

The activities in the central nervous system are mainly related to the synapses. Synapses transfer electric activity from one cell to another. In the brain, the neuronal electrical activities can be classified into two types: action potential and postsynaptic potential. The magnitude of the action potential is larger than postsynaptic potential, but its duration is shorter than postsynaptic potential. Action potentials occur when the electrical excitation of the membrane exceeds a threshold shown in Figure 3.9. In sequence, an action pulse reaches the terminal endings of the presynaptic cell and a neurotransmitter diffuses across the synaptic gap to bind to receptors in specialized membranes of the postsynaptic cell. Then, these events change the transmembrane potential. If it is depolarizing, it is an excitatory

postsynaptic potential (EPSP); if it is hyperpolarizing, it is an inhibitory postsynaptic potential (IPSP) (Malmivuo & Plonsey, 1995). The action potential is an all or none response. This means that, if incoming stimuli exceed the neuron's threshold value, action potentials are produced. Else, action potentials aren't. After the launching of an action potential, for a while action potentials cannot be generated and it is impossible to excite a second spike during or immediately after a first one. This is reason by entering the neuron refractory period (Berne & Levy, 1996; Sanei & Chambers, 2007). Figure 3.10 shows the above activities schematically.

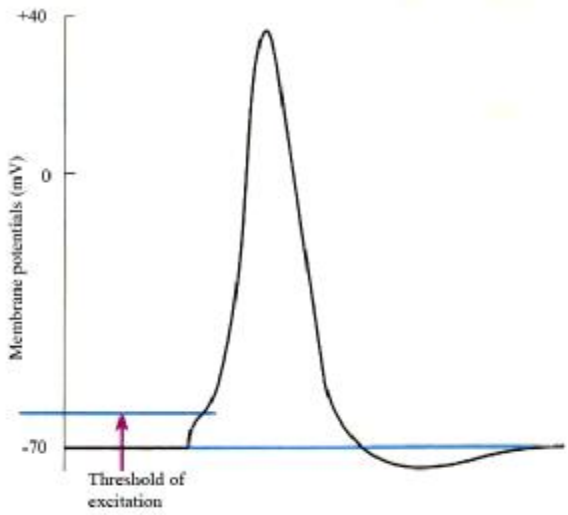


Figure 3.9. An action potential

Postsynaptic potentials typically have amplitudes of 5-10mV and a time span 10–50 msec. In order to obtain threshold excitation, the amplitudes of many postsynaptic potentials have to be superimposed in the soma of a neuron. A neuron can make up to 10000 synaptic junctions with other neurons. The electrical activities of neurons generate currents along the cell membrane and produce an electric field. Macroscopic observation of this electric field requires the synchronization of electrical activity of a large number of dipoles oriented in parallel. EEG comes from the summation of synchronously generated postsynaptic potentials.

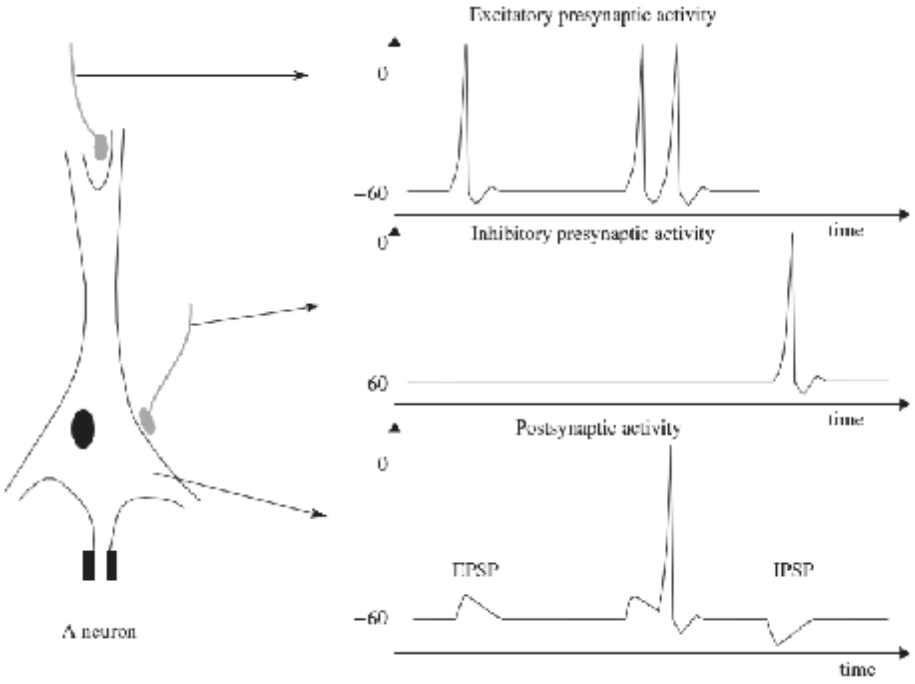


Figure 3.10. The neuron membrane potential changes and current flow during synaptic activation (Picture from Sanei & Chambers, 2007)

3.6.2. Multiresolution System Based on EPSP

The motivation of using excitatory postsynaptic potential as scaling function has already been given in the above section of the text. We generate a scaling function based on excitatory postsynaptic potential. Analytical expression of the EPSP is given as (Arica, 2007)

$$f(t) = \frac{c.d}{d-c}(e^{-ct} - e^{-dt})u(t)\ , \tag{3.42}$$

With c = 6 / 5 and d = 7 / 5. Plot of this function is given in Figure 3.11.

In the following, we both orthogonal and a bi-orthogonal multi-resolution system. Decomposition of a signal $x(t)$ at resolution 2^J is

$$x(t) = \sum_k a_k 2^{J/2} f\left(2^J t - k\right) + \sum_k b_k 2^{J/2} y\ \left(2^J t - k\right) \tag{3.43}$$

where $y(t)$ is the wavelet function responsible for representing detail of signal $x(t)$.

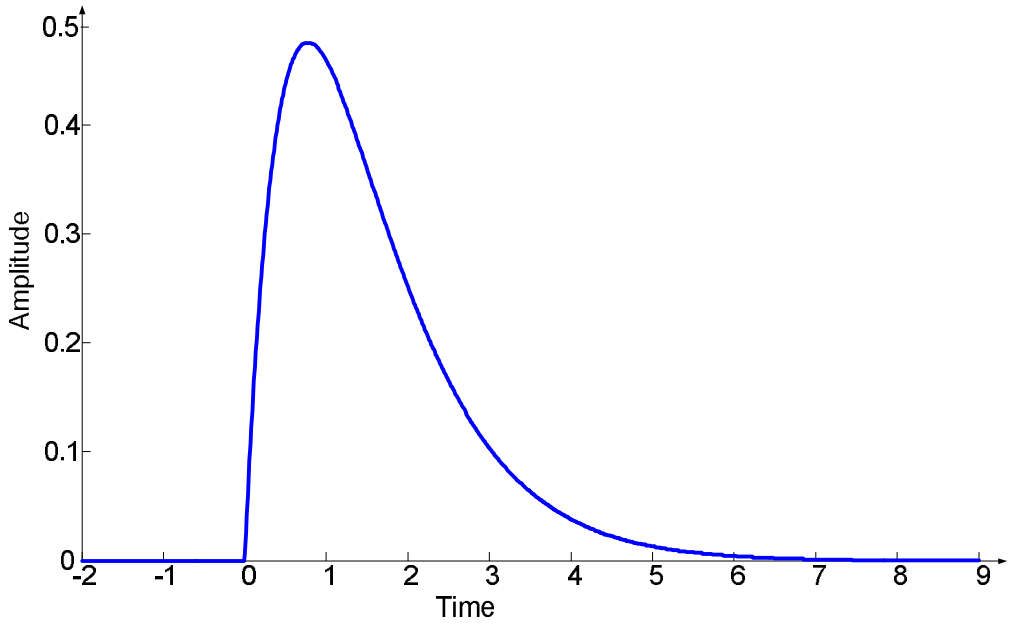


Figure 3.11. EPSP function

The coefficients a_k can be extracted from a signal $x(t)$ by bi-orthogonal complement ($\tilde{f}(t)$) of the scaling function and bi-orthogonal complement ($\tilde{y}(t)$) of the wavelet respectively:

$$a_k = \int_{-\infty}^{\infty} x(t) \cdot 2^{J/2} \tilde{f}\left(2^J t - k\right) dt$$

$$b_k = \int_{-\infty}^{\infty} x(t) \cdot 2^{J/2} \tilde{y}\left(2^J t - k\right) dt \qquad (3.44)$$

In order to extract the coefficients a_k, a bi-orthogonal complement of $f(t)$ is needed and the coefficient a_k is extracted if

$$\int_{-\infty}^{\infty} f(t)\tilde{f}(t-k)dt = d(k) \tag{3.45}$$

Bi-orthogonal counterpart of the scaling function can be generated from itself. Let,

$$\tilde{\Phi}(w) = K(w)\Phi^{*}(w), \tag{3.46}$$

Using the bi-orthogonality in frequency domain we can obtain the bi-orthogonal scaling and wavelet functions:

$$\sum_{l=\infty}^{\infty} \Phi(w-2pl)\tilde{\Phi}(w-2pl) = 1 \tag{3.47}$$

$$\sum_{l=-\infty}^{\infty} \Phi(w-2pl)K(w-2pl)\Phi^{*}(w-2pl) = \sum_{l=-\infty}^{\infty} |\Phi(w-2pl)|^{2} K(w-2pl) \tag{3.48}$$

The equation (3.45) is satisfied in the frequency domain if we choose

$$K(w) = \frac{1}{\sum_{l=-\infty}^{\infty} |\Phi(w-2pl)|^{2}} \tag{3.49}$$

Thus,

$$\tilde{\Phi}(w) = \frac{\Phi(w)}{\sum_{l=-\infty}^{\infty} |\Phi(w-2pl)|^{2}} \tag{3.50}$$

In time domain,

$$\tilde{f}(t) = \sum_{n=-\infty}^{\infty} k(n)f(t-n) \approx \sum_{n=N_1}^{N_2} k(n)f(t-n) \tag{3.51}$$

The time support of $\hat{f}(t)$ is then $[N_1, \quad N+N_2]$ when the time support of $f(t)$ is $[0, N]$.

Recall Fourier transform of dilation equations

$$\Phi(w)=\frac{1}{2}H\left(\frac{w}{2}\right)\Phi\left(\frac{w}{2}\right)$$
$$\hat{\Phi}(w)=\frac{1}{2}\hat{H}\left(\frac{w}{2}\right)\hat{\Phi}\left(\frac{w}{2}\right) \tag{3.52}$$

Replacing $\Phi(w)=\frac{\hat{\Phi}^*(w)}{K^*(w)}$ and $\Phi\left(\frac{w}{2}\right)=\frac{\hat{\Phi}^*\left(\frac{w}{2}\right)}{K^*\left(\frac{w}{2}\right)}$ in the dilation equation,

$$\begin{aligned}\left(K^*(w)\right)^{-1}\hat{\Phi}^*(w) &= \frac{1}{\sqrt{2}}H\left(\frac{w}{2}\right)\left(K^*\left(\frac{w}{2}\right)\right)^{-1}\hat{\Phi}^*\left(\frac{w}{2}\right)\\ \hat{\Phi}^*(w) &= \frac{1}{\sqrt{2}}K^*(w)H\left(\frac{w}{2}\right)\left(K^*\left(\frac{w}{2}\right)\right)^{-1}\hat{\Phi}^*\left(\frac{w}{2}\right)\\ \hat{\Phi}(w) &= \frac{1}{\sqrt{2}}K(w)H^*\left(\frac{w}{2}\right)K^{-1}\left(\frac{w}{2}\right)\hat{\Phi}\left(\frac{w}{2}\right)\end{aligned} \tag{3.53}$$

Therefore,

$$\begin{aligned}&\hat{H}(w)=K(2w)K^{-1}(w)H^*(w)\Leftrightarrow\\ &\hat{h}(n)=F^{-1}\left[K(2w)K^{-1}(w)\right]*h(-n)\end{aligned} \tag{3.54}$$

And the corresponding two-scale equations of the wavelets are computed by the following equations.

$$\Psi(w)=\frac{1}{2}G(\frac{w}{2})\Phi\left(\frac{w}{2}\right), \qquad G(w)=-e^{-jw}\overline{H}(w-p)$$
$$\overline{\Psi}(w)=\frac{1}{2}\overline{G}(\frac{w}{2})\overline{\Phi}\left(\frac{w}{2}\right), \qquad \overline{G}(w)=-e^{jw}H(w-p) \tag{3.55}$$

In time domain,

$$y(n)=\sum_k g(k)f(2n-k), \quad g(k)=(-1)^k\overline{h}(k-1)$$
$$\overline{y}(n)=\sum_k \overline{g}(k)\overline{f}(2n-k), \quad \overline{g}(k)=(-1)^k h(k+1) \tag{3.56}$$

The dilation equations of the scaling functions are also reproduced in the following.

$$f(t)=\sum_k h(k)f(2t-k)$$
$$\overline{f}(t)=\sum_k \overline{h}(k)\overline{f}(2t-k) \tag{3.57}$$

Scaling and wavelet functions and their bi-orthogonal complements for custom wavelet are illustrated in Figure 3.12. Plots of the filters of custom multi-resolution system are shown in Figure 3.13.

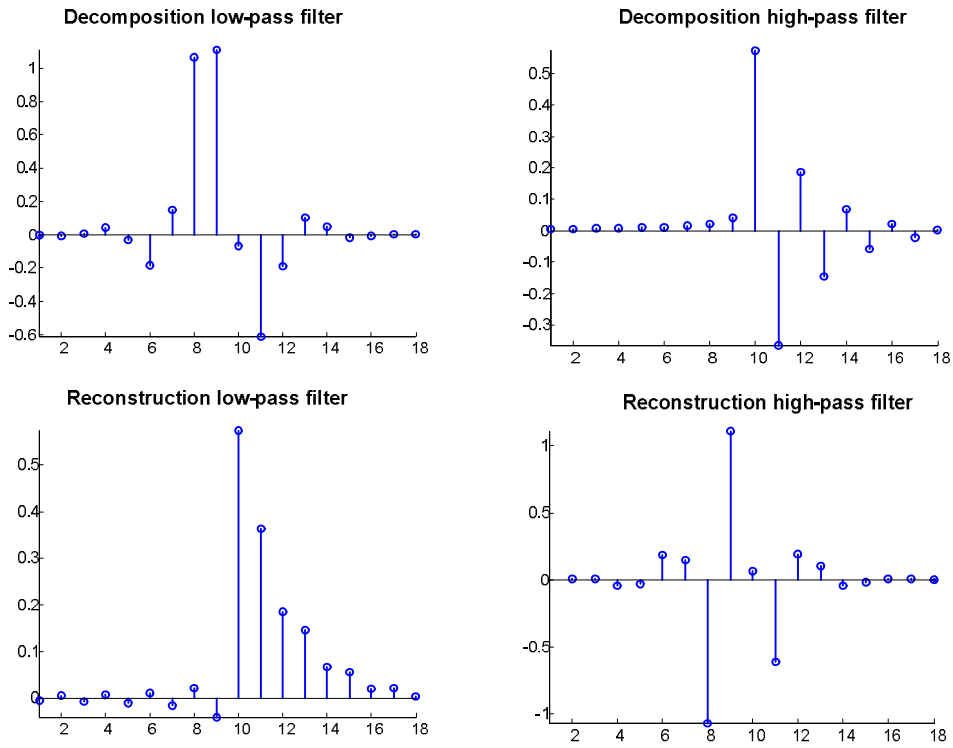


Figure 3.12. The four filters of custom multi-resolution system

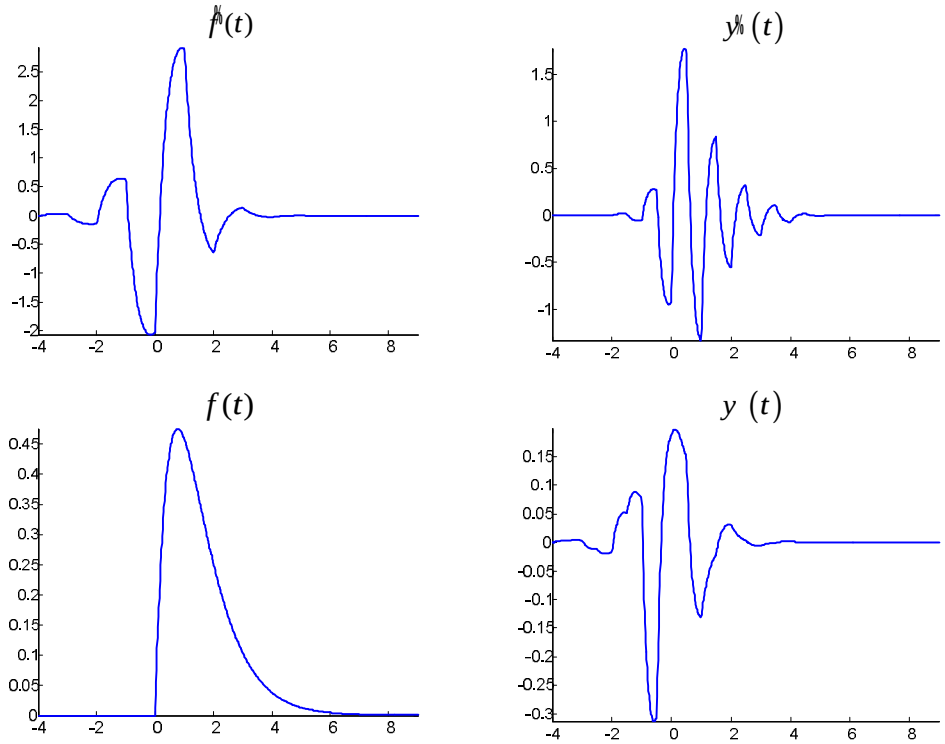


Figure 3.13. Bi-orthogonal scaling and wavelet functions and their bi-orthogonal complements for custom wavelet.

Similarly, it is possible to generate an orthogonal multi-resolution system. Let, orthogonal function, $j_o(t)$ is related to $j(t)$ in the frequency domain as $\Phi_o(w)=K(w)\Phi(w)$. From (3.47), we write the orthogonality condition in the frequency domain:

$$\sum_{l=-\infty}^{\infty}\Phi_o(w-2pl)\Phi_o(w-2pl)=1 \tag{3.58}$$

Then, we get,

$$\begin{aligned}\sum_{l=-\infty}^{\infty}\Phi_o(w-2pl)\Phi_o(w-2pl)&\\ =\sum_{l=-\infty}^{\infty}\Phi(w-2pl)K(w-2pl)\Phi(w-2pl)K(w-2pl)&\\ =\sum_{l=-\infty}^{\infty}|K(w-2pl)|^2|\Phi(w-2pl)|^2&\end{aligned} \tag{3.59}$$

The orthogonality condition is satisfied in the frequency domain if we choose

$$K(w)=\frac{1}{\sqrt{\sum_{l=-\infty}^{\infty}\left|\Phi(w-2pl)\right|^2}} \tag{3.60}$$

Therefore,

$$\Phi_o(w)=\frac{\Phi(w)}{\sqrt{\sum_{l=-\infty}^{\infty}\left|\Phi(w-2pl)\right|^2}} \tag{3.61}$$

This equation in time domain is as;

$$j_o(t)=\sum_{n=-\infty}^{\infty}k(n)f(t-n)\approx\sum_{n=N1}^{N2}k(n)f(t-n) \tag{3.62}$$

Let,

$$b(w) = \sum_{l=-\infty}^{\infty} |\Phi(w - 2pl)|^2 \tag{3.63}$$

Hence,

$$K(w) = 1/\sqrt{b(w)} \tag{3.64}$$

Consider that the the dilation equation

$$\Phi(w) = \frac{1}{2} A\,(\frac{w}{2}) \Phi(\frac{w}{2}) \tag{3.65}$$

Replacing the orthogonalization equation we attain

$$\begin{aligned} \sqrt{b(w)}\,\Phi_o(w) &= \frac{1}{2} A\,(\frac{w}{2}) \sqrt{b(w/2)}\,\Phi_o(\frac{w}{2}) \\ \Phi_o(w) &= \frac{1}{2} A\,(\frac{w}{2}) \frac{\sqrt{b(w/2)}}{\sqrt{b(w)}} \Phi_o(\frac{w}{2}) \end{aligned} \tag{3.66}$$

If dilation equation of the orthogonal scaling function is

$$\Phi_o(w) = \frac{1}{2} H\,(\frac{w}{2}) \Phi_o(\frac{w}{2}) \tag{3.67}$$

then the low-pass filter of the orthogonal system is,

$$H(w) = \frac{1}{2} A\,(w) \frac{\sqrt{b(w)}}{\sqrt{b(2w)}} \tag{3.68}$$

In orthogonal case $H^{*}(z) = H(z^{-1})$ therefore

$$\begin{aligned} G(z) &= -z^{-1}H(-z^{-1}) \\ \tilde{G}(z) &= -zH(-z) = G(z^{-1}) \end{aligned} \tag{3.69}$$

$$H(z)H(z^{-1}) + H(-z)H(-z^{-1}) = 2 \tag{3.70}$$

in z-domain. The time domain of equivalent of these equations

$$g_n = (-1)^n h_{-n+1} \tag{3.71}$$

$$\sum_{l=-\infty}^{\infty} h_l h_{l+2n} = d_n \tag{3.72}$$

Using the bi-orthogonality property the coefficients a_k's at scale J can also be extracted by estimate the following formula

$$a_k = \int_{2^j(k+A)}^{2^j B} x(t)2^{J/2}\tilde{f}(2^j t - k)dt \tag{3.73}$$

where A and B are time limits of the $\tilde{f}(t)$. In practical applications we have discrete signals sampled uniformly with sampling interval of Δ. The equation needs to be modified for the discrete signals. Replace t with $n\Delta$.

$$\begin{aligned} a_k &= \sum_{n=2^{-j}\Delta^{-j}(k+A)}^{2^{-j}\Delta^{-j}B} x(n\Delta)2^{J/2}\tilde{f}(2^j n\Delta - k)\Delta \\ &= \sum_{n=2^{-j}\Delta^{-j}(k+A)}^{2^{-j}\Delta^{-j}B} x(n\Delta)2^{J/2}\tilde{f}(2^j\Delta(n - 2^{-j}\Delta^{-1}k)\Delta \end{aligned} \tag{3.74}$$

Let, $y(n) = x(n\Delta)$ and $s(n) = \tilde{f}(2^j\Delta n)$ and $K = 2^{-j}\Delta^{-1}$. Then,

$$a_k = \Delta\sum_n y(n)s(n - Kk) = \Delta[y(k) * s(-k)]_{\downarrow K} \tag{3.75}$$

3.7. EEG Signal Features

EEG signal gives the information about the condition of the brain. The shape of the wave may contain useful information about the state of the brain. Therefore, extracting the EEG signal parameters is highly useful method in EEG signal processing. Generally, the features used in EEG signal analysis are based on spatial, temporal, and frequencial information. In this section, some EEG feature for representing EEG signal are determined and applied to classify EEG data as an estimator. 14 different feature types for one second EEG data from the stimulus onset are introduced.

3.7.1. Curve Length

Curve length of the signal is defined by the sum of the lengths of the line segments between successive samples of a signal.

$$CL[n] = \frac{1}{N} \sum_{m=(n-1)N+1}^{nN} \left| x[m] - x(m-1) \right| \tag{3.76}$$

where $x[m]$ is an EEG time series, and N is the window length.

The curve length is used for observing amplitude and frequency changes and dimensionality of the signal (D'Alessandro et al., 2003).

3.7.2. Signal Energy

Average energy of signal $x(m)$ is:

$$E[n] = \frac{1}{N} \sum_{m=(n-1)N+1}^{nN} x[m]^2 \tag{3.77}$$

3.7.3. Nonlinear Energy

$$NE[n] = \frac{1}{N} \sum_{m=(n-1)N+1}^{nN} x[m]^2 - x[m-1]x(m+1) \tag{3.78}$$

This operator is sensitive to both amplitude and frequency changes. It is ideal for local (time) analysis of signals, Furthermore it is computationally efficient, and simple to calculate (Hamila et al., 1999).

3.7.4. Sixth Power Energy

$$SPE[n] = \frac{1}{N} \sum_{m=(n-1)N+1}^{nN} x[m]^6 \tag{3.79}$$

The sixth power energy formula calculates the sixth power of the signal and it is used for observing small amplitude differences in the EEG. Magnitude differences are increased with the power of the signal, since small signals increase less than signals with larger amplitudes.

3.7.5. Mean Frequency

The mean frequency of a spectrum is calculated as the sum of the product of the spectrogram intensity (in dB) and the frequency, divided by the total sum of spectrogram intensity.

$$f_m = \frac{\sum_{i=0}^{n} I_i f_i}{\sum_{i=0}^{n} I_i} \tag{3.80}$$

where f_m, mean frequency; n, number of frequency bins in the spectrum; f_i, frequency of spectrum at bin i of n and I_i, intensity (dB scale) of spectrum at bin i of n.

3.7.6. Reyni Entropy

Power spectral density (PSD) can be obtained using Fourier transformation. The PSD represents the distribution of power as a function of frequency. For each frequencies, power P_f and total power P_T are obtained from Fourier Transform and normalization power p_f is calculated (Kannathal et al., 2005).

$$p_f = \frac{P_f}{P_T} \tag{3.81}$$

Then, spectral entropy called Renyi's quadratic entropy is calculated using p_f

$$RE = -\log(\sum_f p_f^2) \tag{3.82}$$

3.7.7. Shannon Entropy

Shannon entropy SE is given by the following equation (Lin, 1991):

$$SE = \sum_x p(x) \log p(x) \tag{3.83}$$

where SE is the Shannon entropy, $p(x)$ is the discrete probability distribution function (PDF).

3.7.8. Average Method

Average method is a simple conversion method. The EEG data recorded through a second are divided into windows each of with a size of d. If the mean of the signal is above the mean of EEG data, the feature is taken 1, otherwise 0 (Petrosian, 2002).

3.7.9. Differential Method

In "differential" method like average method, EEG signal was converted to binary sequence. This method has two steps. At the first step, the difference between two consecutive samples along to one second EEG signal is calculated and divided into windows with size of d. Then, feature was assigned to be 1 if average of the value of this window is positive and 0 if it is negative (Petrosian, 2002).

3.7.10. Barlow Parameters

Barlow parameters are amplitude (*A*), Frequency (*F*) and Spectral Purity Index (*SPI*) are defined as follows:

$$A_b(x(t)) = abs(x(t)) \tag{3.84}$$

$$F_b(x(t)) = \frac{abs(\frac{dx(t)}{dt})}{A_b(x(t))} \tag{3.85}$$

$$SPI_b(x(t)) = \frac{F_b(x(t))^2}{abs(\frac{dx(t)^2}{dt^2})} \tag{3.86}$$

After calculating the parameters, each mean of the parameters are obtained and each one is assigned as a feature.

3.7.11. Hjorth Parameters

The Hjorth parameters are called activity, mobility and complexity describing the properties of the EEG signal *x*.

$$A(x(t)) = \mathrm{var}(x(t)) \tag{3.87}$$

$$M(x) = \sqrt{\frac{A(\frac{dx(t)}{dt})}{A(x(t))}} \tag{3.88}$$

$$C(x(t)) = \frac{M(\frac{dx(t)}{dt})}{M(x(t))} \tag{3.89}$$

After calculating the parameters, each mean of the parameters are obtained and each one is assigned as a feature (Obermaier et al., 2001).

3.7.12. Petrosian Fractal Dimension

Petrosian Fractal Dimention is defined as:

$$PFD = \frac{\log_{10} N}{\log_{10} N + \log_{10}(\frac{N}{N + 0.4N_d})} \tag{3.90}$$

where N is the series length and N_δ is the number of changes in the sign of signal derivative (Petrosian, 2002).

3.7.13. Max Frequency Match Filter

In order to obtain EEG feature using max frequency match filter, the maximum frequency is obtained from the signal spectrum, then cosine function is

formulated with this frequency. After that, matching filter was employed between cosine function and EEG signal *x(m)*.

$$w(k) = \sum_{j} x(j)\cos(2p\ f_m(k-j)) \tag{3.91}$$

Where *w* is convolution between *x* and cosine function.

Then, below procedure is employed,

$$ax = \mathbf{R}\max(w)$$
$$mx = \max(abs(w))$$

$$feaMF = \frac{ax}{mx} \tag{3.92}$$

Max frequency match filter is calculated to divide angle of maximum value of filter result and maximum absolute value of filter result.

3.7.14. Median Method

In the median method, the median of the EEG signal data recorded through a second is assigned as a feature.

3.8. Classification Methods

3.8.1. Linear Discriminant Analysis (LDA)

Linear classifiers use linear functions to distinguish classes within a data. They are probably the most popular algorithms for EEG applications. This technique has a very low computational requirement, simple to use and generally provides good results (Garrett et al., 2003; Lotte et al., 2007).

The goal in linear discriminant analysis (LDA) is to compute a discriminant vector that separates two or more classes as well as possible. Here we consider only

the two-class case. Suppose that we have a set of *d* dimensional samples x_i and corresponding class of C_1 and C_2. Linear combination of *x* is (Duda, Hart, & Stork, 2001; Alpaydın, 2004)

$$y = w^t x \tag{3.93}$$

This is the projection of *x* on *w* and $y_1,\ldots y_n$ divided into the subset of Y_1 and Y_2.

μ_i and m_i are means of samples from C_i before and after projection, respectively given by,

$$m_i = \frac{1}{n_i}\sum_{x\in C_1} x \tag{3.94}$$

$$m_i = \frac{1}{n_i}\sum_{y\in Y_i} y = \frac{1}{n_i}\sum_{y\in Y_i} w^t x = w^t m_i \tag{3.95}$$

The scatter of samples of after the projection;

$$s_i^2 = \sum_{y\in Y_i} (w^t x - m_i)^2 \tag{3.96}$$

Two classes will be well separated after projection. The fisher linear discriminant is *w* that maximizes so $m1-m2$ should be large and $s_1^2 + s_2^2$ to be small as in Figure 3.14.

$$J(w) = \frac{(m_1 - m_2)^2}{s_1^2 + s_2^2} \tag{3.97}$$

To obtain *J*(.), now we can define the between-class scatter matrix S_B and the within-class scatter matrix S_W

$$S_B = (m_1 - m_2)(m_1 - m_2)^t \tag{3.98}$$

$$S_w = \sum_{k=1}^{2} \sum_{i \in C_k} (x_i - m_k)(x_i - m_k)^t \tag{3.99}$$

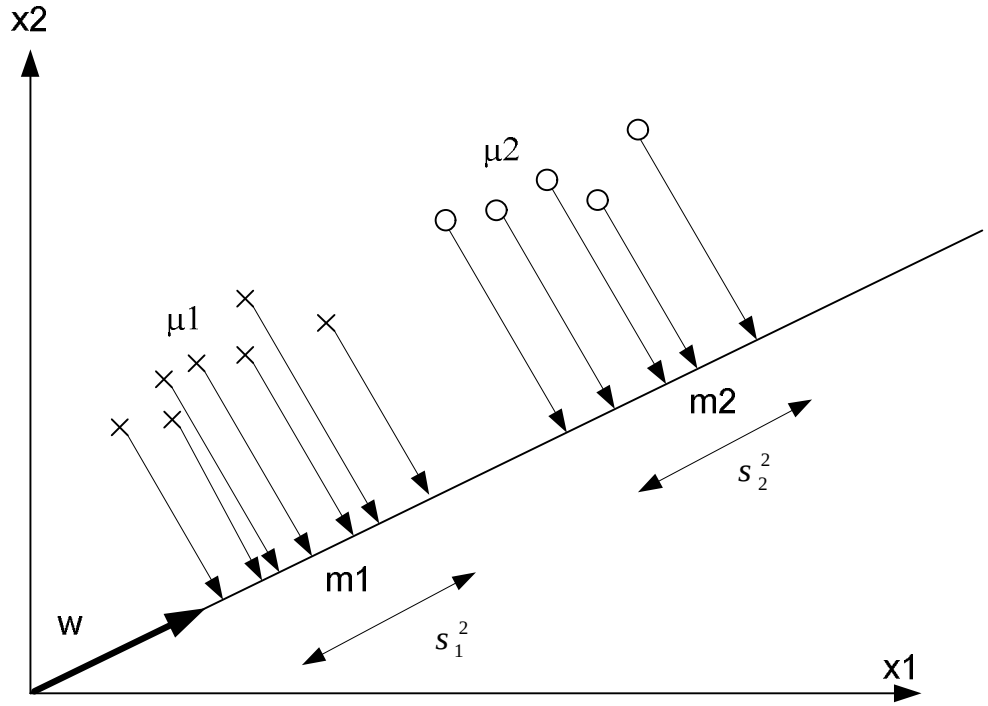


Figure 3.14. Two dimensional, two class data projected on w. (modified from Alpaydın, 2004).

That is, we can write scatter matrices after the projection, between-class scatter becomes $w^t S_B w$ and within-class scatter becomes $w^t S_W w$. It is to be first large and second scatter to be small. With the help of these two matrices, the criterion function can be written as

$$J(w) = \frac{w^t S_B w}{w^t S_W w} \tag{3.100}$$

This is known Rayleigh quotient.

By computing the derivative of *J* and setting it to zero, one can show that the optimal solution for *w* satisfies the following equation

$$w = S_W^{-1}(m_1 - m_2) \tag{3.101}$$

w is obtained for fisher linear discriminant and classification problem is reduced to one dimensional. So, classification is satisfied to determine the appropriate threshold.

If the densities are multivariate normal with equal covariance matrices $\sum$, threshold can be calculated directly (Duda et al., 2001).

$$w^t x + w_0 = 0 \tag{3.102}$$

$$w = \sum^{-1}(m_1 + m_2) \tag{3.103}$$

where w_0 is a constant involving w and μ_1, μ_2 are means of class 1 and class 2 respectively.

3.8.2. Neural Networks

Neural networks (NN) are mostly used in EEG research with linear classifiers. NN produce nonlinear decision boundaries with artificial neurons. In this work, we implement a standard, feed-forward, neural network with one hidden layers and one output layer. This feed-forward network is trained using the standard error back-propagation algorithm to minimize the squared error between the output and the input to the network (Muller et al., 2003). Each iteration in BP constitutes two sweeps: forward activation to produce a solution, and a backward propagation of the computed error to modify the weights (Basheer & Hajmeer, 2000).

For two classes problem, Let X is a $p\,x\,N$ matrix of N samples, as p-dimensional columns. Let Y be a $2xN$ matrix of indicator variables designating the class corresponding to each sample in X. Let α be the $(p+1)\,x\,h$ matrix of hidden-layer weights, where h is the number of hidden units, and β be the $2\,x\,(h\,+1)$ matrix of output-layer weights. The hidden layer output Z and the final network output O are calculated as (Garrett et al., 2003)

$$Z = f(a^T X) \tag{3.104}$$

$$O = f(b^T X) \tag{3.105}$$

Where

$$f(a) = 1/(1+e^{-a}) \tag{3.106}$$

The error back-propagation learning algorithm minimizes the squared error $(Y-O)^2$ summed over all outputs and samples. The gradient descent is performed by updating the weights as

$$d = (Y-O)\cdot O\cdot(1-O) \tag{3.107}$$

$$\Delta a = g\,X(bd\cdot Z\cdot(1-Z))^T \tag{3.108}$$

$$\Delta b = g\,Zd^T \tag{3.109}$$

where γ is a small constant. These update equations are iterated until the squared error in the network output on a subset of untrained data is minimized. The resulting weights are used to classify new data by picking the output with the largest value (Garrett et al., 2003).

3.9. Feature Selection Methods

Signals obtained by the EEG recordings may include redundant information and may also weaken the generalization performance of the classifier.

Feature selection procedure aims to identify and remove as much irrelevant and redundant information as possible. Also, feature selection simplify data visualization and data understanding, reduces the measurement and storage requirements, reduces training and utilization times and improve prediction performance (Guyon & Elisseeff, 2003; Saeys et al., 2007).

Two approaches to feature selection are commonly used that they are the wrapper methods and the filter methods.

Filter technique uses general characteristics of the data. In most cases a feature relevance score is calculated, and low-scoring features are removed (Guyon, 2008). Afterwards, this subset of features is presented as input to the classification algorithm. In this method, high-dimensional datasets are scaled easily. Feature subsets can be fed to different classifiers.

Wrapper method uses embed classifier model within the feature subset search (Kohavi & John, 1997). For this, possible feature subsets are defined, and various subsets of features are generated and evaluated. Specific subset of features is obtained by training and testing with a classification model. To find optimal feature subset, heuristic search methods are used such as deterministic and randomized search algorithms.

As a result, filter techniques computationally simple and fast, and they are independent of the classification algorithm. Whereas, advantages of wrapper approaches include the interaction between feature subset search and model selection, and the ability to take into account feature dependencies.

Both feature selection methods was employed for our classify algorithm. We used fisher criteria and Pearson correlation as filter method and used backward stepwise selection as wrapper method.

Consider a set of input variables X, and corresponding output variable Y. The Pearson correlation coefficient is defined as:

$$C_p = \frac{\mathrm{cov}(X_i, Y)}{\sqrt{\mathrm{var}(X_i)\,\mathrm{var}(Y)}} \tag{3.110}$$

If two random variables are linearly dependent, then their correlation coefficient is ± 1. If the variables are uncorrelated, the correlation coefficient is 0. If two features are independent then they are also uncorrelated. Correlation closely related to Fisher's criterion, t-test criterion, and other similar criteria.

The Fisher criterion provides the normalized level of discrimination between two classes problem. Therefore, it is possible to select the top ranked feature presenting higher discrimination. Fisher criteria can be calculated as (Duda et al., 2001):

$$FC_j = \frac{(m_{j1} - m_{j2})^2}{s_{j1}^2 - s_{j2}^2} \tag{3.111}$$

where m_{j1} and m_{j2} are averages belongs to two classes over all training trials for each feature *j*, and s_{j1}^2 and s_{j2}^2 are also variances of classes for each feature *j*.

On the other hand, by the wrapper approach, the classifier algorithm is run on the dataset and then different sets of features are removed from the data. The feature subset with the highest evaluation is chosen as the final set. The resulting classifier is then evaluated on an independent test set that is not used during the feature subset search. Wrapper feature selection methods can be divided as forward stepwise selection and backward stepwise selection. In the forward stepwise selection, searching starts for one feature and in each step, features are added one by one. Conversely, in the backward stepwise selection method, it starts for all features and then features are removed one by one until only one remains. We use backward stepwise selection in this work.

Wrapper method was employed with LDA classifiers and n-fold cross validation. Wrapper algorithm is as follows (Tanaka et al., 2006):

S1) Calculate classifier performance using all features.

S2) Remove one of the features and calculate classifier performance using remaining features with n-fold cross validation.

S3) Repeat (S2) for each possible feature combination.

S4) Select the best feature combination obtained from step (S3), and go to step (S2) repeat the elimination process.

S5) Repeat (S4) until all features is eliminated.

After the all possible feature combination is evaluated. The feature combination that gives the largest performance from the all sub-features is selected. This sub-feature set can be fed to classifier algorithm as selected features.

3.10. Validation Procedures

3.10.1. Bootstrapping

The bootstrap was introduced by Efron (1979) that it is a computationally intensive statistical tool designed to assess statistical accuracy.

The bootstrap allows to researcher to repeat the experiment. With the bootstrap, the observations are randomly reassigned, and the estimates are recomputed. These assignments and re-computations are done thousands of times and treated as repeated experiments. This approach is used when researchers are managing small samples (Zoubir, 1998).

The basic idea underlying the bootstrap is to produce a random sample from the original pool of data, with replacement and obtained by sampling. This procedure can be repeated many times in order to create an empirical distribution of the statistic. Then, the sample is used to compute the estimate of the parameter by the researcher. Distribution obtained using bootstrap generally represents a good approximation of original probability distribution.

Bootstrap principle can be described as follow. Let $X = \{X_1, X_2, .., X_w\}$ be a sample. X_i 's are independent and identically distributed random variables, each having distribution F obtained from experiment. Then constructing empirical

distribution F' and a sample is drawn from this selected distribution. This sample, $X^* = \{ X_1^*, X_2^{**}, ..., X_n^* \}$, is called the bootstrap resample (Zoubir, 1998).

3.10.2. N-fold Cross-Validation

N-fold cross-validation is one way to improve estimate of a classifier performance.

The data set is divided into n partitions such that the partitions are near-equal size. This procedure is repeated n times. Each time, one of the n subsets is used as the test set and the other n-1 subsets are put together to a training set. The generalization error is assessed for each of the n test sets and averaged over n. Every data point appears in a test set exactly once, and appears in a training set n-1 times. This method can be computationally very expensive and it is seen a disadvantage (Molinaro et al., 2005).

This validation was applied various works in EEG research (Anderson & Sijercic, 1996; Pfurtscheller et al., 1999; Polat & Güneş, 2007) . All results presented here were obtained through this cross validation procedure.

4. FINDINGS AND DISCUSSIONS

The main aim of this thesis is to classify EEG data recorded during familiar and unfamiliar face recognition experimental paradigm. We tried to find out whether the developed algorithm is capable of distinguishing VEPs between familiar and unfamiliar face visual stimuli. For this purpose, all signal processing procedures were done according to the flow charts shown in Figure 4.3, Figure 4.4 and Figure 4.5.

All the data used in this work was obtained from Başkent University Adana Hospital and Research Center. Twenty six healthy volunteers' data were used in this work. 172 digitized photographs of faces, 86 of them are familiar and others are unfamiliar, were selected as the stimuli. According to the experiment paradigm, volunteers pressed the button if they recognize the shown face. However, volunteers didn't recognize all the familiar photos. As a result of that, familiar and unfamiliar EEG data sets occur in different size for each individual volunteer. Familiar and unfamiliar EEG data sets information are shown in Table 4.1.

Besides that, the EEG data of the BCI competition III recorded from two subjects is used to test the algorithm as visual evoked potentials. Our classification approach on this dataset will be explained in section 4.4.

Table 4.1. Familiar and unfamiliar EEG data set size according to volunteers.

Volunteer	F. Size	Unf. Size	Volunteer	F. Size	Unf. Size
1	84	88	14	69	103
2	78	94	15	79	93
3	71	101	16	86	86
4	84	88	17	80	92
5	70	102	18	85	87
6	69	103	19	97	75
7	88	84	20	85	87
8	81	91	21	105	67
9	73	99	22	90	82
10	68	104	23	80	92
11	89	83	24	85	87
12	91	81	25	83	89
13	87	85	26	81	91
			Total	2138	2334
			Average	82,2	89,8

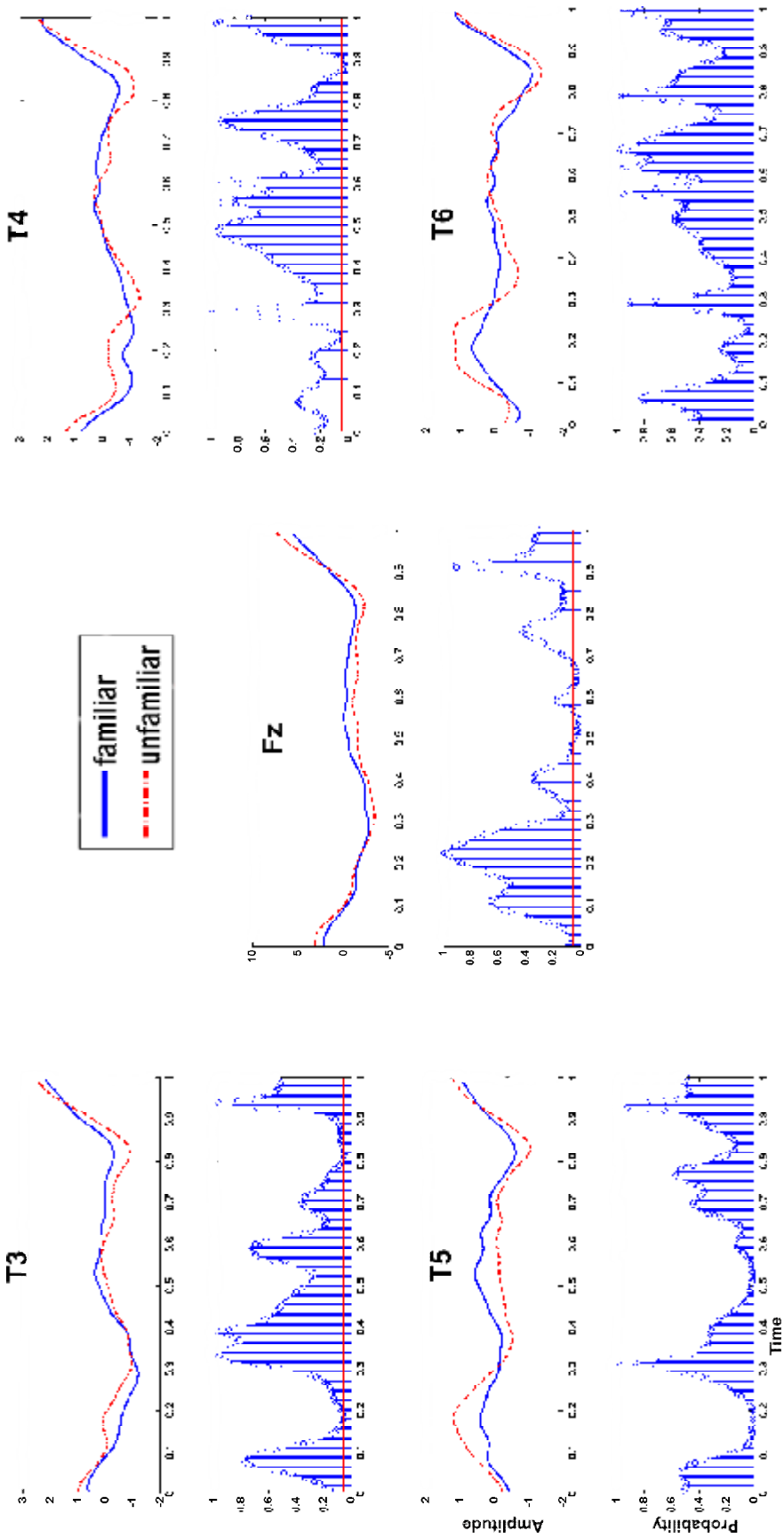


Figure 4.1. Grand average ERPs of all volunteer familiar and unfamiliar data from the each of the channels occipital, temporal, parietal and central regions and corresponding α-value of the t-test under the ERP plots. Red line on the t-test plots are the significant level at α-value=0.05.

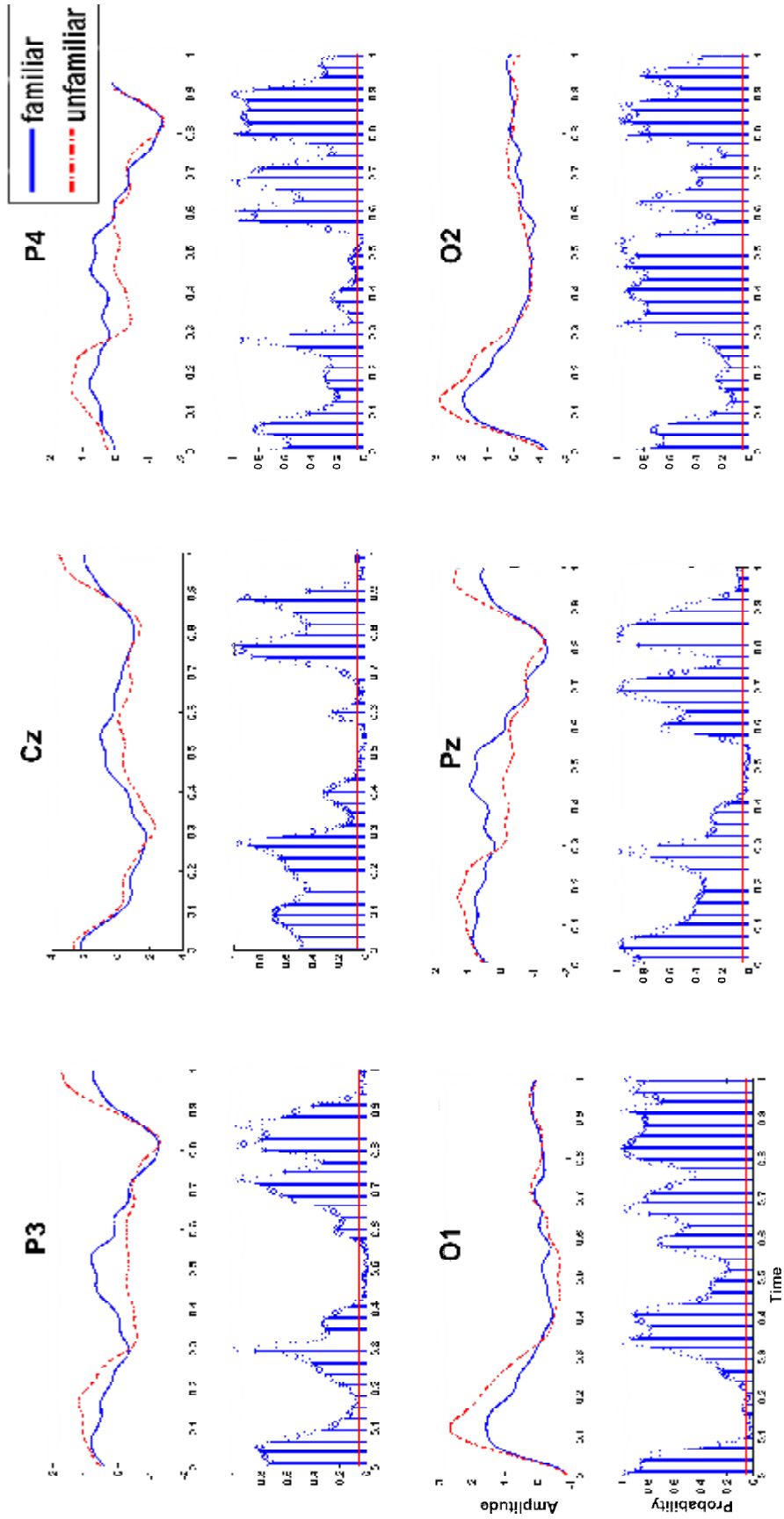


Figure 4.1. Continued.

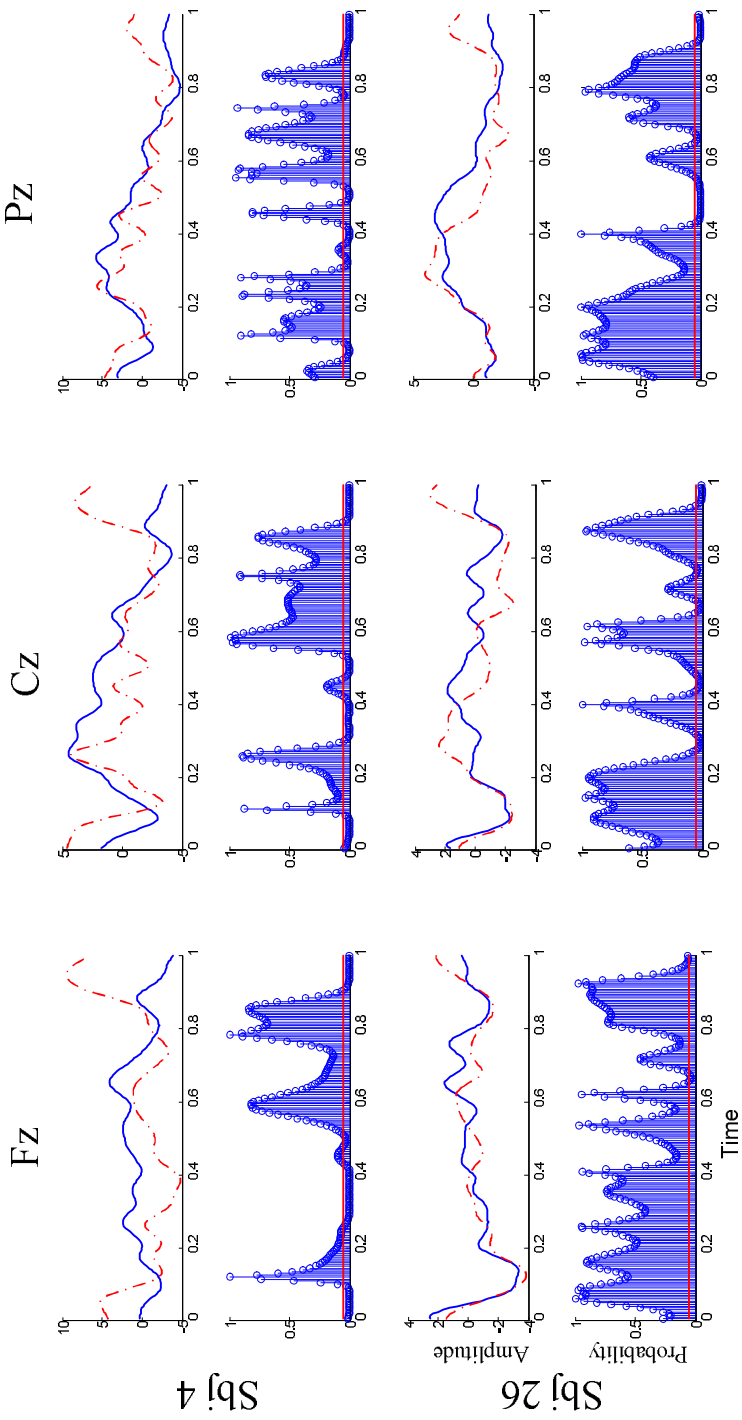


Figure 4.2. Average ERPs of the volunteers 4, 26, 3 and 22 familiar and unfamiliar data from the central regions and corresponding α-value of the t-test under the ERP plots. Red line on the t-test plots are the significant level at α-value=0.05. Selected subjects have the highest two and lowest two accuracy performance in the 'epsp' wavelet decomposition algorithm in Table 4.3 respectively.

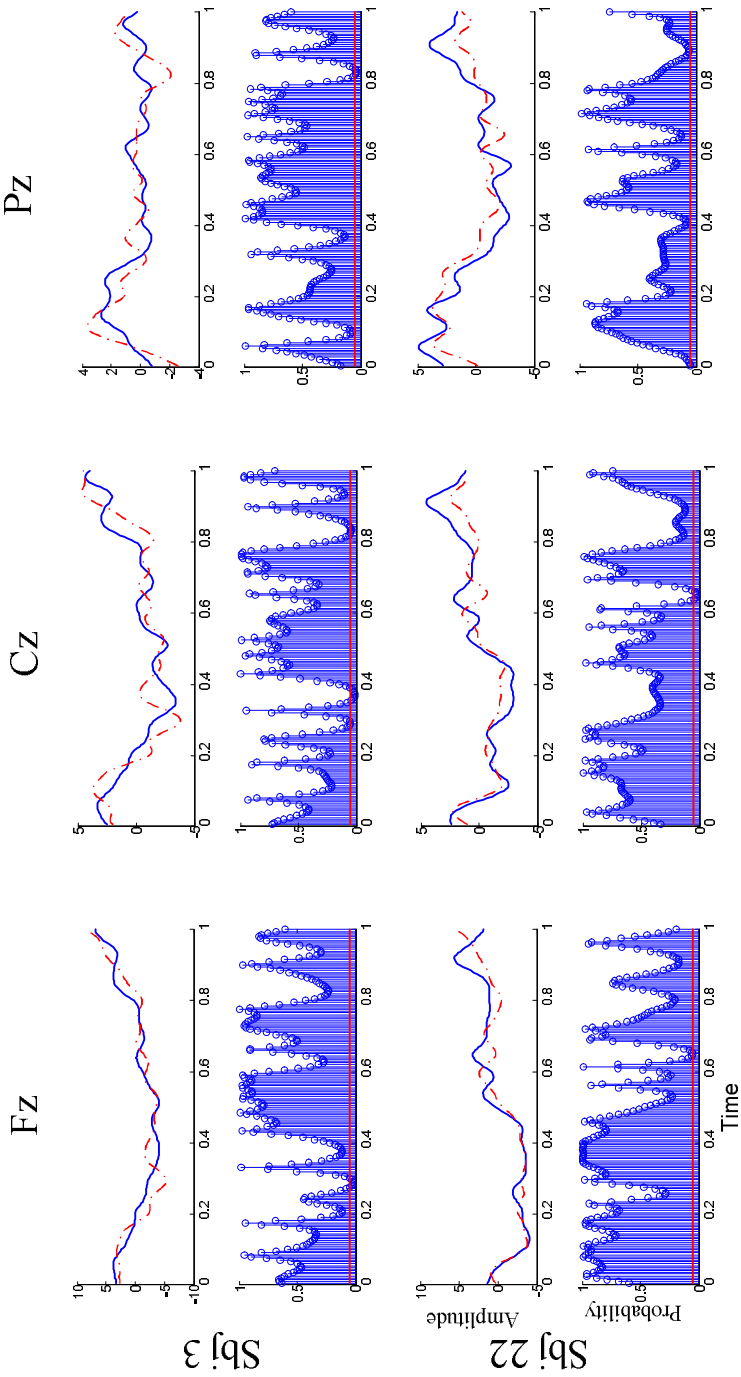


Figure 4.2. Continued.

Figure 4.1 illustrates the comparisons between familiar and unfamiliar face data from the each of the channels occipital, temporal, parietal and central regions. The figures include grand average ERPs of all volunteer familiar and unfamiliar data and corresponding α-values of the t-test below the ERP plot in Figure 4.1. The number of correct responses in familiar and unfamiliar stimuli was 2138 and 2334 respectively. Red line on the t-test plots show the significant level at α-value=0.05. According to the t-test result, it is observed that distinction of the familiar and unfamiliar data is not clear. Major parts of the one second data in all brain regions do not show significant differences between two classes. However, if we analyzed the graphs together with t-test results along the time latency, there are significant differences in time segments 100ms - 250 ms for T3, T4, T5, T6 O1 and O2 electrodes, between 450 to 550 ms for Fz, Cz, Pz, P3 and P4 electrodes, and between 800ms to 900 ms for T3 and T4 electrodes. These observations are consistent with previous face recognition studies (Anaki et al., 2007; Neumann & Schweinberger, 2008; Genetti et al., 2009).

Besides, average ERPs of the volunteers who have the highest two and lowest two accuracy performances in the 'epsp' wavelet decomposition algorithm in Table 4.3 was shown in Figure 4.2 to examine the subject related response. In this figure, average ERPs of familiar and unfamiliar data from the central regions and corresponding α-values of the t-test are illustrated for the volunteer number 4, 26, 3 and 22. At a glance, t-test results show consistency with the classification results of our algorithm. Similarly to our result, volunteers 4 and 26 who have the highest classification performance have lower α-values of t-test than volunteers 3 and 22 with the lowest classification performance. Another observation derived from Figure 4.2 is the effect of N170 and N800 latency in the volunteers 4 and 26 data. These potentials may be influenced by the task relevance of recognizing face identity.

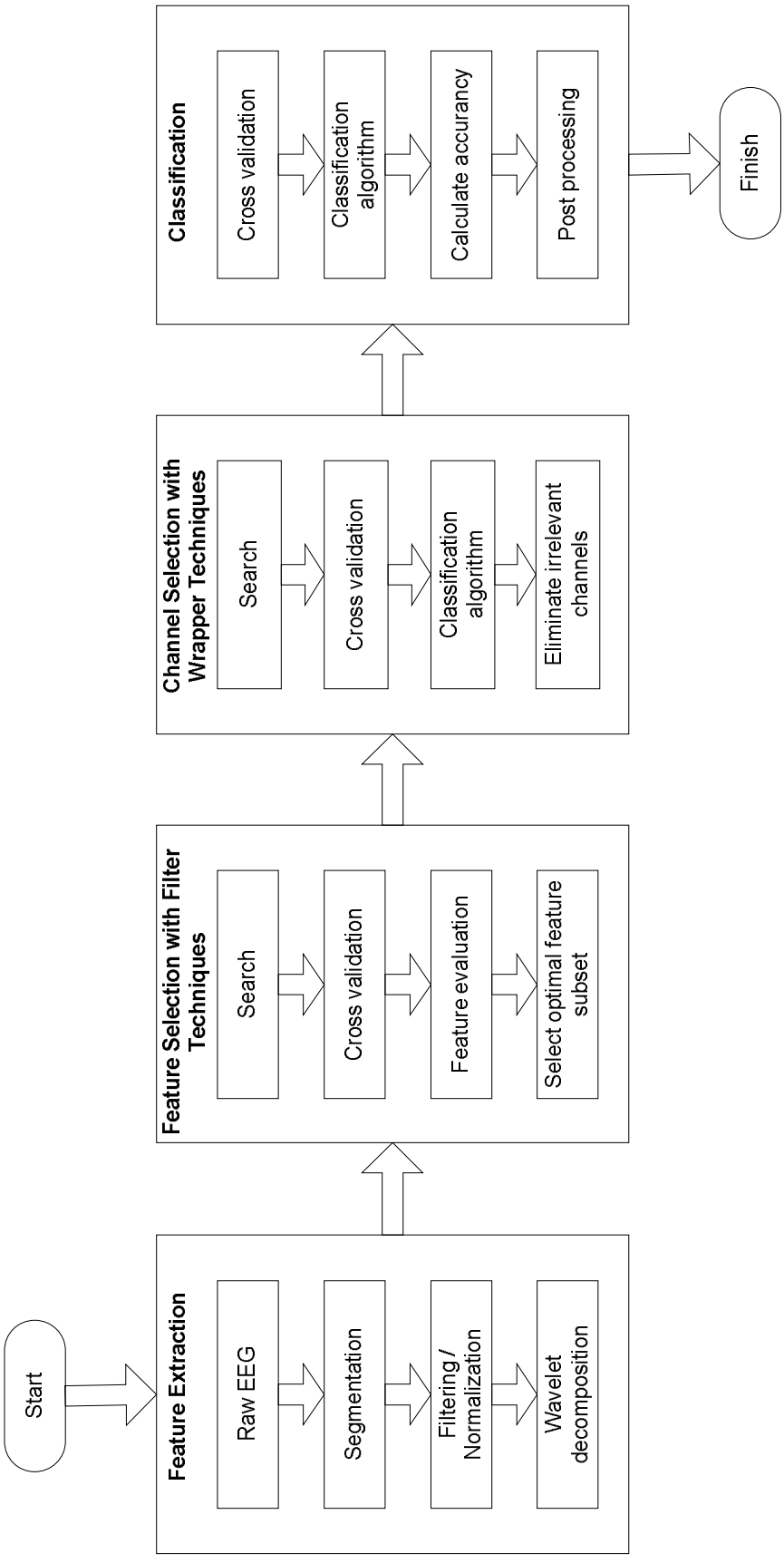


Figure 4.3. Signal processing scheme of classification of familiar - unfamiliar evoked EEG using wavelet decomposition.

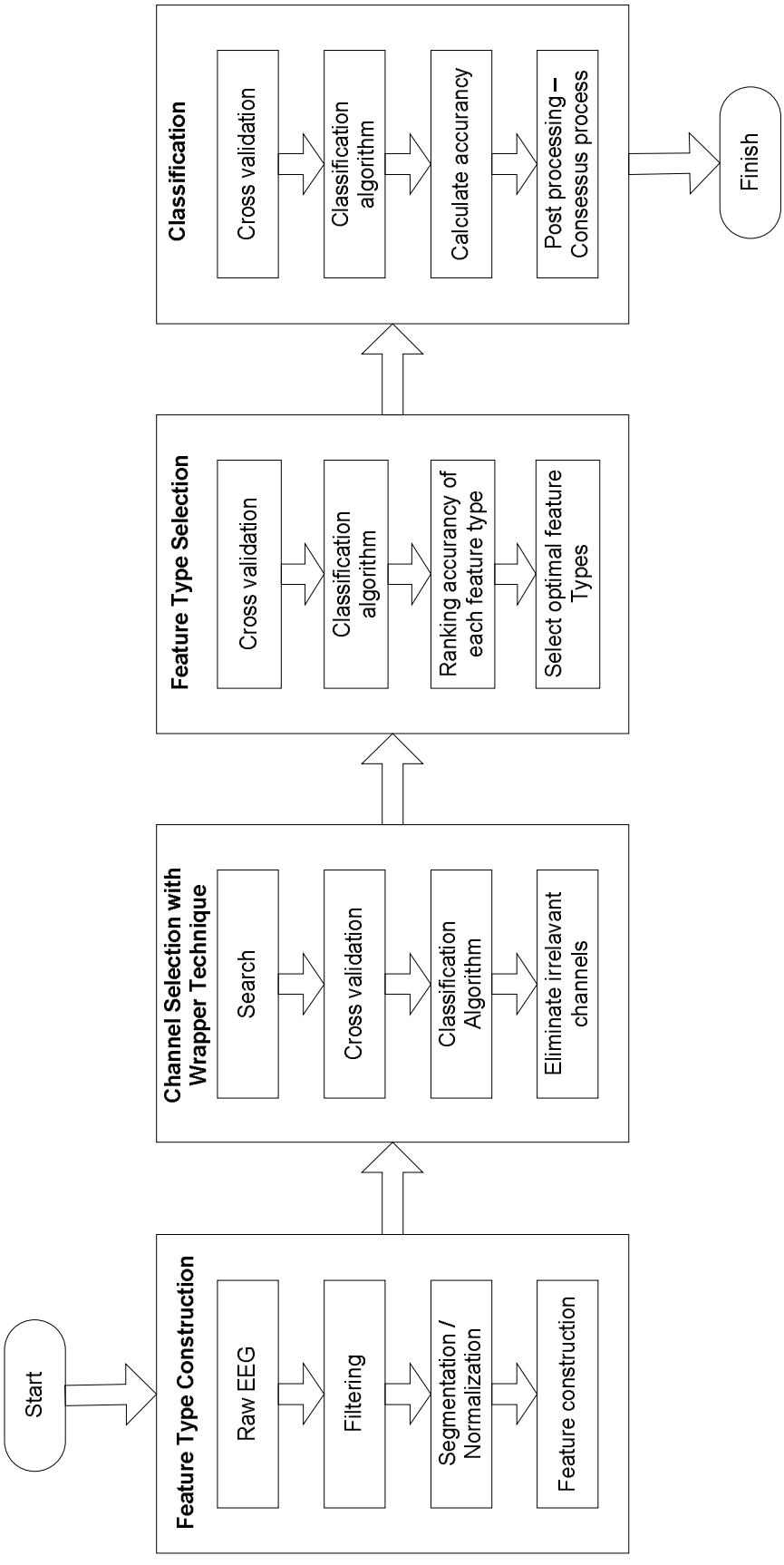


Figure 4.4. Signal processing scheme of classification of familiar - unfamiliar evoked EEG using feature types with consensus methods

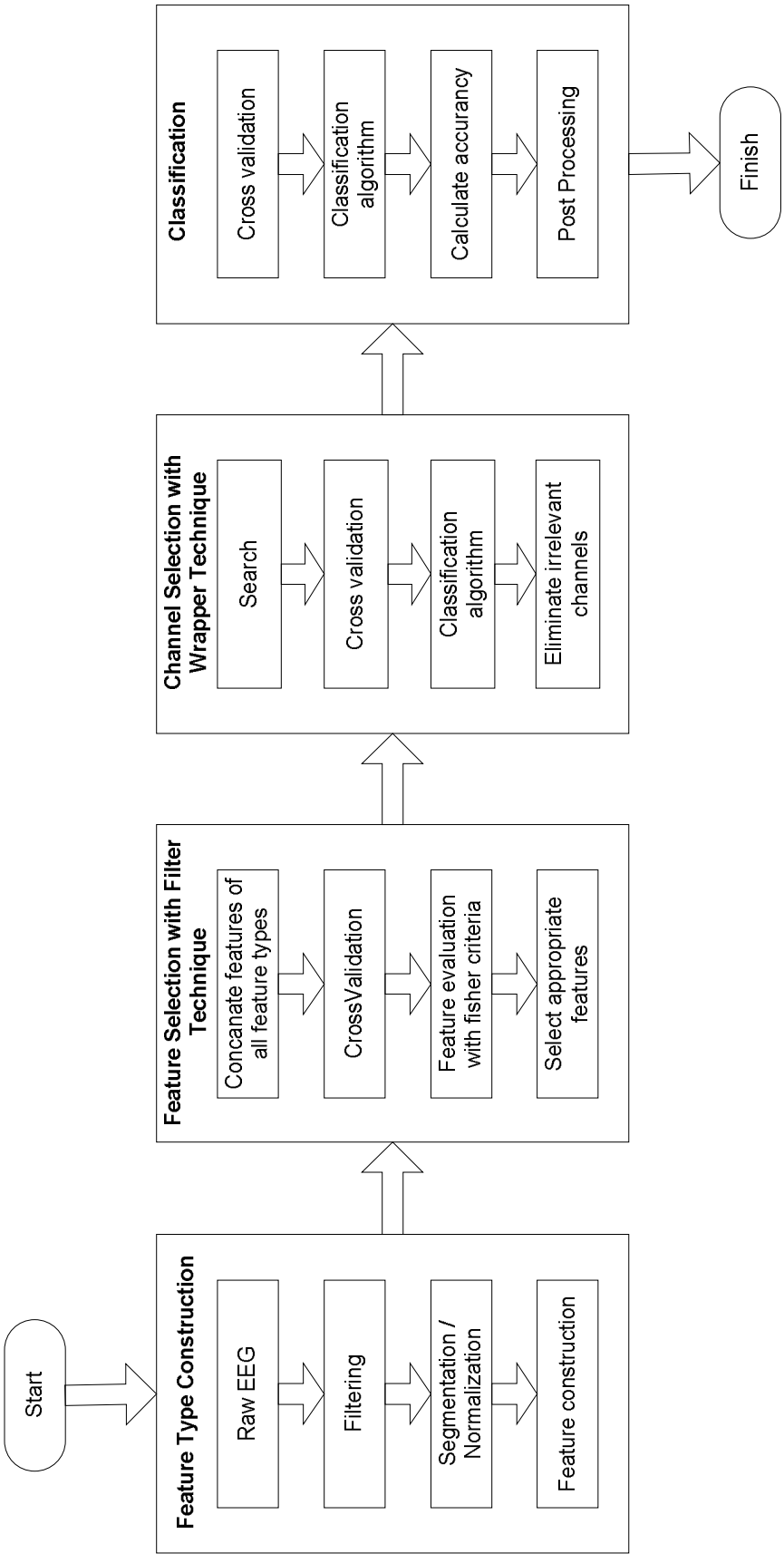


Figure 4.5. Signal processing scheme of classification of familiar - unfamiliar evoked EEG using feature types with concatenate methods

4.1. Model Evaluation of the System

We used 5-fold cross-validation analysis to examine our models in order to estimate of a classifier performance of the models. For that examination, the data set is divided into 5 near-equal size partitions. Then one of the 5 subsets is used as test set and the other four subsets are put together into training set.

The results were quantified with the following statistical parameters: sensitivity (Q_d), specificity (Q_n) and overall accuracy (Q_o). These parameters were respectively used to measure the accuracy of positive prediction, negative prediction and the overall accuracy of the system. These measurements were calculated by using the following values:

TP (true positive): The number of correctly classified familiar set,

FP (false positive): The number of unfamiliar set incorrectly classified as familiar,

TN (true negative): The number of correctly classified unfamiliar set,

FN (false negative): The number of familiar set incorrectly classified as unfamiliar.

The metrics were calculated by using these values with the following equations:

$$\begin{aligned} Q_d &= TP/(TP+FN) \\ Q_n &= TN/(TN+FP) \\ Q_o &= (TP+TN)/(TP+TN+FP+FN) \end{aligned} \tag{4.1}$$

Sensitivity, specificity, and overall accuracy are the terms which are most commonly associated with a binary classification test, and they are used as statistically measure of the performance of the test. In general, when sensitivity indicates how well the test predicts one category, specificity measures how well the test predicts the other category. Accuracy is expected to measure how well the test predicts both categories. Therefore , a good binary classification test always results

with high values for all the three factors, whereas a poor binary classification test results with low values for all.

4.2. Pre-processing of the Visual Evoked EEG Data

The EEG data was extracted by implementing bandpass filtering. As stated previously the EEG is decomposed in 5 bands: Delta rhythm (0.5-4Hz), Theta rhythm (4-8 Hz), Alpha rhythm (8-13 Hz), Beta rhythm (13-26 Hz) and Gamma rhythm (26 Hz<).

Visual evoked potential (VEP) is a brief electrophysiological activity recorded on scalp in response to a visual stimulus. In order to extract VEP, EEG data should be filtered nearly 15 Hz with lowpass filter. Also EEG data can be normalized as following purpose.

A high-dimensional data vector may represent quite different properties. The descriptor metric might differ substantially from column to column. To avoid distortion problems, the data is preprocessed before being used as input for the methods. The data values were normalized according to the z-score shown in equation 4.2.

$$z_j = (x_j - m_j) / s_j \tag{4.2}$$

where $x_{.j}$ is the j^{th} data value, m_j is the mean and s_j is the standard deviation. This scaling process reveals data with zero mean and unit variance.

4.3. Results with Familiar - Unfamiliar Visual Evoked Data

In order to classify familiar -unfamiliar related EEG, three main approaches were implemented. As mentioned previously, 26 volunteers' data was examined during these algorithms. Two classes (familiar and unfamiliar) were explored from

these data and classifier outputs were respectively assigned to these classes as 1 and 0.

4.2.1. Classification with Wavelet Decomposition

In this study, essentially multiresolution approximation coefficients of the EEG data were used as descriptors for the familiar - unfamiliar experimental paradigm. In another word, EEG data was transformed for classification.

Implemented algorithm for this purpose is shown in Figure 4.3. The algorithm mainly consists of four units: feature extraction, feature selection, channel selection and classification. All these procedures are performed offline. Initially, EEG data was filtered with bandpass filter with bandwidth of 1 to 70 Hz, and then was applied notch filter at 50 Hz for eliminating the noise of electrical equipment. Afterward, all data for each channel was pulled out in between 0 to 1 s posterior to the beginning of stimulus. Finally, wavelet decomposition of the filtered data was performed up to level 3.

The algorithm was implemented by using Matlab (Mathworks Inc.), and Matlab statistical and wavelet toolboxes (mathworks.com, 2010). The wavelet transform's output can be significantly affected by the choice of wavelet. Some wavelets are more appropriate than others for particular types of input signals (Samar et al., 1999; Kadambe & Bourdeaux-Bartels, 2002; Glassman, 2005).

A review on wavelet Analysis of Neuroelectric Waveforms by Samar (1999) stated for wavelet shape;

"The wavelet transform is free to use wavelets as its basis functions that have shapes that are as close as possible to the shapes of the neuroelectric events they are analyzing. Like a key designed to fit a lock, the best analyzing function for a neuroelectric event is one that matches that event in shape as closely as possible."

In this viewpoint, we used a function that resembles shape of excitatory post-synaptic potentials waveform to construct a scaling function. Then, filters of our function were introduced to the wavelet toolbox and named as 'epsp'. The

decomposition filter length was 18. We also utilized bi-orthogonal spline wavelets with decomposition and reconstruction filters orders; (8, 2), (8, 6). We also employed Daubechies wavelet, Symlet and Coiflet. Note that we consider wavelets with decomposition filter orders same with or close to decomposition filter order of our wavelet. Selected wavelet for our work and its properties are shown Table 4.2. Also Figure 4.6 illustrates the filter coefficient and Figure 4.7 illustrates scaling and wavelet function of using wavelets respectively.

Table 4.2. Wavelet families, short names and filter length of the wavelet using our work.

Wavelet Family	**Wavelet Short Name**	**Length**
Excitatory Postsynaptic Potential Based	Epsp	18
Bi-Orthogonal Spline	bior2.8	18
	bior6.8	18
Daubechies	db8	17
	db9	19
Coiflet	coif3	18
Symlet	sym8	17
	sym9	19

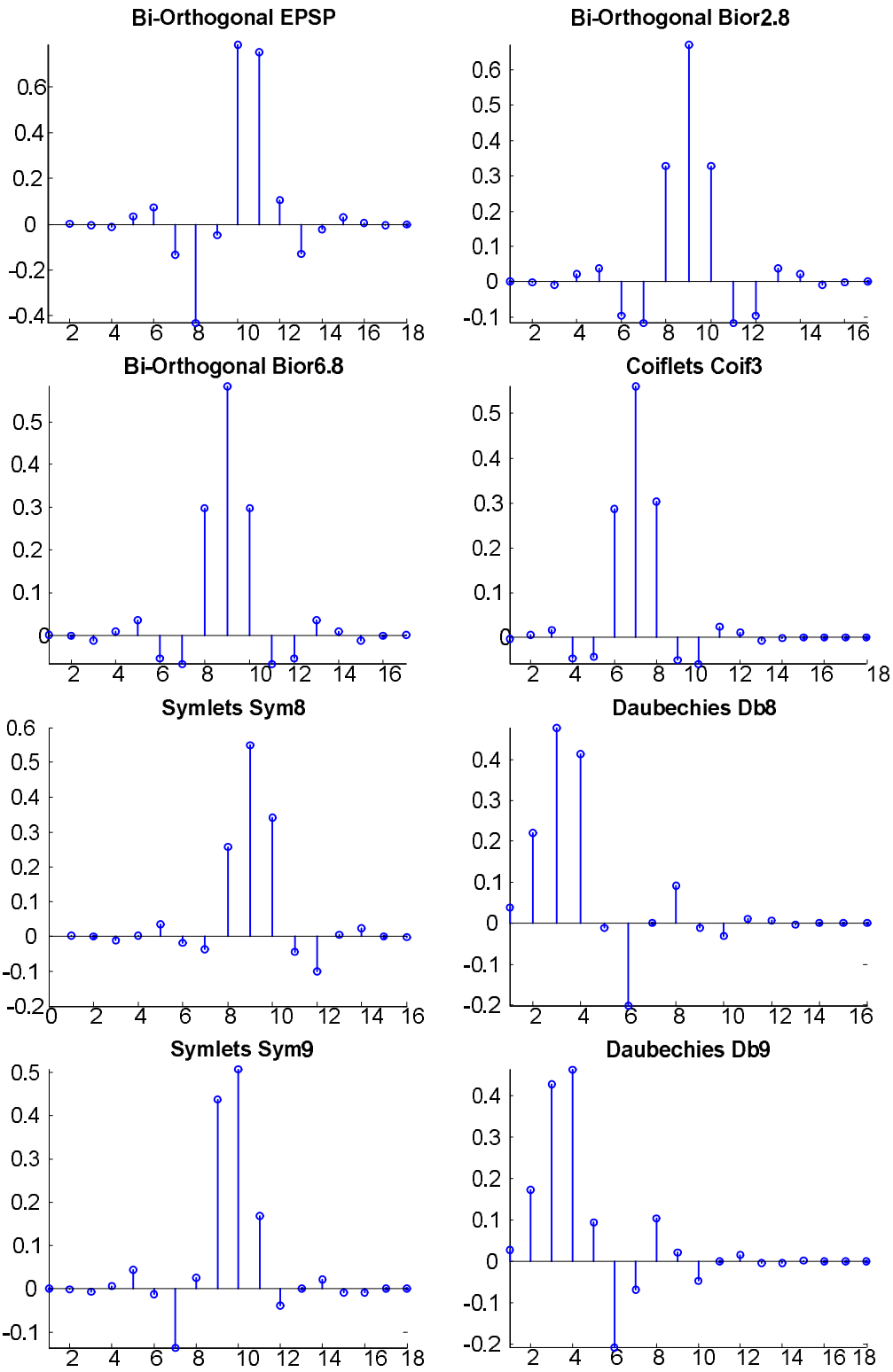


Figure 4.6. Filter coefficients of the wavelet using wavelet decomposition methods.

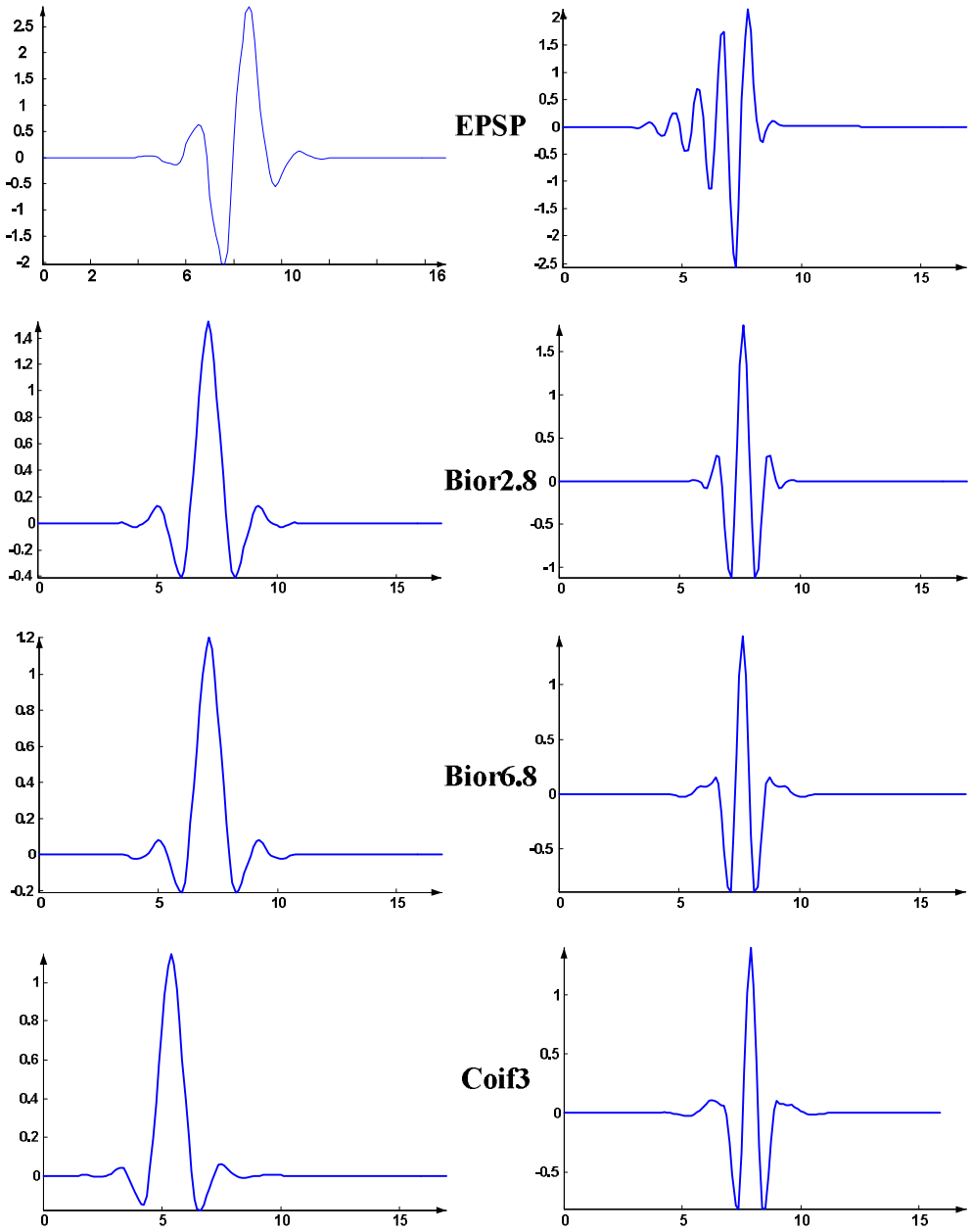


Figure 4.7. Scaling (left) and Wavelet (right) functions of the wavelet using wavelet decomposition methods.

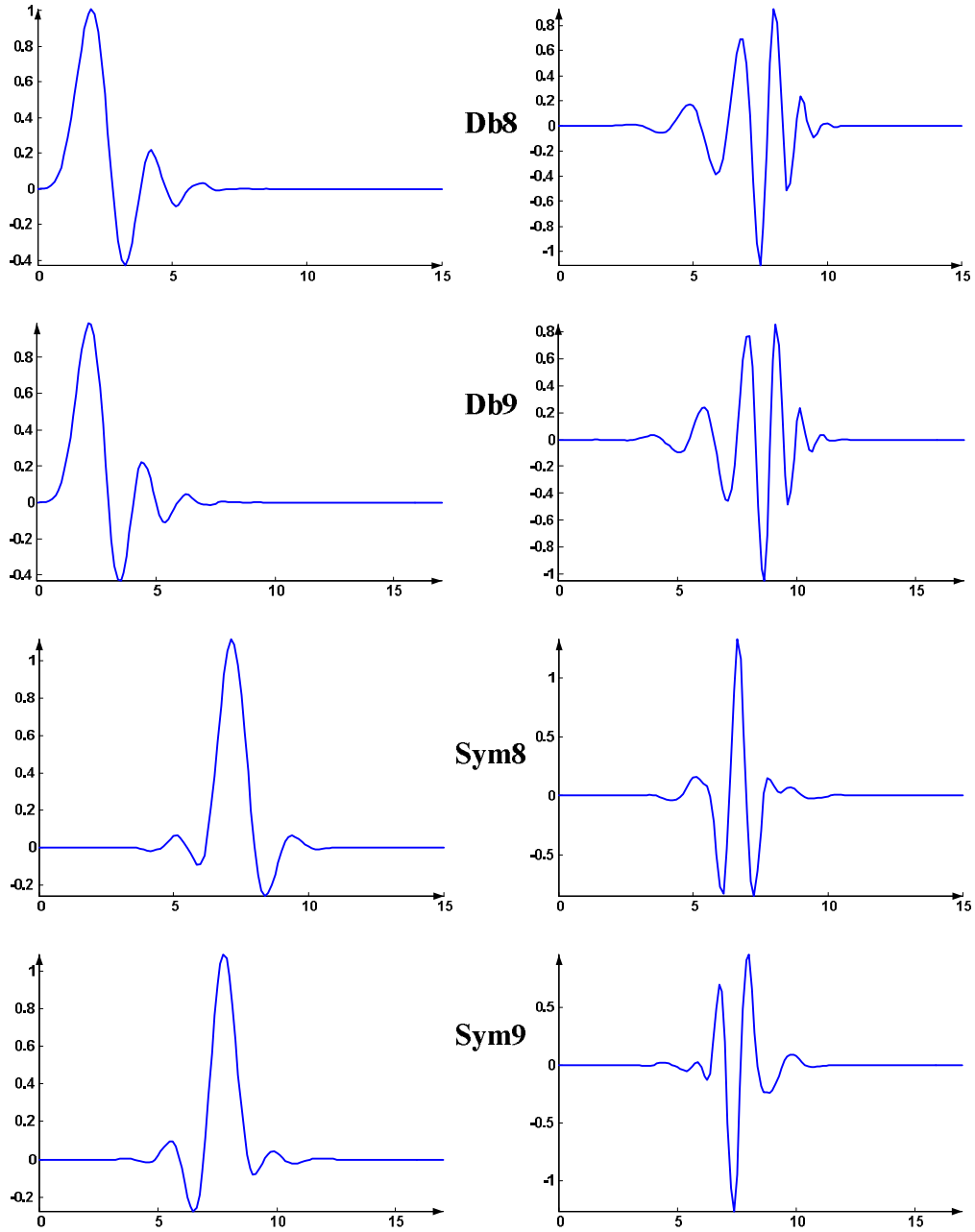


Figure 4.7. Continued.

Approximation coefficient of the wavelet decomposition at level 3 was used as features for our algorithm. Feature size for each channel became 39 for wavelets 'epsp', 'bior2.8', 'bior6.8', 'db9', 'coif3', 'sym9' for 1 second EEG data and wavelet decomposition level at 3, and feature size became 38 for other wavelets. These amounts of feature should be reduced for the efficient classification, and better classification accuracy is obtained by using the small number of features. Feature selection unit with filter techniques was designed for this purpose. The feature evaluations in the algorithm were done by five-fold cross validation. Then optimal four features were selected for each channel. Afterward, 19 channels EEG data were reduced to best relevant channels by channel selection unit. Wrapper technique was employed in this part. Finally, classification part of algorithm was run with selected channel and four features in each channel. In this process, selected channels and features were concatenated for each trial and these features used as input for classification unit. Fisher's linear discriminator was used for familiar - unfamiliar VEP classification. Also five-fold cross validation was employed for classification performance quality. Classification accuracy in percent for subject number from 1 to 26 is indicated in Table 4.3 and Specificity (Qn) and Sensitivity (Qd) of classification results of this method is indicated in Table 4.4. Also selected channels which selected by the channel selection unit using custom wavelet 'epsp' is depicted in Table 4.5. Histogram of the these selected channels is illustrated in Figure 4.8. Also mostly selected five channels which selected by channel selection unit for all wavelets and for all volunteers were indicated in Table 4.6. Besides, selected features for each volunteer by feature selection unit for the selected 5 channels is shown Figure 4.9. Additionally, backpropagation neural networks with properties mentioned in section 3.8.2. was used for the classification method. Results from this approach was given in Table 4.10.

Furthermore, Common Spatial Patterns (CSP) was used instead of wrapper technique for channel selection. CSP is a method that extracts the features of data to maximize the discriminability of two classes. However, CSP analysis was used to obtain the first and last 'm' rows index in wavelet decomposition. These indexes are

also most discriminative channels numbers and these channels could be used in channel selection unit in Figure 4.3 as selected channels.

According to complete results that provided using our custom wavelet with LDA classifier which shown in Table 4.3 vary between 63% and 77%. Besides, when we look to average of the same results for all 26 volunteers, we found that it is 69,66 % and the standard deviation is 4,02. From these results, our wavelet gives the best overall mean and standard deviation value as compared the other wavelet functions.

Another observation derived from Table 4.3 was getting the best result position among used wavelets for each volunteer. In addition to this observation we found that our wavelet became 8 times the top result among wavelets for all 26 volunteers and that it is almost double of any other wavelet's success. The similar results were also observed for the backpropagation classifier methods shown in Table 4.10. Obtained accuracy performances relatively is lower than results using LDA classifier. However, the results in both seems proportionate for all volunteers and all wavelets.

Additionally, bootstrapping validation method was used instead of the 5-fold validation in the multiresolution algorithm. Classification accuracies are given in the Table 4.9. Again, observations from the results are similar to previously mentioned results with 5-fold validation in Table 4.3. As seen in the Table 4.9, classification accuracies were better than results in the Table 4.3 for all wavelets and volunteers. Moreover, standard deviation of all volunteer's results is less than the results of 5-fold validation. This shows that bootstrapping method is a usable approach for the validation process.

Another approach of wavelet decomposition was tried to extract features. The following statistical features were used to represent the time frequency distribution of the EEG signals: Maximum of the wavelet coefficients , Minimum of the wavelet coefficients, Energy of the wavelet coefficients, Standard deviation of the wavelet coefficients in approximation. Results of this approach are shown in Table 4.11. these results were not satisfied to improve accuracy. But results seems to parallel of results in the Table 4.3.

In another experiment was done as transformation the EEG data with the EPSP scaling function instead of wavelet decomposition step in algorithm in Figure 4.3. Results of this approach are shown in Table 4.7. Approximation coefficients of the signal were found by the convolution between signal and scaling function at resolution level J. These approximation coefficients that obtained from this transformation were used as features for the classification.

It is obvious that, if EPSP scaling function used as algorithm and results for resolution index J is above 5,2 , accuracy are significantly better than the results obtained by wavelet decomposition algorithm for all other wavelet. Mean accuracy take the highest value at resolution index 6,4 in despite to standard deviation is high at this index level. The optimum balance between the accuracy mean and standard deviation takes place at resolution 6,0.

All statements above and results indicate that our wavelet function suitable for classification of visual related EEG data.

Table 4.3. Classification accuracies in percent for subject number from 1 to 26 with 5-fold validation using LDA classification. The custom wavelet (epsp) is compared with some well known wavelets. The decomposition filter length of the epsp is 18 and the filter length of the other wavelets is close to or equal to 18.

Volunteer No	epsp	bior2.8	bior6.8	coif3	db8	sym8	db9	sym9
1	69,09	67,88	66,67	69,70	67,88	69,70	70,91	66,67
2	71,18	73,53	74,12	66,47	72,35	70,59	70,59	70,00
3	67,06	64,71	64,71	67,65	62,94	65,88	62,35	63,53
4	72,35	68,82	65,88	66,47	68,24	71,76	68,82	77,65
5	64,24	61,21	61,21	62,42	61,21	62,42	57,58	63,03
6	67,27	67,88	66,67	67,88	67,27	69,70	72,73	67,27
7	65,29	68,82	63,53	60,59	66,47	64,71	66,47	62,35
8	71,18	71,76	70,59	67,06	71,76	72,94	73,53	71,18
9	72,73	70,91	72,12	72,73	67,27	73,33	71,52	71,52
10	65,45	66,06	70,91	60,61	64,24	65,45	63,64	64,85
11	63,53	69,41	67,06	61,76	62,35	62,35	63,53	61,76
12	75,15	67,88	64,85	69,70	66,67	66,67	68,48	67,88
13	70,59	70,59	68,24	70,59	71,18	73,53	68,24	71,76
14	67,65	64,71	65,29	64,71	64,71	69,41	66,47	65,29
15	71,18	70,00	71,76	74,12	68,82	71,76	71,18	72,35
16	70,91	68,48	63,03	66,06	61,82	66,67	66,67	67,88
17	71,76	68,24	69,41	70,59	65,29	65,29	66,47	64,71
18	71,18	75,29	75,29	76,47	74,71	76,47	71,18	73,53
19	65,45	61,21	61,21	58,18	61,21	61,82	61,21	60,00
20	68,24	66,47	69,41	68,24	66,47	67,65	68,24	65,88
21	77,06	74,71	71,18	71,76	75,29	72,35	74,12	74,12
22	67,06	67,65	65,29	64,12	67,06	62,35	69,41	66,47
23	69,70	64,24	64,24	63,03	62,42	64,85	68,48	63,64
24	67,27	73,94	69,70	67,27	67,88	70,30	69,70	69,09
25	72,73	66,67	68,48	73,94	69,09	70,30	71,52	70,30
26	75,88	70,59	68,82	69,41	68,82	74,71	70,00	74,71
Accuracy Mean	69,66	68,53	67,68	67,37	67,06	68,58	68,19	67,98
Standard Deviation	3,57	3,67	3,73	4,60	3,90	4,19	3,97	4,51
Number of Occurrences of Winner	8	3	3	4	0	4	4	1

Table 4.4. Specificity (Qn) and Sensitivity (Qd) of classification results of the wavelet decomposition method according to different wavelets. All values are given in % and rounded.

Volunteer No	epsp		bior2.8		bior6.8		coif3		db8		sym8		db9		sym9	
	Qn	Qd	Qd	Qd	Qn	Qd	Qn	Qd	Qn	Qd	Qn	Qd	Qn	Qd	Qn	Qd
1	74	63	74	60	78	56	77	61	76	59	77	60	77	65	75	57
2	73	69	76	73	75	74	68	66	73	73	73	72	74	70	73	68
3	69	67	65	65	65	65	69	67	63	63	65	67	65	61	64	63
4	75	70	72	67	69	65	68	66	73	65	76	70	73	67	82	75
5	75	54	69	52	69	50	71	52	69	50	71	54	67	46	71	55
6	71	66	70	67	67	68	70	68	71	65	73	68	74	73	69	66
7	65	67	69	69	65	63	63	59	66	68	66	64	67	66	62	63
8	70	73	71	74	70	72	63	73	70	75	74	75	73	77	71	72
9	75	71	78	66	75	70	78	70	72	64	82	69	75	68	75	71
10	66	66	67	66	72	70	64	59	67	62	67	64	64	64	70	63
11	73	55	74	64	74	59	69	53	70	54	71	53	72	54	69	54
12	81	68	79	58	76	56	80	59	76	56	76	57	78	59	75	58
13	69	73	71	70	68	70	71	71	70	74	74	74	69	68	72	72
14	65	70	63	67	62	69	62	68	63	67	66	74	65	68	65	66
15	72	71	70	70	74	70	77	73	69	70	74	71	71	73	74	72
16	72	71	68	72	62	64	65	68	62	61	66	68	66	68	67	69
17	71	73	69	69	70	72	72	71	63	69	64	68	66	67	65	66
18	68	75	73	77	73	77	76	77	73	77	75	78	68	76	71	78
19	67	65	64	59	63	60	62	56	63	61	64	61	63	60	62	58
20	71	66	69	64	72	68	71	67	70	64	69	67	72	66	67	65
21	67	87	66	83	60	83	61	82	65	86	63	82	64	83	65	83
22	71	64	71	65	70	62	66	62	70	64	65	60	72	67	68	65
23	77	62	71	58	72	57	71	56	71	55	72	60	75	62	70	56
24	73	62	79	71	77	65	72	62	72	65	75	66	73	67	75	65
25	73	73	66	68	69	69	76	74	69	70	70	71	74	71	68	74
26	80	73	77	63	76	61	76	62	74	63	80	69	75	64	81	68
Accuracy Mean	72	68	71	67	70	66	70	65	69	65	71	67	70	67	70	66

Table 4.5. Selected channels by the channel selection steps of the wavelet decomposition method using custom wavelet 'epsp'

Volunteer No	Selected Channels for our Wavelets for each volunteer
1	Fp1, Fp2, F4, C4, P3, P4, O1, O2, T3, T5, T6
2	Fp1, F3, F4, C3, O1, O2, T3, T5, T6, Fz, Cz, Pz
3	Fp1, C3, C4, P3, P4, O1, F7, F8, T3, T4, T6, Fz
4	F4, P3, P4, O1, F8, T3, T4, Cz, Pz
5	Fp2, F3, F4, C4, P4, O2, F7, T3, T4, T5, Pz
6	F4, C3, O2, F7, F8
7	P4, O1, T4, T6
8	F4, C4, P3, O1, F8, T3, Fz, Cz
9	Fp2, F3, F4, P4, O1, T5, Fz
10	Fp2, F4, C4, P4, O2, F7, T3, T6, Cz
11	P4, T6, Fz, Pz
12	Fp1, C3, C4, P3, O1, O2, F8, T3, T4, T5, T6, Cz, Pz
13	Fp1, P4, O1, F7, F8, T3, Fz, Pz
14	Fp1, P3, P4, O1, F8, T6, Fz, Pz
15	P4, F7, T5, T6, Cz, Pz
16	Fp1, Fp2, O1, O2, T3, T4, T5
17	Fp2, C3, T3, T4, T6
18	Fp1, F3, P4, O2, F7, T3, T5, Fz, Pz
19	T5, Fz
20	Fp1, F4, C4, P4, O1, T5, Fz, Cz
21	Fp2, F3, P3, O1, O2, F8, T4, Fz, Cz
22	Fp1, F8, Cz
23	Fp2, P4, T4
24	Fp1, F3, F4, P4, O2, F7, F8, T5, T6, Fz, Cz, Pz
25	Fp1, F3, C4, P4, F8, T3, T6, Fz, Cz
26	Fp1, Fp2, O2, T5, Fz, Cz, Pz

Table 4.6. Wavelet names and corresponding most selected five channels by channel selection steps of the wavelet decomposition method from all volunteers

wavelet name	Most selected five channels in 19 channels				
epsp	P4	Fz	Fp1	O1	T3
bior2.8	O2	F7	T3	Cz	F3
bior6.8	F7	O2	T4	T3	Cz
coif3	T6	Pz	Fp1	F3	P3
db8	F7	Fp1	C3	T4	T5
sym8	F7	T4	O1	Cz	Fp1
db9	T4	O2	T3	Cz	Fp1
sym9	T5	O2	T4	T6	Pz

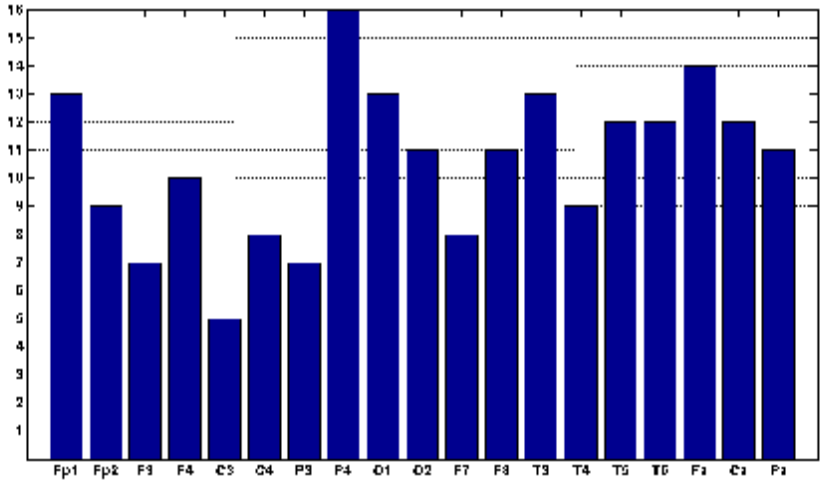


Figure 4.8. Histogram of the selected channel by wrapper method. Y axis indicate number of selection for the 26 volunteers

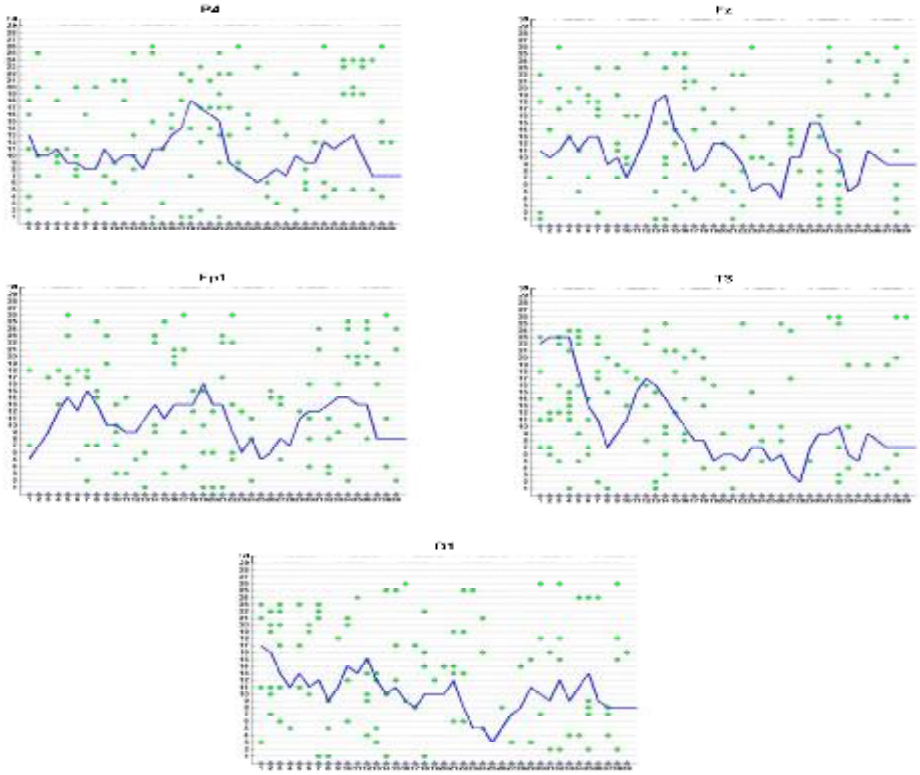


Figure 4.9. Selected features by Fishers Criteria in the feature selection unit. X-axis indicates the features, y-axis indicates the number of volunteer, green points indicate selected features and line indicates sum of the selected features over 26 volunteers.

Table 4.7. Classification accuracies in percent for subject number from 1 to 26 by using excitatory postsynaptic potential approximation method with level 2^J.

J / Volunteer No	4,00	4,40	4,80	5,20	5,60	6,00	6,40
1	64,24	65,45	69,09	73,33	70,30	74,55	77,58
2	68,82	74,71	71,76	73,53	77,06	73,53	78,82
3	63,53	62,35	67,06	73,53	73,53	75,29	78,24
4	68,82	64,12	72,94	77,06	75,29	78,82	81,18
5	60,00	63,64	64,85	66,67	71,52	69,09	69,70
6	62,42	66,67	70,30	70,30	74,55	77,58	78,18
7	64,12	65,88	69,41	70,59	70,59	72,94	72,94
8	67,06	68,24	70,59	74,12	70,00	75,29	73,53
9	64,85	71,52	69,09	75,15	76,36	75,76	77,58
10	65,45	63,03	66,67	67,88	71,52	71,52	72,73
11	70,59	65,29	61,76	65,88	62,94	70,59	62,94
12	65,45	69,70	73,94	72,12	73,94	77,58	79,39
13	68,82	68,82	67,65	74,12	72,94	74,12	78,24
14	61,76	64,12	71,18	70,59	71,76	72,35	71,18
15	68,82	67,06	68,24	75,88	77,06	78,82	82,35
16	66,67	70,30	69,09	69,70	76,36	72,73	80,00
17	64,71	71,18	68,24	73,53	73,53	74,12	81,76
18	71,76	71,18	78,24	74,12	76,47	80,00	80,59
19	64,24	69,09	67,27	66,67	69,09	70,91	79,39
20	67,06	70,00	68,82	72,94	74,71	82,35	78,24
21	63,53	71,76	77,65	78,82	73,53	78,24	78,24
22	58,24	68,24	68,24	74,12	70,00	77,06	75,29
23	68,48	68,48	67,88	75,15	69,70	72,12	68,48
24	67,27	68,48	73,94	69,70	69,70	72,73	74,55
25	66,67	72,73	67,88	72,12	75,15	73,94	69,70
26	69,41	70,00	70,00	72,35	72,35	77,65	78,24
Accuracy Mean	65,88	68,16	69,68	72,31	72,69	74,99	76,12
Standard Deviation	3,23	3,22	3,57	3,23	3,21	3,24	4,74

Table 4.8. Classification accuracies in percent for subject # from 1 to 26 using CSP as the channel selection approach of the wavelet decomposition method. The custom wavelet (epsp) is compared with some well known wavelets. Most discriminative ten channels were selected according to CSP transform.

Volunteer No	epsp	bior2.8	bior6.8	coif3	db8	sym8	db9	sym9
1	60,00	55,15	53,94	46,67	58,79	55,76	63,03	49,70
2	59,41	61,18	58,24	61,18	54,12	56,47	59,41	46,47
3	61,76	51,76	49,41	54,71	51,18	55,29	55,29	52,35
4	62,94	61,76	60,59	67,06	66,47	64,71	62,35	60,00
5	53,33	48,48	52,12	43,03	47,88	43,64	41,21	49,09
6	53,33	57,58	53,33	53,33	48,48	58,79	56,97	50,91
7	63,53	50,59	52,35	50,59	53,53	57,06	55,88	54,12
8	60,00	52,35	57,06	58,82	59,41	58,82	48,82	57,65
9	61,82	63,03	58,79	55,76	58,18	60,00	53,33	53,94
10	59,39	56,36	56,97	50,91	58,79	57,58	57,58	57,58
11	56,47	54,12	54,71	54,12	50,59	43,53	53,53	54,71
12	61,82	64,24	55,76	59,39	54,55	57,58	62,42	55,76
13	65,88	57,65	64,12	57,06	61,18	57,06	61,18	54,71
14	58,82	57,06	60,00	62,35	55,88	51,76	54,12	59,41
15	56,47	55,88	56,47	53,53	53,53	51,18	54,12	51,76
16	53,94	58,79	58,18	59,39	58,79	60,61	60,61	55,15
17	60,59	53,53	55,29	60,59	54,71	53,53	57,06	56,47
18	66,47	67,06	72,94	72,94	70,59	75,29	71,76	68,24
19	44,24	50,91	53,94	50,30	53,33	53,33	50,30	51,52
20	61,18	63,53	61,76	57,06	67,06	62,94	63,53	60,00
21	59,41	61,76	61,18	68,82	67,06	58,82	60,00	66,47
22	55,88	57,06	59,41	54,12	52,94	57,06	58,24	57,65
23	54,55	49,09	45,45	41,21	43,03	46,67	49,70	47,27
24	65,45	58,18	56,36	60,00	55,15	54,55	53,94	55,15
25	64,85	68,48	57,58	66,67	64,85	60,00	59,39	60,00
26	66,47	56,47	60,00	50,59	55,29	57,65	57,65	55,88
Accuracy Mean	59,54	57,39	57,15	56,55	56,74	56,53	56,98	55,46
Standard Deviation	5,09	5,35	5,16	7,56	6,57	6,42	5,93	5,15
Number of occurrence of Max	12	4	3	4	1	3	2	1

Table 4.9. Classification accuracies in percent for subject number from 1 to 26. The custom wavelet (epsp) is compared with some well known wavelets. Bootstrapping cross validation was used instead of 5-fold validation

Volunteer No	epsp	bior2.8	bior6.8	coif3	db8	sym8	db9	sym9
1	79,73	77,33	78,79	78,91	80,97	79,15	80,30	78,91
2	79,94	82,47	82,62	79,97	80,03	79,85	79,50	78,47
3	77,88	76,44	76,79	76,29	74,50	77,00	77,03	77,41
4	79,18	78,71	78,65	77,44	78,56	79,38	80,50	77,62
5	79,09	77,91	76,52	77,30	78,52	77,85	75,39	77,55
6	76,30	77,82	77,94	75,94	77,18	79,61	75,48	77,06
7	77,15	77,03	78,15	76,38	76,18	78,38	77,35	75,85
8	79,18	79,91	79,06	77,97	79,91	77,38	78,35	77,47
9	78,64	79,88	79,79	79,12	80,79	78,48	78,33	77,30
10	80,24	78,82	78,33	78,64	77,94	78,33	78,12	78,18
11	77,44	76,47	76,79	75,38	76,35	76,82	76,82	76,68
12	83,12	78,45	79,36	78,09	77,09	79,18	79,91	80,45
13	79,76	78,56	79,47	79,41	78,21	77,06	77,88	77,26
14	78,97	79,74	77,32	78,62	78,53	78,47	79,50	78,00
15	79,44	80,15	79,21	81,85	80,76	81,44	81,47	80,00
16	78,97	79,30	78,27	77,61	78,21	78,33	78,91	78,30
17	78,29	78,74	76,97	77,24	76,85	78,74	77,85	78,94
18	79,56	80,47	81,65	80,68	80,82	79,59	81,82	80,03
19	76,61	77,52	76,73	76,18	76,39	77,61	76,58	75,67
20	77,68	77,35	78,79	79,32	79,06	79,53	79,24	78,50
21	82,91	80,74	80,82	80,62	81,56	81,85	79,56	82,06
22	79,18	79,29	77,44	77,21	77,56	76,65	78,88	76,62
23	78,58	78,79	79,24	79,24	79,64	78,24	77,97	77,30
24	81,39	80,30	80,55	79,55	78,82	79,09	81,24	79,73
25	80,97	78,55	80,52	79,45	79,45	77,76	80,18	79,24
26	81,24	78,76	80,18	80,68	80,71	80,15	78,91	80,15
Accuracy Mean	79,29	78,83	78,84	78,43	78,64	78,69	78,73	78,26
Standard Deviation	1,69	1,41	1,59	1,67	1,80	1,31	1,70	1,52
Number of Occurrences of Winner	10	4	1	1	4	4	2	1

Table 4.10. Classification accuracies in percent for subject number from 1 to 26 with 5-fold validation using Backpropagation Neural Network classification. The custom wavelet (epsp) is compared with some well known wavelets. The decomposition filter length of the epsp is 18 and the filter length of the other wavelets is close to or equal to 18.

Volunteer No	epsp	bior2.8	bior6.8	coif3	db8	sym8	db9	sym9
1	67,27	67,88	68,48	65,45	66,06	64,24	64,85	64,24
2	62,35	68,24	68,24	65,29	70,00	65,29	66,47	65,88
3	63,53	63,53	64,12	64,71	62,94	62,94	63,53	62,94
4	72,35	75,29	71,18	71,18	71,18	71,18	71,18	74,71
5	67,27	63,64	63,64	59,39	62,42	62,42	62,42	61,21
6	63,64	69,09	65,45	67,27	66,67	64,24	64,85	65,45
7	68,82	62,35	62,94	67,06	65,29	65,29	62,94	63,53
8	65,29	65,88	65,88	62,94	65,29	62,35	65,29	63,53
9	64,85	61,21	66,06	63,03	63,64	66,06	65,45	63,64
10	65,45	64,85	63,03	62,42	65,45	63,64	64,24	68,48
11	67,65	61,18	64,12	65,88	62,94	64,71	65,88	64,12
12	69,09	67,88	67,27	68,48	66,06	67,88	68,48	71,52
13	67,06	65,29	67,06	67,65	62,94	62,35	64,71	65,29
14	73,53	67,06	68,82	70,59	69,41	69,41	65,88	69,41
15	66,47	63,53	62,35	64,71	64,12	60,59	62,94	62,35
16	64,24	64,85	66,67	64,85	67,88	67,27	65,45	63,64
17	68,82	64,12	64,12	64,71	65,88	68,82	67,06	65,29
18	71,18	70,00	71,18	72,94	71,76	70,59	72,35	74,12
19	61,21	63,03	61,82	61,21	63,03	62,42	59,39	61,82
20	64,12	68,24	68,24	65,88	68,82	68,24	67,65	65,29
21	67,65	68,82	68,82	68,24	70,59	68,82	67,06	71,76
22	62,35	61,76	61,18	61,18	60,00	60,00	60,59	61,18
23	64,24	62,42	67,27	60,00	61,82	63,64	61,82	63,03
24	66,67	69,09	69,09	72,12	69,09	64,24	70,91	68,48
25	70,30	72,73	69,09	74,55	70,30	69,09	68,48	72,12
26	73,53	67,65	67,65	70,00	68,82	71,18	70,59	70,00
Accuracy Mean	66,88	66,14	66,30	66,22	66,25	65,65	65,79	66,27
Standard Deviation	3,39	3,57	2,82	4,01	3,28	3,28	3,26	4,04
Number of Occurrences of Winner	8	4	4	4	4	2	0	4

Table 4.11. Classification accuracies in percent for subject number from 1 to 26. The custom wavelet (epsp) is compared with some well known wavelets. Approximation statistics was used instead of approximation coefficient and 5-fold validation is used.

Volunteer No	epsp	bior2.8	bior6.8	coif3	db8	sym8	db9	sym9
1	66,67	66,06	63,64	64,24	64,24	66,67	63,64	63,64
2	62,94	60,00	60,00	58,24	59,41	58,82	60,59	59,41
3	67,06	66,47	67,65	62,35	70,59	65,29	60,59	68,24
4	75,88	72,35	69,41	61,18	63,53	65,29	67,06	66,47
5	69,09	61,21	58,18	62,42	61,21	58,79	64,85	60,00
6	66,67	64,24	64,24	66,67	63,64	67,27	69,70	69,70
7	61,18	69,41	62,94	69,41	70,00	64,12	65,88	61,76
8	62,35	63,53	62,35	59,41	60,00	58,82	60,59	59,41
9	63,64	61,82	62,42	61,21	64,24	59,39	63,64	59,39
10	68,48	64,85	64,85	63,64	63,03	66,67	61,21	66,67
11	60,59	59,41	55,29	58,82	57,06	62,35	57,06	57,06
12	71,52	66,06	70,30	67,27	69,70	72,73	66,06	70,91
13	66,47	61,76	61,76	64,12	67,06	64,71	66,47	64,12
14	65,88	64,71	63,53	61,76	67,65	65,29	62,35	64,71
15	60,00	60,00	61,18	61,18	59,41	59,41	68,24	65,29
16	68,48	58,18	61,82	66,67	66,06	60,61	66,67	68,48
17	65,88	63,53	68,82	66,47	62,94	61,18	68,82	61,76
18	65,29	66,47	67,06	71,18	70,00	67,06	74,12	68,24
19	63,64	63,03	61,82	63,03	60,61	61,82	66,06	60,61
20	70,59	63,53	64,12	62,35	60,00	60,59	66,47	60,59
21	62,94	65,88	67,06	60,59	62,94	65,29	61,76	65,29
22	64,71	65,29	65,29	61,76	62,35	66,47	58,82	62,94
23	62,42	61,82	58,79	60,61	61,21	58,79	62,42	60,00
24	57,58	62,42	62,42	65,45	60,61	61,21	63,03	67,27
25	58,18	63,03	62,42	55,15	63,03	60,61	59,39	63,03
26	65,88	62,94	62,35	65,88	67,65	56,47	63,53	62,35
Accuracy Mean	65,15	63,77	63,45	63,12	63,78	62,91	64,19	63,74
Standard Deviation	4,16	3,10	3,51	3,59	3,77	3,78	3,83	3,71
Number of Occurrences of Winner	8	2	2	0	7	4	6	4

4.2.2. Classification with features of Section 3.7.

As stated in chapter 3, several descriptors were used to characterize the EEG structures by taking the features of data. Signal parameters extracting method can be suitable way to analyze and classify EEG signals. In this study, we have used various measures to study and investigate the familiar and unfamiliar related EEG signals. We produce 14 different feature types for one second EEG data started right after the stimulus onset. These feature type can be categorized as follow: entropy based features, such as signal energy, nonlinear energy, sixth power energy, Shannon's entropy, frequency based features as reyni entropy and mean frequency, max frequency match filter, amplitude based features as average and difference method, Petrosian fractal dimension, median method and parametric based features as Barlow and Hjorth parameters methods. In the following table shows that all feature types and number of features in a feature type which detail in Table 4.12.

Table 4.12. Feature types for classification algorithm and number of features of each feature type.

No	Feature Types	Number of Features
1	Curve Length	5
2	Signal Energy	5
3	Nonlinear Energy	5
4	Sixth Power Energy	5
5	Mean Frequency	1
6	Reyni Entropy	1
7	Shannon Entropy	1
8	Average Method	5
9	Difference Method	5
10	Barlow Parameters	3
11	Hjorth Parameters	3
12	Petrosian Fractal Dimension	1
13	Max Frequency Match Filter	1
14	Median Method	1

Two kinds of strategy were developed with using feature types for classification familiar -unfamiliar related EEG data as shown in Figure 4.4 and Figure 4.5. First of them is the consensus method and other one is the concatenate method.

Both algorithms began with the construction unit of feature types .Here an overview; firstly, raw EEG data was filtered with band pass filter of bandwidth 0.5-15 Hz and then EEG data was segmented to familiar and unfamiliar. Afterward, EEG data that segmented into one second parts starting right after stimulus onset and normalized with zero mean and unit variance was employed to feature construction procedure. 42 features were constructed as shown in Table 4.12 from 14 feature type. Then, channel selection and feature type selection units were run for signal enhancement purpose respectively. Finally, classification algorithm was employed with Fisher linear discriminant method to discriminate the familiar - unfamiliar related VEP.

In the consensus method shown in Figure 4.4, each feature type was processed separately until the end of the algorithm. Then, consensus method was applied to combine and generate the common result. The proposed combination scheme explained as fallow: there are 14 different classifiers for 14 feature types. Each of these classifiers produces output results such as where k=1,…,14, is the pattern and j is the class label 0 or 1. In feature type selection unit, feature types ranked by these classifier results and sorted from higher to lower, afterwards optimal feature types were selected according to the sorted result. Classification process was run with using the selected feature type. The majority vote rule was used to combine the classifier results as familiar or unfamiliar. The final result is determined by result of majority vote procedure applied to classifier results.

In the concatenate method shown in Figure 4.5, features that comes from all feature types was concatenated in beginning of the feature selection unit. The rest of the algorithm was the similar to wavelet decomposition algorithm.

Results of both methods are given in the following tables Table 4.13 and Table 4.14. According to the results given in Table 4.13 and Table 4.14, these methods produced almost similar classification performance compared to wavelet decomposition method and scaling approximation method. On the other hand, in case of comparison two methods, results of the concatenate method are slightly better than results of the consensual method. This situation can be explained like that; grouping

the coefficients by concatenating method improves the classification accuracy. The difference between the accuracies is nearly 3%.

As it can be clearly seen in the Table 4.13 that the first, second and sixth feature types in Table 4.12 were mostly selected feature types. These feature types are related to temporal and entropy based information of the data. This indicates that difference between the familiar and unfamiliar data is generally connected to the amplitude of the signals. In other word, ERPs related to familiar and unfamiliar face stimuli have different energy levels and elicited component.

Table 4.13. Classification accuracy in percent for subject No from 1 to 26 by using feature types with consensus method with sensitivity, specificity and overall accuracy measures. Also, selected feature types by the algorithm are given in right.

Volunteer No	Sensitivity-Qd	Specificity-Qn	Overall accuracy-Qo	Selected feature types
1	65,54	70,22	68,94	1 2 4 6 11 14
2	73,48	70,18	70,24	1 7 8 11
3	74,97	74,76	72,62	1 3 7 8 9
4	70,24	89,34	75,60	1 2 14
5	61,11	76,54	68,94	1 2 5 6 7 9 10
6	80,74	77,15	76,19	1 4 10 14
7	73,34	79,02	75,60	1 6 11 13 14
8	72,47	56,13	60,71	1 2 3 5 13 14
9	71,85	68,24	69,05	1 2 6 10
10	72,80	71,00	70,83	1 4 6
11	65,44	65,30	64,88	1 2 3 11 13 14
12	62,59	70,08	67,70	1 2 4 5 7 8
13	71,58	59,10	61,90	1 2 5 11
14	80,74	64,83	70,19	1 2 5 7
15	75,97	71,96	72,62	1 2 4 5 6 7
16	71,47	64,64	65,48	1 5 10 12
17	77,37	66,88	70,24	1 3 11 13
18	75,42	77,54	75,78	1 2 3 4 14
19	76,07	62,72	66,07	1 7 9 14
20	68,19	79,35	73,21	1 2 10
21	79,53	60,25	70,24	1 3 4 6 8 11
22	66,16	74,26	69,64	1 6 10 12 14
23	66,94	76,69	72,02	1 2 5 6 13
24	78,83	68,57	71,43	1 6 8 12
25	75,91	67,37	70,81	1 3 4 5
26	59,82	72,25	66,67	1 3 4
Accuracy Mean	71,87	70,55	69,91	
Standard Deviation	5,92	7,32	4,00	

Table 4.14. Classification accuracy in percent for subject number from 1 to 26 by using feature types with concatenate method with sensitivity, specificity and overall accuracy measures. Also selected channels by the channel selection steps is in right side and most selected channels is in right bottom side

V. No	Sens.	Spec.	Overall acc	Selected channels
1	67,00	78,93	72,12	Fp2 , F3 , O1 , O2 , F7 , F8 , T4 , Cz,
2	70,78	74,32	71,67	Fp1 , F4 , C4 , P3 , O1 , O2 , F8 , T5 , T6 , Fz , Pz,
3	74,37	79,61	75,14	Fp1 , Fp2 , F3 , C3 , C4 , P3 , O1 , O2 , T3 , T6 , Fz , Pz,
4	71,26	80,71	74,59	P3 , O1 , F7 , T4 , T6 , Cz , Pz,
5	69,40	70,64	68,11	Fp2 , F3 , P4 , O1 , O2 , F8 , T3 , T4 , T6 , Fz,
6	69,44	74,14	71,89	F3 , F4 , C3 , P3 , P4 , O1 , O2 , F8 , T3 , T4 , T6 , Fz , Pz,
7	69,03	74,23	70,81	Fp2 , P3 , P4 , O2 , F7 , F8 , T3 , T6 , Cz , Pz,
8	71,61	76,36	72,63	Fp1 , Fp2 , F4 , C4 , P3 , O1 , O2 , F7 , T3 , T4 , T5 , Fz , Cz , Pz,
9	61,51	65,70	63,68	Fp2 , F3 , F4 , C3 , C4 , P3 , F7 , T5 , T6 , Cz , Pz,
10	69,13	76,61	72,63	Fp1 , F4 , C3 , C4 , P3 , P4 , T3 , T5 , Fz , Cz,
11	70,24	70,47	69,47	Fp1 , C4 , P4 , O1 , O2 , T6,
12	68,31	73,04	70,53	Fp1 , F3 , F4 , C3 , C4 , O1 , O2 , T6 , Fz,
13	76,27	81,37	78,42	Fp2 , F3 , F4 , O1 , O2 , T4 , T5 , Cz,
14	70,37	75,71	71,58	Fp2 , C3 , C4 , P4 , F8 , T4 , T5 , T6 , Fz , Cz,
15	62,39	68,41	65,26	F8 , T4 , Cz , Pz,
16	77,04	74,85	75,26	F3 , F4 , C3 , C4 , P4 , O2 , F8 , T4 , T5 , Fz , Cz , Pz,
17	75,39	74,79	74,74	F4 , C3 , C4 , P3 , P4 , O1 , O2 , T4 , T5 , T6 , Cz , Pz,
18	72,91	78,44	75,38	Fp2 , F3 , P4 , O1 , O2 , F7 , T3 , T5 , Fz , Cz,
19	66,81	68,92	67,69	Fp2 , C3 , C4 , F7 , Pz,
20	73,96	74,50	73,85	Fp1 , Fp2 , F3 , P3 , P4 , T3 , T4 , Cz , Pz,
21	75,55	74,13	74,15	Fp2 , F3 , C4 , P3 , O1 , O2 , F8 , T5 , T6 , Fz , Pz,
22	65,70	63,09	63,90	C3 , C4 , O1 , T5 , Fz,
23	73,48	66,22	68,78	Fp1 , C3 , C4 , O1 , F8 , T3 , T4 , T5 , Pz,
24	71,33	68,98	69,27	Fp1 , F3 , C4 , O2 , F7 , F8 , T3 , T6 , Fz , Cz,
25	69,26	68,81	68,29	Fp1 , Fp2 , C4 , F8 , T4 , T6 , Pz,
26	76,24	71,59	73,17	F3 , P3 , P4 , T6,
Acc. Mean	70,50	73,32	71,19	**Most Selected Five Channels**
Std.	3,97	4,84	3,74	'C4', 'O1', 'O2', 'T6', 'Pz'

4.4. Results of BCI Competition III P300 Speller Data

Now developed multiresolution and approximation method that introduced in the previous sections, are used to classify on the dataset produced by a P300 speller matrix during the BCI competition III (Krusienski & Schalk, 2004) from 2 different subjects at different acquisition sessions. We need features of signals to feed the classifier. These signals have been preprocessed after building the features.

Initially, 0.1 to 15 Hz band of the EEG data filtered out to extract VEPs. We pull out all data for each channel in between 0 to 1 s posterior to the beginning of intensification. In training step we use only time interval of 150-650 ms. This window is large enough to capture all required time features. An averaged P300 signal over Cz electrode is given in Figure 4.13 and some examples of segmented signals were given in Figure 4.14. Afterwards, wavelet decomposition of the VEP data is performed up to level 4.

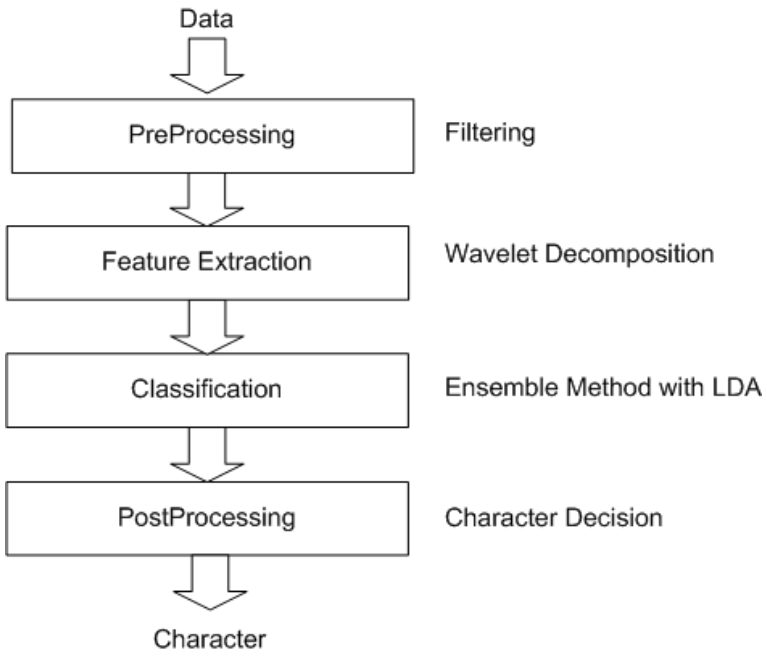


Figure 4.10. General signal processing flow chart for the P300 Speller Paradigm.

All analysis was performed offline for classification performance. Figure 4.10 represents the flow chart for classification algorithm of the P300 Speller Paradigm and Figure 4.12 shows the detailed version of the this algorithm (Çelik & Arıca,

2010). The test set of the data contains 100 symbols and performance accuracy is equal to true predicted symbol. Table 4.16 depict the classification results for Subject A and B versus six wavelet types and number of repetitions for three electrode sets and for 5, 10 and 15 repetitions. Mean performances are shown in Table 4.17.

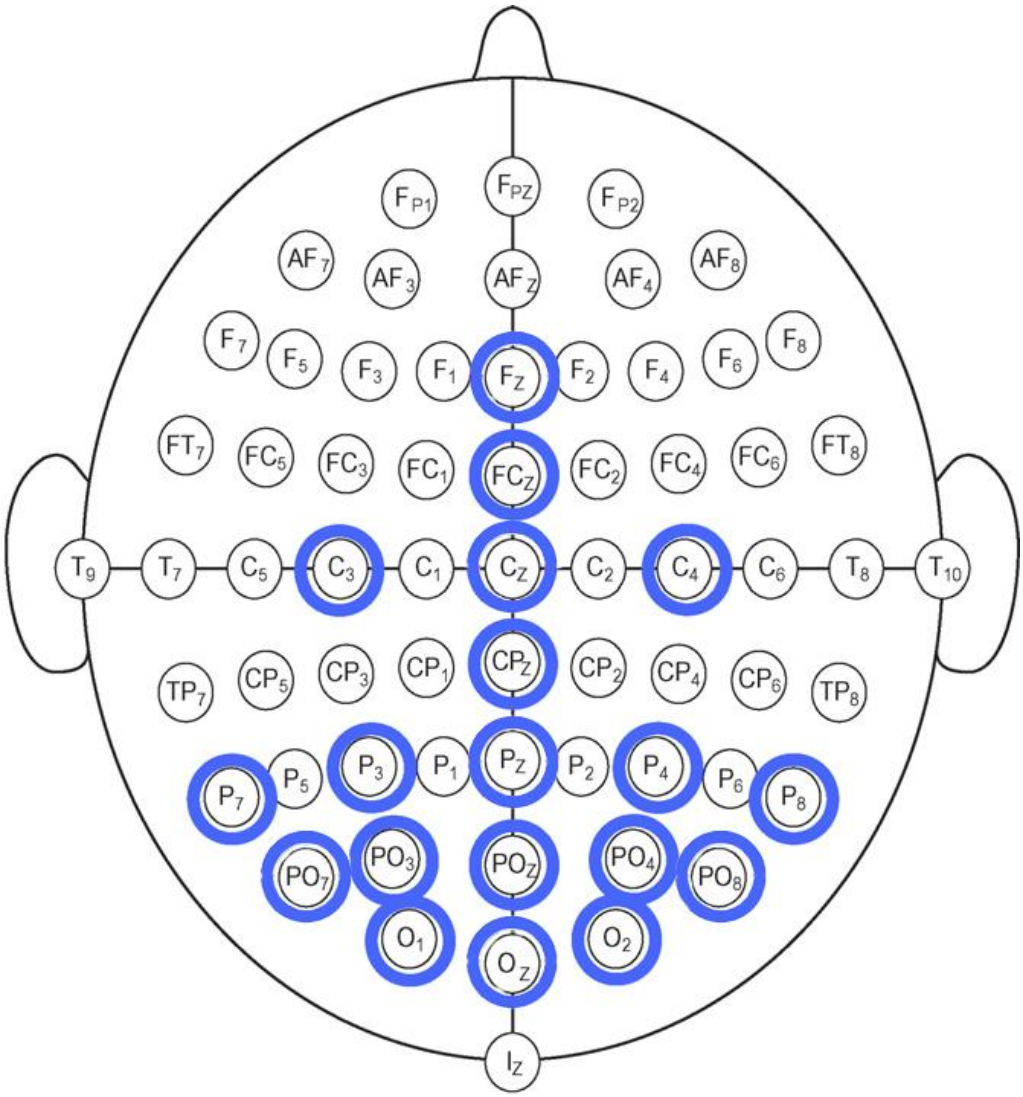


Figure 4.11. The 64-channel electrode montage and the predefined channel set.

Three electrode configurations were studied (Çelik & Arıca, 2010); the standard 19 channels international 10-20 electrode system, all 64 channels and predefined19 channels as illustrated in Figure 4.11. The predefined 19 channels represent the posterior, central and occipital regions that have strong correlations of P300 response (Krusienski et al., 2008).

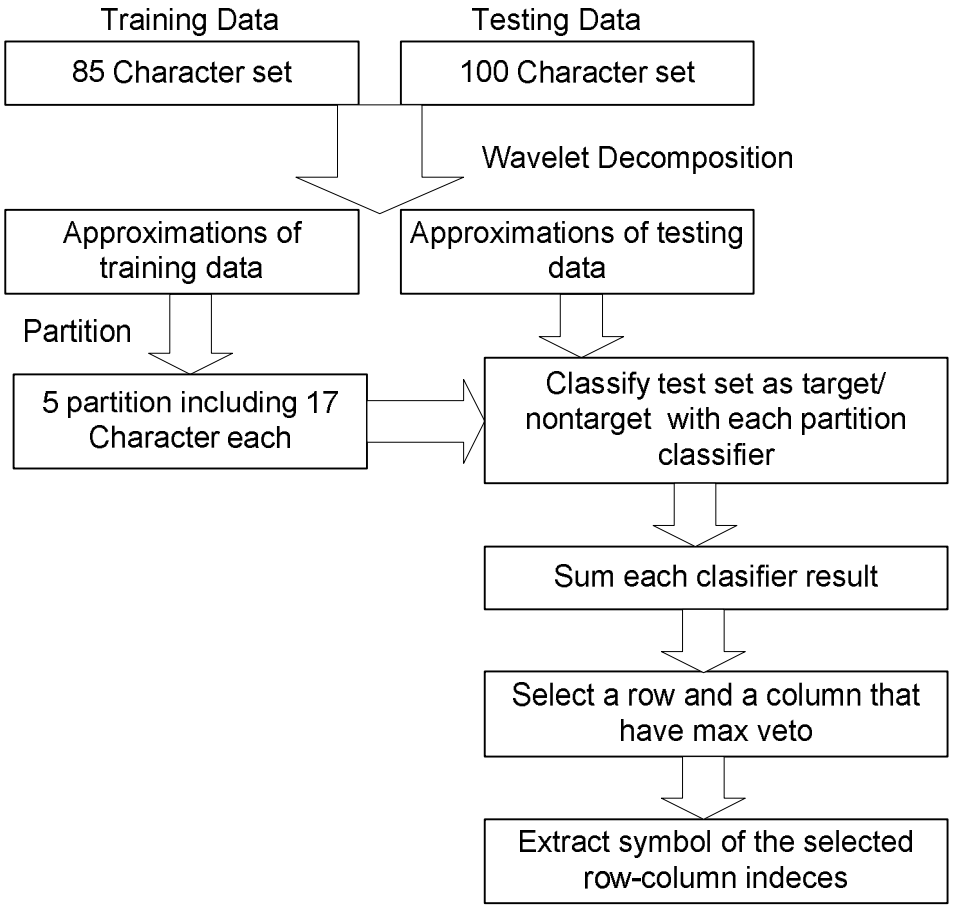


Figure 4.12. Detailed signal processing scheme of the work

Multiresolution approximation coefficients of the EEG data of these configurations are computed; namely the data is transformed.

P300 Speller paradigm has two problems. First, P300 ERP component that occurs after desired character intensified, named a post-stimulus signal have to predict. Afterwards, desired character has to be correctly predicted so this deals with a 36-class classification problem.

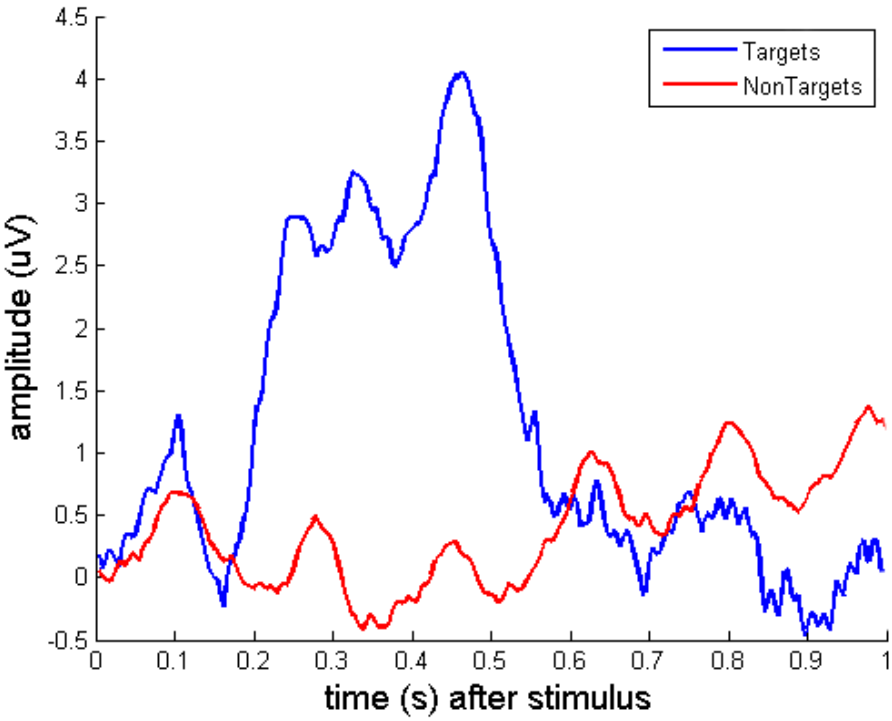


Figure 4.13. A P300 Potential averaged responses over Cz electrode.

BCI III competition dataset consist of 85 desired characters. For the spelling of a single character, each of the 12 rows and columns of the matrix is intensified. This sequence of intensifications is repeated 15 times for each character. Hence, post stimulus spelling segment correspond to 12x15x85=15300 signals. Also, EEG collected over 64 channels.

The classification strategy is presented for the P300 Speller paradigm. This strategy consists of two steps. At first, a multiple classifier is described to detect the P300 component. Secondly, a routine deals are set up with how classification results of first step are transformed into a decision for the desired character.

In this multiple classifier approach an ensemble of classifiers is used (see in Figure 4.12). The ensemble method was implemented for SVM by Rakotomamonjy and Guigue (2008). This method is used for LDA, but it differs from Rakotomamonjy and Guigue (2008) study for size of partitions and selected channels. The training dataset is divided into five equal size parts. Each part is composed of signals associated with 17 characters. Characters composing each part

built up from 85 sequences by randomly selecting 17 characters. A classifier for each part is constructed for each part and each classifier in the ensemble is trained on its part. Test set is applied to each of the five classifier for distinction of the targets that include P300 component and non-targets that do not include P300 component. The voting of the classifiers (the sum of the classifier results) was used to determine the target character. The highest votes for column and row intensifications are identified and then the character at these row-column indices of the character matrix is assigned as predicted character.

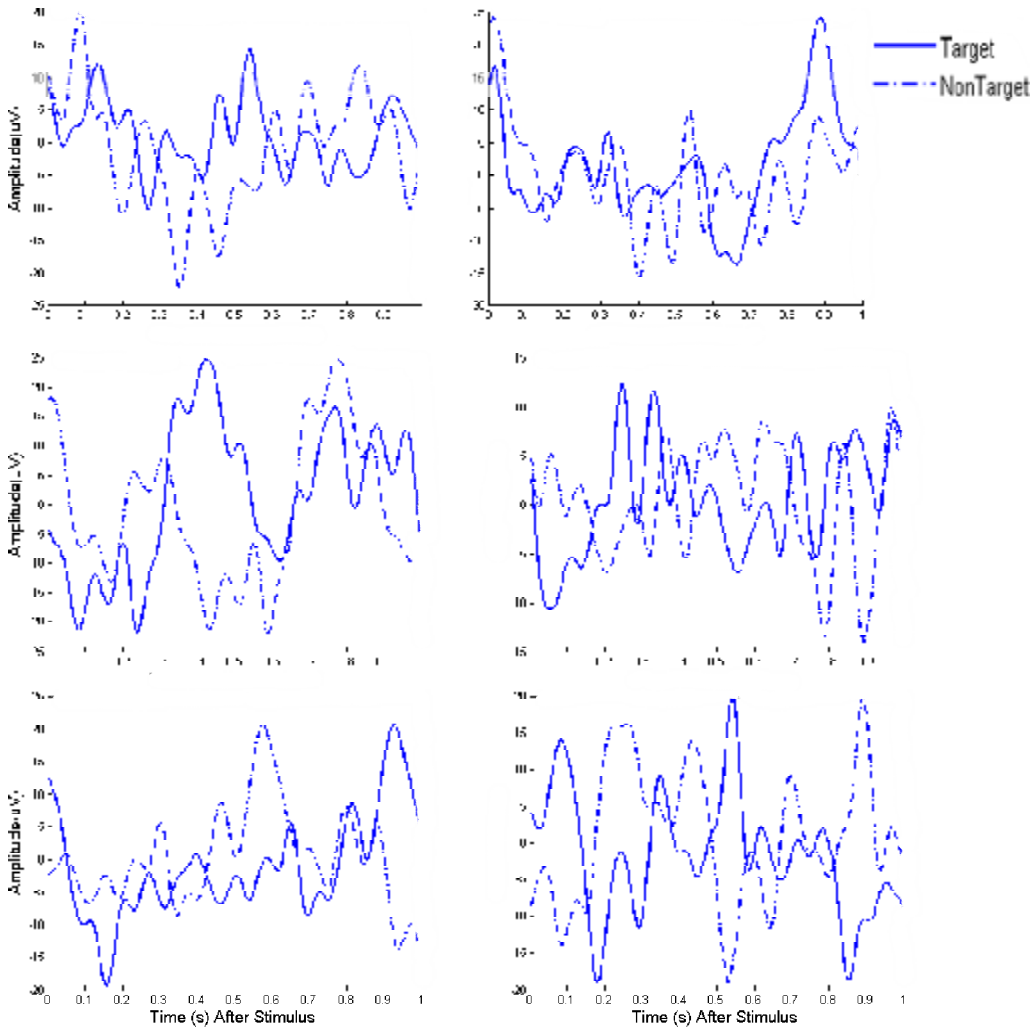


Figure 4.14. A couple of one second speller signals.

The algorithm was realized by using Matlab (Mathworks Inc.), and Matlab statistical and wavelet toolboxes (mathworks.com, 2010). Filters of our multiresolution system were introduced to the wavelet toolbox and named as 'epsp'. The decomposition filter length was 18. We also utilized bi-orthogonal spline wavelets with decomposition and reconstruction filters orders; (8, 2), (8, 6) and filter length of 18. We also employed Daubechies wavelet, Symlet and Coiflet with filter lengths of 16, 16, and 18 respectively. Note that wavelets are considered with decomposition filter orders same with or close to decomposition filter order of our wavelet.

As it can be seen from Table 4.16, classification accuracy of subject A at 5 and 10 repetitions is low with respect to subject B. However, the performances of both subjects at 15 repetitions are similar. In case of mean performances, the best performances obtained from the predefined electrode set and the extended 64 electrode with Daubechies wavelet; 95% and 94.5% respectively. The highest performance of the standard 10/20 electrode set has been obtained with Symlet. Classification accuracy result of the custom wavelet is near to the average performance of the other wavelets. The average accuracy of all wavelets for the standard, the extended and the predefined electrode set are 86.25%, 91.1% and 93% respectively (see in Table 4.17). This result shows that the predefined 19 channels perform better than the 64 channel and the 10/20 system in average.

Table 4.15. Highest five performance measures of BCI Competition III . The first column of results shows the results of all 15 repetitions and second column only five repetitions (Original Tables in http://www.bbci.de/competition/iii/results/index.html)

#.	Contributor	Acc (15)	Acc (5)	Research Lab
1.	Alain Rakotomamonjy	96.5%	73.5%	PSI CNRS FRE-2645, INSA De Rouen, France
2.	Li Yandong	90.5%	55.0%	Department of Automation Department Of Biomedical Engineering, Tsinghua University, China
3.	Zhou Zongtan	90.0%	59.5%	Department of Automatic Control, National University Of Defense Technology, China
4.	Ulrich Hoffmann	89.5%	53.0%	Ecole Polytechnique Federale De Lausanne (EPFL), Switzerland
5.	Lin Zhonglin	87.5%	57.5%	Department of Automation, Tsinghua University, China

Note that these BCI competition datasets were studied various researcher and they construct the different and similar approach to our strategy. Blankertz et all BCI Competition III review gives the result of P300 dataset that result is shown in Table 4.15. (Blankertz, et al., 2006).

The accuracy of the study at first position of the rank list of the BCI completion III is 96.5% (Rakotomamonjy & Guigue, 2008). The accuracy achieved by our method is close to this result. The 2nd ranked study reports 90.5% accuracy for 15 repetitions. Our study is placed in 2nd rank with 94.5% of Daubechies wavelet or 91% of the epsp obtained from the predefined channels.

Table 4.16. Classification accuracy in percent for subject A and subject B for spelling the symbols. The custom wavelet (epsp) is compared with some well known wavelets. The decomposition filter length of the epsp is 18 and the filter length of the other wavelets is close to or equal to 18.

		Number of repetitions					
		Subject A			**Subject B**		
		5	**10**	**15**	**5**	**10**	**15**
Standard 10/20 system	epsp	31	61	85	55	80	88
	db8	37	72	85	54	78	86
	coif3	33	64	86	47	74	81
	sym8	33	65	92	46	81	91
	bior2.8	30	65	87	51	73	84
	bior6.8	30	61	86	46	74	84
All 64 Channels	epsp	31	74	91	52	85	90
	db8	25	74	96	57	86	94
	coif3	25	71	86	61	86	88
	sym8	32	69	91	56	87	91
	bior2.8	27	68	92	60	87	92
	bior6.8	26	68	91	57	85	91
Predefined 19 channels	epsp	40	70	91	71	87	91
	db8	47	78	96	72	87	93
	coif3	38	72	93	72	86	90
	sym4	36	70	92	72	87	93
	bior2.8	42	71	95	71	87	93
	bior6.8	41	71	96	69	86	93

Table 4.17. Mean classification accuracy in percent for spelling the symbols. The custom wavelet (epsp) is compared with some well known wavelets. The decomposition filter length of the epsp is 18 and the filter length of the other wavelets is close to or equal to 18.

		Number of repetitions		
		5	**10**	**15**
Standard 10/20 system	epsp	43	70,5	86.5
	db8	45,5	75	85.5
	coif3	40	69	83.5
	sym8	39,5	73	91.5
	bior2.8	40,5	69	85.5
	bior6.8	38	67,5	85
All 64 Channels	epsp	41,5	79,5	90.5
	db8	41	80	95
	coif3	43	78,5	87
	sym8	44	78	91
	bior2.8	43,5	77,5	92
	bior6.8	41,5	76,5	91
Predefined 19 channels	epsp	55,5	78,5	91
	db8	59,5	82,5	94.5
	coif3	55	79	91.5
	sym4	54	78,5	92.5
	bior2.8	56,5	79	94
	bior6.8	55	78,5	94.5

5. RESULTS AND SUGGESTIONS

In this thesis, EEG recordings are analyzed and classified accompanying visual evoked potentials. Familiar and unfamiliar faces are used as a visual stimulus. Faces are rich sources of information and aim of this study is to investigate in response to familiar and unfamiliar faces in the time-frequency domain.

The datasets from Başkent University, Adana Application and Research Center and BCI competition III are used for investigation. The first dataset paradigm is the familiar and unfamiliar face visual stimulus, the second is the P300 speller odd-ball paradigm.

Initially VEP was analyzed by short time Fourier transform to visualize structures in the time frequency domain. Then, the statistical tests were applied to examine to discriminate power.

This thesis presented a novel scaling-wavelet function pair and its bi-orthogonal complements by resembling the waveform of the scaling function to excitatory post-synaptic potential for classification. These approximation coefficients was used to obtain to distinction the familiar-unfamiliar face specific VEP. An EEG signal can be considered as filtered version of sum of electrical signals of a group of neurons such as excitatory and inhibitory post-synaptic potentials, spikes etc. As the skull and scalp acts as low pass filter and since a VEP is a low pass filtered signal we can expect that a VEP is composed by excitatory post-synaptic potentials (EPSPs) as spikes are filtered out by low pass filtering. Since then we use a function that resembles shape of EPSP waveform to construct a scaling function.

In addition to the wavelet decomposition approach, the entropy, frequency and amplitude based features of the EEG data was used to separate familiar and unfamiliar related EEG. The features are the well known and widely used features in EEG signal processing literature. Classification using these features could be facilitated for comparisons between different approaches and testing classification performance of our wavelet approximation method. This study represents an attempt to incorporate the basic informational characteristics for analysis of EEG signals. In particular, it shows the feasibility of combination of those measures for recognition

of familiar- unfamiliar EEG patterns. In addition, various conversion methods are applied during construction of these features.

In order to generalization performance of the classifier output, feature selection and channel selection methods were implemented in the classification algorithms. Aims of the using feature selection to identify and remove redundant information in the data and reduce training and utilization times and storage requirements. In addition to wrapper methods and the filter methods as feature selection, common spatial pattern was used for this manner. As a further process, CSP was used to construct coefficients for using as EEG features. Both spatial and spatio-temporal approach of CSP was employed for distinguishing the VEP data. Another generalization method that used in this study was the data validation techniques as n-fold and bootstrapping. They supply to improve estimate of classifier performance.

In conclusion, EEG data supplied from our recording paradigm was used for analysis and classification. All our experiments indicated that the best classification results were obtained with the proposed custom wavelet compared to the others wavelets on our EEG data. Besides, to the authors knowledge, time-frequency analysis with wavelets was not investigated to separate familiar and unfamiliar face related EEG. Our approach using time frequency analysis and a machine learning algorithm was used to determination of event related EEG as familiar or unfamiliar for the first time in literature. On the other hand, results of classification algorithm with EEG data features type were similar to results obtained from wavelet decomposition approach. Furthermore, applying the ensemble method using the custom wavelet to extract approximation coefficients of the VEPs from BCI Competition III P300 Speller data obtained 91% accuracy from the predefined channel set and this result takes second place in the BCI competition III competition results. Obtained results indicate that our approach was provided an option to classify of visual related EEG.

The work in this thesis can be improved adding some approach for some future works. One can be change the design of the experiment. It can be effective way that measure heart rate, measure breathing and tracing the eye movement.

Besides, in order to possibly improve the classification performance of the algorithms. It would also be interesting to take into account combine the different type of feature extraction method. Besides the our feature extraction method parametric method as autoregressive moving average (ARMA) models could be used for feature extraction unit. Additionally, it could be tried different type of nonlinear classifiers. In this study VEP was analyzed and classified, also upper EEG band such as beta and gamma bands can be used. These bands is related to cognition process and these band may be contain information about familiar and unfamiliar distinction problem.

REFERENCES

ALLISON, T., PUCE, A., SPENCER, D., & MCCARTHY, G. (1999). Electrophysiological studies of human face perception. I: Potentials generated in occipitotemporal cortex by face and non-face stimuli. *Cerebral Cortex* , 415.

ALPAYDIN, E. (2004). *Introduction to Machine Learning.* The MIT Press.

ANAKI, D., ZION-GOLUMBIC, E., & BENTIN, S. (2007). Electrophysiological neural mechanisms for detection, configural analysis and recognition of faces. *Neuroimage , 37*, 1407--1416.

ANDERSON, C., & SIJERCIC, Z. (1996). Classification of EEG signals from four subjects during five mental tasks. *Solving Engineering Problems with Neural Networks: Proceedings of the Conference on Engineering Applications in Neural Networks (EANN'96)*, (s. 507--414).

ARICA, S. (2007). An Orthogonal Scaling and Wavelet Function Pair For Analysis and Synthesis of Electroencephalography Signals. *IEEE 15th Signal Processing and Communications Applications, 2007. SIU 2007.* 1--4.

BABILONI, F., CINCOTTI, F., BIANCHI, L., PIRRI, G., MILLÁN J., R., MOURIÑO, J. (2001). Recognition of imagined hand movements with low resolution surface Laplacian and linear classifiers. *Medical Engineering and Physics* (23), 323--328.

BARBEAU, E., TAYLOR, M., REGIS, J., MARQUIS, P., CHAUVEL, P., & LIEGEOIS-CHAUVEL, C. (2008). Spatio temporal dynamics of face recognition. *Cerebral Cortex* , 997.

BASAR, E., SCHMIEDT-FEHR, C., ÖNIZ, A., & BASAR-EROGLU, C. (2008). Brain oscillations evoked by the face of a loved person. *Brain research* , 105--115.

BASHASHATI, A., FATOURECHI, M., WARD, R., & BIRCH, G. (2007). A survey of signal processing algorithms in brain--computer interfaces based on electrical brain signals. *Journal of Neural engineering , 4*, R32.

BASHASHATI, A., WARD, R., & BIRCH, G. (2005). A new design of the asynchronous brain computer interface using the knowledge of the path of features. *Neural Engineering, 2005. Conference Proceedings. 2nd International IEEE EMBS Conference on* , 101--104.

BASHEER, I., & HAJMEER, M. (2000). Artificial neural networks: fundamentals, computing, design, and application. *Journal of Microbiological Methods , 43*, 3--31.

BEGLEITER, H., PORJESZ, B., & WANG, W. (1995). Event-related brain potentials differentiate priming and recognition to familiar and unfamiliar faces. *Electroencephalography and Clinical Neurophysiology* , 41--49.

BENTIN, S., & DEOUELL, L. (2000). Structural encoding and identification in face processing: ERP evidence for separate mechanism. *The cognitive neuroscience of face processing: a special issue of Cognitive neuropsychology , 2000*, 35--54.

BENTIN, S., ALLISON, T., PUCE, A., PEREZ, E., & MCCARTHY, G. (1996). Electrophysiological studies of face perception in humans. *Journal of cognitive neuroscience* , 551--565.

BENTIN, S., DEOUELL, L., & SOROKER, N. (1999). Selective visual streaming in face recognition: Evidence from developmental prosopagnosia. *Neuroreport* , 823.

BERNE, R., & LEVY, M. (1996). *Principles of physiology.* Mosby Elsevier Health Science.

BISHOP, C. M. (1996). *Neural Networks for Pattern Recognition.* Oxford University press.

BLANCHARD, G., & BLANKERTZ, B. (2004). BCI competition 2003-data set IIa: spatial patterns of self-controlled brain rhythm modulations. *IEEE Transactions on Biomedical Engineering , 51*, 1062--1066.

BLANKERTZ, B., MULLER, K., KRUSIENSKI, D., SCHALK, G., WOLPAW, J., SCHLOGL, A. (2006). The BCI competition III: validating alternative approaches to actual BCI problems. *IEEE Transactions on Neural Systems and Rehabilitation Engineering , 14*, 153--159.

BLANKERTZ, B., TOMIOKA, R., LEMM, S., KAWANABE, M., & MULLER, K. (2008). Optimizing spatial filters for robust EEG single-trial analysis. *IEEE Signal Processing Magazine , 25*, 41.

BOBES, M., QUIN˜ONEZ, I., PEREZ, J., LEON, I., & VALDE´S-SOSA, M. (2007). Brain potentials reflect access to visual and emotional memories for faces. *Biological psychology* , 146--153.

BOOSTANI, R., GRAIMANN, B., MORADI, M., & PFURTSCHELLER, G. (2007). A comparison approach toward finding the best feature and classifier in cue-based BCI. *Medical and Biological Engineering and Computing , 45*, 403--412.

BOSTANOV, V. (2004). BCI competition 2003-data sets Ib and IIb: feature extraction from event-related brain potentials with the continuous wavelet transform and the t-value scalogram. *IEEE Transactions on Biomedical engineering , 51*, 1057--1061.

BRUCE, V., & YOUNG, A. (1986). Understanding face recognition. *British journal of psychology* (77), 305--327.

BURGES, C. (1998). A tutorial on support vector machines for pattern recognition. *Data mining and knowledge discovery* , 121--167.

CAHAREL, S., BERNARD, C., THIBAUT, F., HAOUZIR, S., DI MAGGIO-CLOZEL, C., ALLIO, G. (2007). The effects of familiarity and emotional expression on face processing examined by ERPs in patients with schizophrenia. *Schizophrenia research , 95* (1-3), 186--196.

CAHAREL, S., POIROUX, S., BERNARD, C., THIBAUT, F., LALONDE, R., & REBAI, M. (2002). ERPs associated with familiarity and degree of familiarity during face recognition. *International Journal of Neuroscience , 112*, 1499--1512.

CURRAN, T., & HANCOCK, J. (2007). The FN400 indexes familiarity-based recognition of faces. *NeuroImage , 36* (2), 464--471.

ÇELIK, U., & ARICA, S. (2010). Classification of the Visual Evoked EEG Using Multiresolution Approximation Based on Excitatory Post-Synaptic

Potential Waveform. *2010 IEEE 26-Th Convention Of Electrical And Electronics Engineers In Israel.*

DAL SENO, B., MATTEUCCI, M., & MAINARDI, L. (2010). Online Detection of P300 and Error Potentials in a BCI Speller. *Computational intelligence and neuroscience , 2010*, 1.

D'ALESSANDRO, M., ESTELLER, R., VACHTSEVANOS, G., HINSON, A., ECHAUZ, J., & LITT, B. (2003). Epileptic seizure prediction using hybrid feature selection over multiple intracranial EEG electrode contacts: a report of four patients. *IEEE Transactions on Biomedical Engineering , 50*, 603--615.

DEMARCO, B., & MICHELI-TZANAKOU, E. (2009). A Multiresolution Analysis of the Effect of Face Familiarity on Human Event-Related Potentials. *Biometrics: Theory, Methods, and Applications* (s. 483). içinde Wiley-IEEE Press.

DIETL, T., TRAUTNER, P., STAEDTGEN, M., VANNUCHI, M., MECKLINGER, A., GRUNWALD, T. (2005). Processing of famous faces and medial temporal lobe event-related potentials: A depth electrode study. *Neuroimage* (25), 401--407.

DUBOIS, S., ROSSION, B., SCHILTZ, C., BODART, J., MICHEL, C., BRUYER, R. (1999). Effect of familiarity on the processing of human faces. *Neuroimage , 9*, 278--289.

DUDA, R., HART, P., & STORK, D. (2001). *Pattern classification.* Wiley-Interscience.

EFRON, B. (1979). Bootstrap methods: another look at the jackknife. *The annals of statistics , 7*, 1--26.

EGER, E., SCHWEINBERGER, S., DOLAN, R., & HENSON, R. (2005). Familiarity enhances invariance of face representations in human ventral visual cortex: fMRI evidence. *Neuroimage* , 1128--1139.

EIMER, M. (2000a). Effects of face inversion on the structural encoding and recognition of faces:: Evidence from event-related brain potentials. *Cognitive Brain Research* , 145--158.

EIMER, M. (2000b). Event-related brain potentials distinguish processing stages involved in face perception and recognition. *Clinical Neurophysiology* (111), 694--705.

ELLIS, A., & ROLLS, E. (1992). Cognitive Mechanisms of Face Processing [and Discussion]. *Philosophical Transactions: Biological Sciences* , 113--119.

ELLIS, H., SHEPHERD, J., & DAVIES, G. (1979). Identification of familiar and unfamiliar faces from internal and external features: Some implications for theories of face recognition. *Perception* , 431--439.

FARWELL, L., & DONCHIN, E. (1988). Talking off the top of your head: toward a mental prosthesis utilizing event-related brain potentials. *Electroencephalography and clinical Neurophysiology , 70*, 510--523.

GARRETT, D., PETERSON, D., ANDERSON, C., & THAUT, M. (2003). Comparison of linear and nonlinear methods for EEG signal classification. *IEEE Transactions on Neural Systems and Rehabilitative Engineering* , 141--144.

GAZZANIGA, M., & BIZZI, E. (2000). *The new cognitive neurosciences.* The MIT Press.

GENETTI, M., KHATEB, A., HEINZER, S., MICHEL, C., & PEGNA, A. (2009). Temporal dynamics of awareness for facial identity revealed with ERP. *Brain and cognition , 69*, 296--305.

GLASSMAN, E. (2005). A wavelet-like filter based on neuron action potentials for analysis of human scalp electroencephalographs. *Biomedical Engineering, IEEE Transactions on , 52* (11), 1851--1862.

GOBBINI, M., & HAXBY, J. (2007). Neural systems for recognition of familiar faces. *Neuropsychologia , 45*, 32--41.

GUILLAUME, C., GUILLERY-GIRARD, B., CHABY, L., LEBRETON, K., HUGUEVILLE, L., EUSTACHE, F. (2009). The time course of repetition effects for familiar faces and objects: An ERP study. *Brain Research , 1248*, 149--161.

GUNN, S. (1998). Support vector machines for classification and regression. *ISIS technical report* .

GUYON, I. (2008). Practical feature selection: from correlation to causality. I. Guyon içinde, *Mining Massive Data Sets for Security: Advances in Data Mining, Search, Social Networks and Text Mining, and their Applications to Security* (s. 27--43).

GUYON, I., & ELISSEEFF, A. (2003). An introduction to variable and feature selection. *The Journal of Machine Learning Research , 3*, 1157--1182.

HAMILA, R., ASTOLA, J., ALAYA CHEIKH, F., GABBOUJ, M., & RENFORS, M. (1999). Teager energy and the ambiguity function. *IEEE Transactions on Signal Processing , 47*, 260--262.

HAXBY, J., GRADY, C., HORWITZ, B., UNGERLEIDER, L., MISHKIN, M., CARSON, R. (1991). Dissociation of object and spatial visual processing pathways in human extrastriate cortex. *Proceedings of the National Academy of Sciences of the United States of America , 88* (5), 1621.

HAXBY, J., HOFFMAN, E., & GOBBINI, M. (2002). Human Neural Systems for Face Recognition and Social Communication. *Biological psychiatry* , 59--67.

HAXBY, J., HOFFMAN, E., & GOBBINI, M. (2000). The distributed human neural system for face perception. *Trends in cognitive sciences* (4), 223--232.

HAXBY, J., HORWITZ, B., UNGERLEIDER, L., MAISOG, J., PIETRINI, P., & GRADY, C. (1994). The functional organization of human extrastriate cortex: a PET-rCBF study of selective attention to faces and locations. *Journal of Neuroscience* , 6336.

HEISZ, J., WATTER, S., & SHEDDEN, J. (2006). Automatic face identity encoding at the N170. *Vision research* , 4604--4614.

HENSON, R., GOSHEN-GOTTSTEIN, Y., GANEL, T., OTTEN, L., QUAYLE, A., & RUGG, M. (2003). Electrophysiological and haemodynamic correlates of face perception, recognition and priming. *Cerebral Cortex , 13* (7), 793.

HOFFMANN, U., VESIN, J., & EBRAHIMI, T. (2006). Spatial filters for the classification of event-related potentials. *Proceedings of the 14th*

European Symposium on Artificial Neural Networks (ESANN). Bruges (Belgium).

İNCE, N. F. (2005). *Analysis and Classification of EEG with Adapted Wavelets and Local Discriminant Bases.* Adana: Phd Thesis.

ITIER, R., & TAYLOR, M. (2004). Effects of repetition learning on upright, inverted and contrast-reversed face processing using ERPs. *Neuroimage* , 1518--1532.

ITIER, R., HERDMAN, A., GEORGE, N., CHEYNE, D., & TAYLOR, M. (2006). Inversion and contrast-reversal effects on face processing assessed by MEG. *Brain research* , 108--120.

JAMES, M., JOHNSTONE, S., & HAYWARD, W. (2001). Event-related potentials, configural encoding, and feature-based encoding in face recognition. *Journal of Psychophysiology* , 275--285.

JEFFREYS, D. (1996). Evoked potential studies of face and object processing. *Visual Cognition* , 1--38.

JOHNSTON, R., & EDMONDS, A. (2009). Familiar and unfamiliar face recognition: A review. *Memory* , 577--596.

KADAMBE, S., & BOURDEAUX-BARTELS, G. (2002). A comparison of a wavelet functions for pitch detection of speech signals. *1991 International Conference on Acoustics, Speech, and Signal Processing, ICASSP-91.*, , (s. 449 - 452).

KANNATHAL, N., CHOO, M., ACHARYA, U., & SADASIVAN, P. (2005). Entropies for detection of epilepsy in EEG. *Computer Methods and Programs in Biomedicine , 80*, 187--194.

KANWISHER, N., & MOSCOVITCH, M. (2000). The cognitive neuroscience of face processing: An introduction. *Cognitive Neuropsychology* (17), 1--11.

KANWISHER, N., CHUN, M., MCDERMOTT, J., & LEDDEN, P. (1996). Functional imaging of human visual recognition. *Cognitive Brain Research* , 55--67.

KANWISHER, N., MCDERMOTT, J., & CHUN, M. (1997). The fusiform face area: a module in human extrastriate cortex specialized for face perception. *Journal of Neuroscience* (17), 4302.

KAPER, M., MEINICKE, P., GROSSEKATHOEFER, U., LINGNER, T., & RITTER, H. (2004). BCI competition 2003-data set IIb: Support vector machines for the P300 speller paradigm. *IEEE Transactions on Biomedical Engineering , 51*, 1073--1076.

KOHAVI, R., & JOHN, G. (1997). Wrappers for feature subset selection. *Artificial intelligence , 97*, 273--324.

KRUSIENSKI, D., & SCHALK, G. (2004). Wadsworth BCI Dataset (P300 Evoked Potentials). *BCI Competition III Challenge* .

KRUSIENSKI, D., SELLERS, E., & VAUGHAN, T. (2007). Common spatio-temporal patterns for the P300 speller. *Neural Engineering, 2007. CNE'07. 3rd International IEEE/EMBS Conference on*, (s. 421--424).

KRUSIENSKI, D., SELLERS, E., CABESTAING, F., BAYOUDH, S., MCFARLAND, D., VAUGHAN, T. (2006). A comparison of classification techniques for the P300 speller. *Journal of neural engineering , 3*, 299--305.

KRUSIENSKI, D., SELLERS, E., MCFARLAND, D., VAUGHAN, T., & WOLPAW, J. (2008). Toward enhanced P300 speller performance. *Journal of neuroscience methods , 167*, 15--21.

KRUSIENSKI, D., TOWNSEND, G., & SELLERS, E. (2009). Amplitude Quantization of Event Related Potentials for Brain-Computer Interfaces. *Proceedings of the 4th International IEEE EMBS Conference on Neural Engineering.* Antalya.

LENHARDT, A., KAPER, M., & RITTER, H. (2008). An adaptive P300-based online brain-computer interface. *IEEE transactions on neural systems and rehabilitation engineering: a publication of the IEEE Engineering in Medicine and Biology Society , 16*, 121.

LI, Y., GUAN, C., LI, H., & CHIN, Z. (2008). A self-training semi-supervised SVM algorithm and its application in an EEG-based brain computer interface speller system. *Pattern Recognition Letters , 29*, 1285--1294.

LIANG, N., & BOUGRAIN, L. (2008). Averaging techniques for single-trial analysis of oddball event-related potentials. *4th International Brain-Computer Interface workshop (2008).*

LIN, J. (1991). Divergence measures based on the Shannon entropy. *IEEE Transactions on Information theory , 37*, 145--151.

LIN, Z., & ZHANG, C. (2005). Enhancing Classification by Perceptual Characteristic for the P300 Speller Paradigm. *Neural Engineering, 2005. Conference Proceedings. 2nd International IEEE EMBS Conference on*, (s. 574--576).

LOTTE, F. (2008). *Study of Electroencephalographic Signal Processing and Classification Techniques towards the use of Brain-Computer Interfaces in Virtual Reality Applications.*

LOTTE, F., CONGEDO, M. A., LAMARCHE, F., & ARNALDI, B. (2007). A review of classification algorithms for eeg-based brain-computer interfaces. *Journal of Neural Engineering* , R1--R13.

MALLAT, S. (1989). A theory for multiresolution signal decomposition: The wavelet representation. *IEEE transactions on pattern analysis and machine intelligence , 11*, 674--693.

MALMIVUO, J., & PLONSEY, R. (1995). *Bioelectromagnetism: principles and applications of bioelectric and biomagnetic fields.* Oxford University Press New York.

MARZI, T., & VIGGIANO, M. (2007). Interplay between familiarity and orientation in face processing: An ERP study. *International Journal of Psychophysiology , 65*, 182--192.

MATHWORKS.COM. (2010, September 15). Matlab web site: http://www.mathworks.com adresinden alınmıştır

MCFARLAND, D., ANDERSON, C., MULLER, K., SCHLOGL, A., & KRUSIENSKI, D. (2006). Bci meeting 2005-workshop on bci signal

processing: feature extraction and translation. *IEEE Transactions on Neural Systems and Rehabilitation Engineering , 14*, 135--138.

MCFARLAND, D., MCCANE, L., & WOLPAW, J. (1998). EEG-based communication and control: short-term role of feedback. *IEEE Transactions on Rehabilitation Engineering* (6), 7--11.

MERZAGORA, A., BUNCE, S., IZZETOGLU, M., & ONARAL, B. (2006). Wavelet analysis for EEG feature extraction in deception detection. *Engineering in Medicine and Biology Society, 2006. EMBS'06. 28th Annual International Conference of the IEEE*, (s. 2434--2437).

MIRGHASEMI, H., FAZEL-REZAI, R., & SHAMSOLLAHI, M. (2006). Analysis of P300 classifiers in brain computer interface speller. *Engineering in Medicine and Biology Society, 2006. EMBS'06. 28th Annual International Conference of the IEEE*, (s. 6205--6208).

MIYAKOSHI, M., KANAYAMA, N., NOMURA, M., IIDAKA, T., & OHIRA, H. (2008). ERP study of viewpoint-independence in familiar-face recognition. *International Journal of Psychophysiology* , 119--126.

MNATSAKANIAN, E., & TARKKA, I. (2005). Familiar and nonfamiliar face-specific ERP components. *International Congress Series, 1278*, s. 135--138.

MOHR, B., LANDGREBE, A., & SCHWEINBERGER, S. (2002). Interhemispheric cooperation for familiar but not unfamiliar face processing. *Neuropsychologia , 40* (11), 1841--1848.

MOLINARO, A., SIMON, R., & PFEIFFER, R. (2005). Prediction error estimation: a comparison of resampling methods. *Bioinformatics , 21*, 3301.

MUGLER, E., BENSCH, M., HALDER, S., ROSENSTIEL, W., BOGDAN, M., BIRBAUMER, N. (2008). Control of an internet browser using the P300 event-related potential. *International Journal of Bioelectromagnetism* , 56 - 63.

MULLER, K., ANDERSON, C., & BIRCH, G. (2003). Linear and nonlinear methods for brain-computer interfaces. *IEEE Transactions on Neural Systems and Rehabilitation Engineering , 11*, 165--169.

MÜLLER-GERKING, J., PFURTSCHELLER, G., & FLYVBJERG, H. (1999). Designing optimal spatial filters for single-trial EEG classification in a movement task. *Clinical neurophysiology , 110*, 787--798.

NAM, C., LI, Y., & JOHNSON, S. (2010). Evaluation of P300-Based Brain-Computer Interface in Real-World Contexts. *International Journal of Human-Computer Interaction , 26*, 621--637.

NEUMANN, M., & SCHWEINBERGER, S. (2008). N250r and N400 ERP correlates of immediate famous face repetition are independent of perceptual load. *1239*, 181--190.

NIJBOER, F., SELLERS, E., MELLINGER, J., JORDAN, M., MATUZ, T., FURDEA, A. (2008). A P300-based brain-computer interface for people with amyotrophic lateral sclerosis. *Clinical neurophysiology , 119*, 1909--1916.

OBERMAIER, B., GUGER, C., NEUPER, C., & PFURTSCHELLER, G. (2001). Hidden Markov models for online classification of single trial EEG data. *Pattern Recognition Letters , 22*, 1299--1309.

ÖZGÖREN, M., BAŞAR-EROĞLU, C., & BAŞAR, E. (2005). Beta oscillations in face recognition. *International Journal of Psychophysiology* (55), 51--59.

PALLER, K., GONSALVES, B., GRABOWECKY, M., BOZIC, V., & YAMADA, S. (2000). Electrophysiological correlates of recollecting faces of known and unknown individuals. *Neuroimage , 11*, 98--110.

PETROSIAN, A. (2002). Kolmogorov complexity of finite sequences and recognition of different preictal EEG patterns. *Proceedings of the Eighth IEEE Symposium on Computer-Based Medical Systems, 1995.,*, (s. 212--217).

PFURTSCHELLER, G., & NEUPER, C. (2001). Motor imagery and direct brain-computer interface. *Proceeding of IEEE* (89), 1123-1134.

PFURTSCHELLER, G., MÜLLER-PUTZ, G. R., SCHLÖGL, A., GRAIMANN, B., LEE, F., SCHERER, R. (2006). 15 Years of BCI Research at Graz University of Technology : Current Projects. *IEEE Transactions on Neural Systems and Rehabilitation Engineering* , 205--210.

PFURTSCHELLER, G., NEUPER, C., GUGER, C., HARKAM, W., RAMOSER, H., SCHLÖGL, A. (1999). Current Trends in Graz Brain–Computer Interface (BCI) Research. *IEEE Trans. Rehab. Eng.*

PFURTSCHELLER, G., NEUPER, C., SCHLOGL, A., & LUGGER, K. (1998). Separability of EEG signals recorded during right and left motor imagery using adaptive autoregressive parameters. *IEEE transactions on rehabilitation engineering , 6*, 316--325.

POLAT, K., & GÜNEŞ, S. (2007). Classification of epileptiform EEG using a hybrid system based on decision tree classifier and fast Fourier transform. *Applied Mathematics and Computation , 187*, 1017--1026.

RAKOTOMAMONJY, A., & GUIGUE, V. (2008). BCI competition III: Dataset II-ensemble of SVMs for BCI P300 speller. *IEEE Transactions on Biomedical Engineering , 55*, 1147--1154.

RAMOSER, H., MULLER-GERKING, J., & PFURTSCHELLER, G. (2000). Optimal spatial filtering of single trial EEG during imagined hand movement. *IEEE Transactions on Rehabilitation Engineering* , 441--446.

RIVET, B., SOULOUMIAC, A., GIBERT, G., & ATTINA, V. (2008). P300 Speller Brain-Computer Interface: Enhancement of P300 Evoked Potential by Spatial Filters. *16th European Signal Processing Conference EUSIPCO-2008.* Lausanne : Switzerland.

ROBERT, C., GAUDY, J., & LIMOGE, A. (2002). Electroencephalogram processing using neural networks. *Clinical Neurophysiology* , 694--701.

ROSSION, B., & JACQUES, C. (2008). Does physical interstimulus variance account for early electrophysiological face sensitive responses in the human brain? Ten lessons on the N170. *Neuroimage* , 1959--1979.

ROSSION, B., DELVENNE, J., DEBATISSE, D., GOFFAUX, V., BRUYER, R., & CROMMELINCK, M. (1999). Spatio-temporal localization of the face inversion effect: An event-related potentials study. *Biological Psychology* , 173--189.

ROSSION, B., GAUTHIER, I., TARR, M., DESPLAND, P., BRUYER, R., & LINOTTE, S. (2000). The N170 occipito-temporal component is delayed

and enhanced to inverted faces but not to inverted objects: An electrophysiological account of face-specific processes in the human brain. *Neuroreport* , 69.

ROSSION, B., SCHILTZ, C., ROBAYE, L., PIRENNE, D., & CROMMELINCK, M. (2001). How does the brain discriminate familiar and unfamiliar faces?: a PET study of face categorical perception. *Journal of Cognitive Neuroscience* (13), 1019--1034.

ROWLAND, L., & SHNEIDER, N. (2001). Amyotrophic lateral sclerosis. *New England Journal of Medicine , 344*, 1688.

SAEYS, Y., INZA, I., & LARRAN˜ AGA, P. (2007). A review of feature selection techniques in bioinformatics. *Bioinformatics , 23*, 2507.

SAGIV, N., & BENTIN, S. (2001). Structural encoding of human and schematic faces: holistic and part-based processes. *Journal of Cognitive Neuroscience* , 937--951.

SALVARIS, M., & SEPULVEDA, F. (2009). Visual modifications on the P300 speller BCI paradigm. *Journal of Neural Engineering , 6*, 046011.

SALVARIS, M., & SEPULVEDA, F. (2009). Wavelets and Ensemble of FLDs for P300 Classification. *Proceedings of the 4th International IEEE EMBS Conference on Neural Engineering*. Antalya.

SAMAR, V., BOPARDIKAR, A., RAO, R., & SWARTZ, K. (1999). Wavelet analysis of neuroelectric waveforms: a conceptual tutorial. *Brain and language , 66*, 7--60.

SANEI, S., & CHAMBERS, J. (2007). *EEG signal processing*. Wiley-Interscience.

SCHWEINBERGER, S., PICKERING, E., BURTON, A., & KAUFMANN, J. (2002). Human brain potential correlates of repetition priming in face and name recognition. *Neuropsychologia , 40*, 2057--2073.

SCHWEINBERGER, S., PICKERING, E., JENTZSCH, I., BURTON, A., & KAUFMANN, J. (2002). Event-related brain potential evidence for a response of inferior temporal cortex to familiar face repetitions. *Cognitive Brain Research , 14*, 398--409.

SELLERS, E. (2004). *A P300-based brain-computer interface: Testing an alternative method of communication.* University of South Florida.

SELLERS, E., & DONCHIN, E. (2006). A P300-based brain-computer interface: initial tests by ALS patients. *Clinical Neurophysiology , 117*, 538--548.

SELLERS, E., KRUSIENSKI, D., MCFARLAND, D., VAUGHAN, T., & WOLPAW, J. (2006). A P300 event-related potential brain-computer interface (BCI): the effects of matrix size and inter stimulus interval on performance. *Biological Psychology , 73*, 242--252.

SELLERS, E., KUBLER, A., & DONCHIN, E. (2006). Brain-computer interface research at the University of South Florida Cognitive Psychophysiology Laboratory: the P300 speller. *IEEE Transactions on Neural Systems and Rehabilitation Engineering , 14*, 221--224.

SERBY, H., YOM-TOV, E., & INBAR, G. (2005). An improved P300-based brain-computer interface. *IEEE Transactions on neural systems and rehabilitation engineering* , 89--98.

STRANG, G., & NGUYEN, T. (1996). *Wavelets and filter banks.* Wellesley Cambridge Pr.

SUBASI, A. (2007). EEG signal classification using wavelet feature extraction and a mixture of expert model. *Expert Systems with Applications , 32*, 1084--1093.

SUTTON, S., BRAREN, M., ZUBIN, J., & JOHN, E. (1965). Evoked-potential correlates of stimulus uncertainty. *150*, 1187.

SYKACEK, P., ROBERTS, S., & STOKES, M. (2004). Adaptive BCI based on variational Bayesian Kalman filtering: an empirical evaluation. *IEEE Transactions on Biomedical Engineering , 51*, 719--727.

TAKANO, K., KOMATSU, T., HATA, N., NAKAJIMA, Y., & KANSAKU, K. (2009). Visual stimuli for the P300 brain-computer interface: A comparison of white/gray and green/blue flicker matrices. *Clinical Neurophysiology* .

TANAKA, K., KURITA, T., MEYER, F., BERTHOUZE, L., & KAWABE, T. (2006). Stepwise feature selection by cross validation for EEG-based

Brain Computer Interface. *2006. IJCNN'06. International Joint Conference on Neural Networks,,* (s. 4672--4677).

TANSKANEN, T., NÄSÄNEN, R., OJANPÄÄ, H., & HARIA, R. (2007). Face recognition and cortical responses: Effect of stimulus duration. *Neuroimage* , 1636--1644.

TAVAKOLIAN, K., & REZAEI, S. (2004). Classification of mental tasks using Gaussian mixture Bayesian network classifiers. *2004 IEEE International Workshop on Biomedical Circuits and Systems.*

TEPLAN, M. (2002). Fundamentals of EEG measurement. *Measurement Science Review , 2* (2), 1--11.

THIERRY, G., MARTIN, C., DOWNING, P., & PEGNA, A. (2007). Controlling for interstimulus perceptual variance abolishes N170 face selectivity. *Nature neuroscience* , 505--511.

TROJE, N., & KERSTEN, D. (1999). Viewpoint-dependent recognition of familiar faces. *PERCEPTION-LONDON-* , 483--488.

UNSER, M., & ALDROUBI, A. (1996). A review of wavelets in biomedical applications. *Proceedings of the IEEE , 84*, 626--638.

VUILLEUMIER, P., & POURTOIS, G. (2007). Distributed and interactive brain mechanisms during emotion face perception: evidence from functional neuroimaging. *Neuropsychologia* , 174--194.

WATANABE, S., MIKI, K., & KAKIGI, R. (2005). Mechanisms of face perception in humans: A magneto- and electro-encephalographic study. *Neuropathology* (25), 8--20.

WOLPAW, J., BIRBAUMER, N., MCFARLAND, D., PFURTSCHELLER, G., & VAUGHAN, T. (2002). Brain--computer interfaces for communication and control. *Clinical neurophysiology* , 767--791.

XU, W., SHEN, M., WANG, S., & CHAN, F. (2005). Analysis of time-varying coherence of EEG during face recognition based on harmonic transform. *Annual International Conference of the IEEE Engineering in Medicine and Biology Society., 6*, s. 5927.

YOUNG, A., HAY, D., MCWEENY, K., FLUDE, B., & ELLIS, A. (1985). Matching familiar and unfamiliar faces on internal and external features. *Perception* , 737--746.

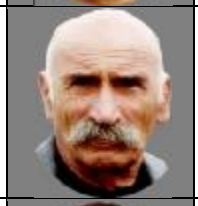
ZOUBIR, A. A. (1998). The bootstrap and its application in signal processing. *IEEE signal processing magazine , 15*, 56--76.

CIRRICULUM VITAE

Umut ÇELİK received the B.S. degree in Electrical and Electronics Engineering from University of Cukurova in 2000 and the M.S. degree in 2004 from Mustafa Kemal University, Antakya in the field of Electrical-Electronics Engineering. His master thesis title is "A Vehicle License Plate Recognition System" supervised by Asst. Prof Mustafa ORAL. He worked as a research assistant in the Department of Electrical Electronic Engineering at Mustafa Kemal University between January 2002 and March 2004. He is currently working as a research assistant in Department of Electrical Electronics Engineering at Çukurova University. He has been involved in research in Digital Image Processing, Biomedical Signal Processing and Computational Intelligence.

APPENDIXES

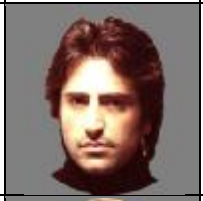
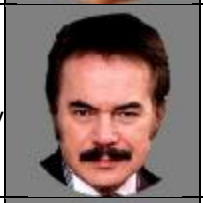
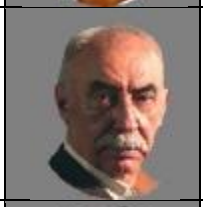
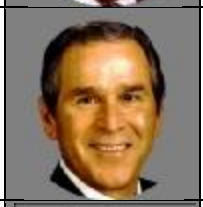
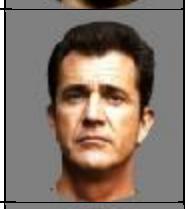
APPENDIX I. Familiar (Famous) Stimulus Photos and Names

No	Name	Photos	No	Name	Photos	No	Name	Photos
1	Bülent Çolak		7	Mehmet Aslantuğ		13	Deniz Çakir	
2	Sarp Apak		8	Dağhan Külegeç		14	Hülya Avşar	
3	Tuncel Kurtiz		9	Ufuk Özkan		15	Ebru Gündeş	
4	Emre Karayel		10	Brad Pitt		16	Ilyas Salman	
5	Ersin Korkut		11	Fatih Terim		17	Tayyip Erdogan	
6	Selçuk Yöntem		12	Halit Kocatepe		18	Ahmet Kaya	

APPENDIX I Continued.

No	Name	Photos	Name	Photos	No	Name	Photos
19	Kadir Inanir		Ilker Başbuğ		35	Acun Ilıcalı	
20	Barış Manco		Josh Holloway		36	Oya Başar	
21	Abdullah Gul		Kemal Sunal		37	Cem Yılmaz	
22	Gulse Birse		Kenan Imirzalıoğlu		38	Şehsuvar Aktaş	
23	Fırat Tanış		Bill Clinton		39	Tarik Akan	
24	Safak Sezer		Kemal Kılıçtaroğlu		40	Rıdvan Dilmen	
25	Hülya Koçyigit		Kivanc Tatlitug		41	Zülfü Livaneli	
26	Ibrahim Tatlıses		Uğur Yücel		42	Halil Ergün	

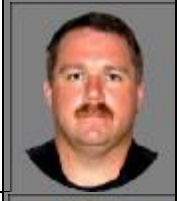
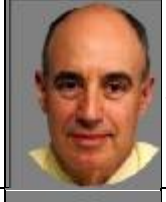
APPENDIX I Continued.

No	Name	Photos	No	Name	Photos	No	Name	Photos
43	Mahsun Kırmızıgül		51	Oğuzhan Koç		59	Ahmet Necdet Sezer	
44	M. Ali Birand		52	Orhan Gencebay		60	Sibel Can	
45	Şener Şen		53	George W. Bush		61	Tarkan	
46	Michael Jackson		54	Özgü Namal		62	Mel Gibson	
47	Ali Kirca		55	Petek Dinçöz		63	Tolga Cevik_	
48	Müjde Ar		56	Vladimir Putin		64	Oktay Kaynarca	
49	Barack Hussein Obama		57	Şebnem Ferah		65	Pelin Karahan	
50	Leonardo Dicaprio		58	Altan Erkekli		66	Ali Sunal	

APPENDIX I Continued.

No	Name	Photos	No	Name	Photos	No	Name	Photos
67	Uğur Dündar		75	Levent Ülgen		83	Timuçin Esen	
68	Yılmaz Erdoğan		76	Beren Saat		84	Murat Eken	
69	Angelina Jolie		77	Demet Evgar		85	Cezmi Baskın	
70	Terry O'Quinn		78	Ozan Güven		86	Metin Akpınar	
71	Okan Bayülgen		79	Olgun Şimşek				
72	Ata Demirer		80	Tolga Karel				
73	Gazanfer Özcan		81	Hakan Şukur				
74	Deniz Baykal		82	Cüneyt Arkın				

APPENDIX II. Unfamiliar Stimulus Photos

No	Photos	No	Photos	No	Photos	No	Photos	No	Photos
1		8		15		22		29	
2		9		16		23		30	
3		10		17		24		31	
4		11		18		25		32	
5		12		19		26		33	
6		13		20		27		34	
7		14		21		28		35	

APPENDIX II Continued.

No	Photos	No	Photos	No	Photos	No	Photos	No	Photos
36		44		52		60		68	
37		45		53		61		69	
38		46		54		62		70	
39		47		55		63		71	
40		48		56		64		72	
41		49		57		65		73	
42		50		58		66		74	
43		51		59		67		75	

APPENDIX II Continued.

No	Photos	No	Photos	No	Photos	No	Photos
76		79		82		85	
77		80		83		86	
78		81		84			

APPENDIX III. Participant Information

P. No	Age	Sex	Education	Exp. hour	True Familiar	True Unfamiliar	Total Fmlr	Total Unfmlr	Is useable?
1	24	M	U	PM					No
2	28	M	G	AM	84	86	84	88	Yes
3	21	M	U	PM	78	86	78	94	Yes
4	21	M	U	PM	70	85	71	101	Yes
5	24	M	G	AM	84	86	84	88	Yes
6	21	M	U	PM	69	85	70	102	Yes
7	26	M	G	AM	64	81	69	103	Yes
8	20	F	G	PM	83	81	88	84	Yes
9	20	F	U	PM	79	84	81	91	Yes
10	22	F	U	PM	74	44	79	56	No
11	29	M	U	PM	72	85	73	99	Yes
12	21	M	U	PM	68	86	68	104	Yes
13	31	M	G	AM	86	83	89	83	Yes
14	21	M	U	PM	83	78	91	81	Yes
15	24	M	U	PM	86	85	87	85	Yes
16	25	M	G	PM	69	86	69	103	Yes
17	22	M	U	PM	78	85	79	93	Yes
18	32	F	G	PM	82	63	105	67	No
19	26	M	G	PM	86	86	86	86	Yes
20	21	M	U	PM	79	85	80	92	Yes
21	20	M	U	PM	82	83	85	87	Yes
22	23	M	U	PM	86	75	97	75	Yes
23	21	M	U	PM	85	86	85	87	Yes
24	21	M	U	PM	86	67	105	67	Yes
25	23	M	U	AM	86	82	90	82	Yes
26	33	F	G	AM	79	85	80	92	Yes
27	23	M	G	PM	84	85	85	87	Yes
28	22	M	U	PM	81	84	83	89	Yes
29	21	F	U	PM	79	84	81	91	Yes

(U=Undergraduate, G=Graduate, M=Male, F=Female)

APPENDIX IV. Informed Consent Form

İZİN BELGESİ

Yrd. Doç. Dr. Sami ARICA ve Araş. Gör. Umut ÇELİK tarafından yürütülen **"Hareketle ve Görsellikle İlişkili EEG'nin Zaman Frekans Analizi ve Sınıflaması"** adlı çalışma için EEG verimin alınmasını ve bu verinin adı geçen çalışma kapsamında kullanılmasını gönüllü olarak kabul ederim.

Bu çalışmanın amacının, kapsamının ve EEG ölçümü için kullanılacak yöntemlerin tarafıma ayrıntılı olarak anlatıldığını, EEG ölçümüne katılmaya ikna olduğumu, bu verilerin çalışma kapsamında kullanılmasının çalışmaya katkı sunacağını düşünerek herhangi bir karşılık olmadan tamamen gönüllülük esasına göre bu çalışmada yer aldığımı, bu verilerin kullanılmasını durdurma hakkımın saklı olduğunu bildiğimi ve aşağıdaki bilgilerimin doğru olduğunu beyan ederim.

Tarih: 23. /06/2010

İsim: [redacted]

İmza: [redacted]

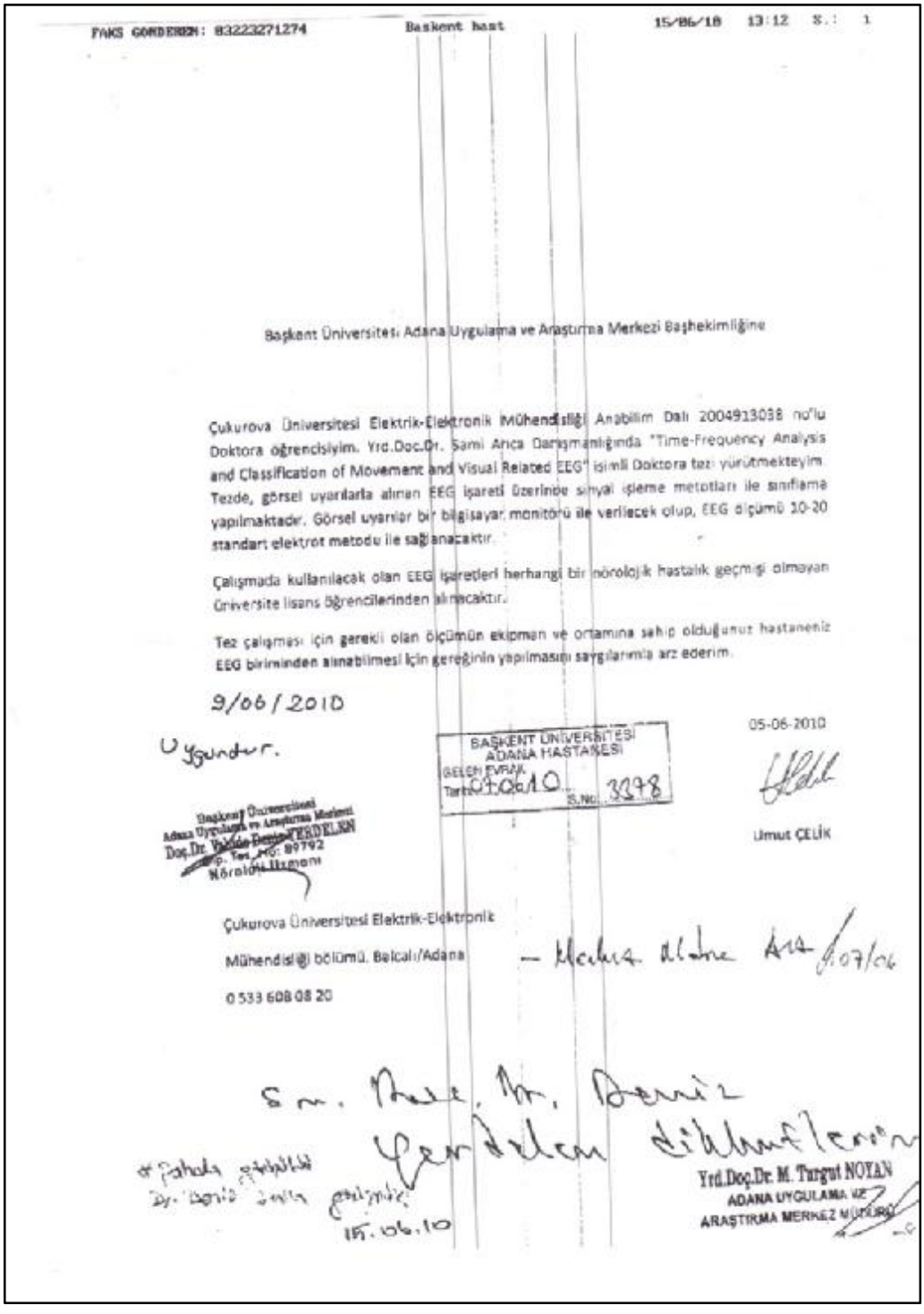
Mesleği: [redacted]

Yaşı: 32

İletişim Bilgileri: Çukurova Üniversitesi

Müh. Mim. Fak. Balcalı Adana

APPENDIX V. Approved Form by Neurology Department Committee and Management of Başkent University, Adana Application and Research Center



FAKS GONDEREN: 83223271274 Baskent hast 15/06/10 13:12 S.: 1

Başkent Üniversitesi Adana Uygulama ve Araştırma Merkezi Başhekimliğine

Çukurova Üniversitesi Elektrik-Elektronik Mühendisliği Anabilim Dalı 2004913038 no'lu Doktora öğrencisiyim. Yrd.Doç.Dr. Sami Arıca Danışmanlığında "Time-Frequency Analysis and Classification of Movement and Visual Related EEG" isimli Doktora tezi yürütmekteyim. Tezde, görsel uyarılarla alınan EEG işareti üzerinde sinyal işleme metotları ile sınıflama yapılmaktadır. Görsel uyarılar bir bilgisayar monitörü ile verilecek olup, EEG ölçümü 10-20 standart elektrot metodu ile sağlanacaktır.

Çalışmada kullanılacak olan EEG işaretleri herhangi bir nörolojik hastalık geçmişi olmayan Üniversite lisans öğrencilerinden alınacaktır.

Tez çalışması için gerekli olan ölçümün ekipman ve ortamına sahip olduğunuz hastaneniz EEG birimlerinden alınabilmesi için gereğinin yapılmasını saygılarımla arz ederim.

9/06/2010

Uygundur.

Başkent Üniversitesi Adana Uygulama ve Araştırma Merkezi Doç.Dr. Yıldız Dursun ERDELEN Sicil No: 89792 Nöroloji Uzmanı

BAŞKENT ÜNİVERSİTESİ ADANA HASTANESİ GELEN EVRAK Tarih: 07.06.10 S.No: 3378

05-06-2010

Ümut ÇELİK

Çukurova Üniversitesi Elektrik-Elektronik Mühendisliği bölümü. Balcalı/Adana

0 533 608 08 20

Sn. Başk. Dr. Deniz Yardımcısı Dikkat'e

Yrd.Doç.Dr. M. Turgut NOYAN
ADANA UYGULAMA VE ARAŞTIRMA MERKEZ MÜDÜRÜ

*Fotoğraf çekebilir Dr. Deniz Sanca görüşmüş. 15.06.10